Development and Use of a New Three-Dimensional Mechanistic Water Quality Model of Jordan Lake to Predict Responses of Reduced Nutrient Loading

by

William Langley, Babatunde Adeyeye, and James D. Bowen
Civil and Environmental Engineering Department
University of North Carolina at Charlotte

A Report to the North Carolina Policy Collaboratory,
Chapel Hill, North Carolina

June 29, 2020

Table of Contents

1. INTRODUCTION

1.1 Background

The North Carolina Policy Collaboratory was established by the state legislature to utilize and disseminate the environmental research expertise of the University of North Carolina for practical use by state and local governments. In 2016, the legislature approved a budget provision to develop a new, comprehensive nutrient management regulatory framework. The provision directed the Collaboratory to oversee a continuing study and analysis of nutrient management strategies and the compilation of existing water quality data for Jordan Lake. During 2019, a number of research projects, referred to collectively as the Jordan Lake Nutrient Management Study, were initiated under this provision. The resulting scientific findings have been integrated into a three-dimensional mass-balance-based simulation model of Jordan Lake. The Jordan Lake Nutrient Response Model, reported on herein, evaluates (1) the Lake's potential for eutrophication relative to nutrient loads, streamflow patterns, and climate, for both current conditions and future scenarios, and (2) the potential for nutrient mitigation by implementing best management practices, regulatory measures and restoration efforts.

The Jordan Lake watershed lies within the Cape Fear River basin in the Piedmont region of North Carolina (Figure 1). The Jordan Lake Nutrient Response Model is a numerical simulation of physical, chemical, and biological processes in the lake and underlying sediments. Water, nutrients, and organic matter constitute input loads to the lake at its inflow boundaries. Within the lake and its sediments, physical, chemical, and biological transformations occur under the prevailing conditions of heat and light. The quality of water in the lake and its outflow are transformed as a result.

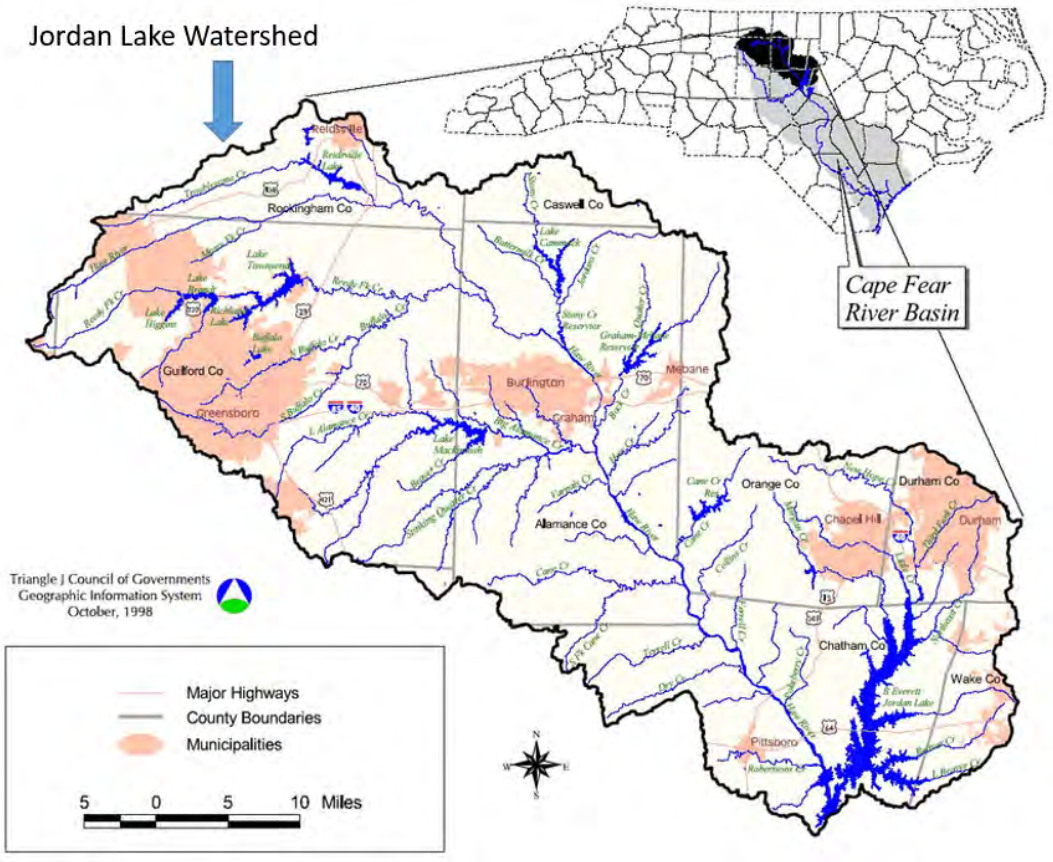

Figure 1. Jordan Lake watershed within the Cape Fear River basin of the Piedmont region of North Carolina

1.2 Study Objectives

This report describes the setup, calibration, and scenario testing with a newly developed Jordan Lake Nutrient Response Model that used a five year monitoring dataset (2014-2018). The model was developed to test how reductions in watershed loadings of nutrients, specifically nitrogen and phosphorus, would be expected to affect the water quality conditions in the lake. Of primary interest are the chlorophyll a concentrations in the lake for various load reduction scenarios. Chlorophyll a is an essential pigment in phytoplankton cells that is commonly used as quantitative measure of algal abundance. A second project objective was to better understand the interactions between the Jordan Lake watershed, the underlying benthic sediments of Jordan Lake, and the physical, chemical, and biological conditions in the water column of Jordan Lake.

The work follows an earlier study (Tetra Tech 2002, Tetra Tech Inc. 2003) that used monitoring data from 1993-2001 to create a nutrient response model of the lake as a coupled EFDC/WASP application (Hamrick 1992, Ambrose, Wool et al. 1993). The model described in this report takes advantage of a large amount of newly collected physical, chemical, and biological information on the lake, and reflects the latest conditions with respect to development within the Jordan Lake watershed. The newly developed model also takes advantage of advances in the

capabilities of mass-balance based water quality models. The Jordan Lake model developed here utilizes a new computational model grid and a predictive sediment diagenesis submodel. These advances allow for a better accounting of the short and long-term responses that would be expected under a scenario that significantly reduces nutrient loading to the lake.

1.3 Organization of the Study Report

The following section provides a description of the numerical model (EFDC) that was used as the basis of the Jordan Lake nutrient response model. A literature review of similar EFDC modeling projects is also provided. Some background information on Jordan Lake and a summary of the observed chlorophyll a concentrations for the 2014-2018 model time period are provided in the system description section. Specification of Model Input File and Calibration describe the data sources used and the method for calibrating the model to the observed data on the physical, chemical, and biological conditions during the five-year model time period. The next two sections use the model to describe the functioning of the system. Simulated releases of a non-reactive dye are used to determine the residence times of waters entering the lake, and the circulation and mixing of waters in various regions of the lake. A loading analysis is also presented that quantitatively compares the sources of water and inorganic and organic forms of phosphorus and nitrogen to the lake. Scenarios that look at the short and long-term impacts of various levels of reduction in watershed nutrient loading are then presented. Other scenarios consider the consequences of other changes to the system such as the removal of causeways that restrict circulation within the New Hope Creek arm of the lake. A discussion and conclusions section ends the report.

2. MODEL SETUP

2.1 Model Description

The Environmental Fluid Dynamics Code (EFDC) model was used to model simulate the hydrodynamics and water quality of the lake. EFDC(Hamrick 1992) is a general-purpose surface water modeling package for simulating three-dimensional (3-D) water circulation, mass transport, sediments and biogeochemical processes in surface waters. The graphical user interface EFDC Explorer 8.4 (Craig 2018) was used for pre- and post-processing of data.

EFDC solves numerically the three-dimensional, vertically hydrostatic, free surface, Reynold's averaged momentum equations for a variable-density fluid (Hamrick 1992). Turbulent kinetic energy, turbulent length scale, salinity and temperature transport equations are also solved. Wetting and drying of shallow areas is simulated using a mass conservation scheme(Hamrick 1992).

A 16-state variable (Table 1) version EFDC water quality model was used for this study (Tetra Tech 2007). Five variables found in the full 21-state variable model were not included for this study. (chemical oxygen demand (COD), total available metal (TAM), total suspended solids (TSS), and bioavailable (SA) and non-bioavailable silicate (SU)). The state variables included were able to simulate the algal dynamics using three state variables (cyanobacteria, diatoms, green algae), nutrient dynamics using three inorganic (total phosphate, nitrate nitrogen, ammonium) and six organic state variables (refractory and labile particulate nitrogen and

Table 1. EFDC Water Quality State Variables (Tetra Tech 2007). Abbreviations refer to constituents as shown in Figure 2.

No.	Water Quality State Variable	Abbreviation	Unit
1	Cyanobacteria (blue-green algae)	Bc	g/m^3
2	Diatoms (algae)	Bd	g/m^3
3	Green algae (others)	Bg	g/m^3
4	Refractory particulate organic carbon	RPOC	g/m^3
5	Labile particulate organic carbon	LPOC	g/m^3
6	Dissolved organic carbon	DOC	g/m^3
7	Refractory particulate organic phosphorus	RPOP	g/m^3
8	Labile particulate organic phosphorous	LPOP	g/m^3
9	Dissolved organic Phosphorous	DOP	g/m^3
10	Total phosphate	TPO_4	g/m^3
11	Refractory particulate organic nitrogen	RPON	g/m^3
12	Labile particulate organic nitrogen	LPON	g/m^3
13	Dissolved organic nitrogen	DON	g/m^3
14	Ammonium	NH_4	g/m^3
15	Nitrate nitrogen	NO_3^-	g/m^3
16	Dissolved Oxygen	DO	g/m^3

phosphorus, dissolved organic nitrogen), carbon cycling between algal and detrital fractions using three additional state variables (refractory and labile particulate carbon, dissolved organic

carbon), and dissolved oxygen dynamics using one additional state variable. EFDC simulated the spatially and temporally varying mass balance of each of these state variables and the exchange of mass between the state variables to simulate processes in the water column such as nutrient uptake via photosynthesis, nutrient release via respiration and predation, and nutrient recycling between organic and inorganic forms (Figure 2).

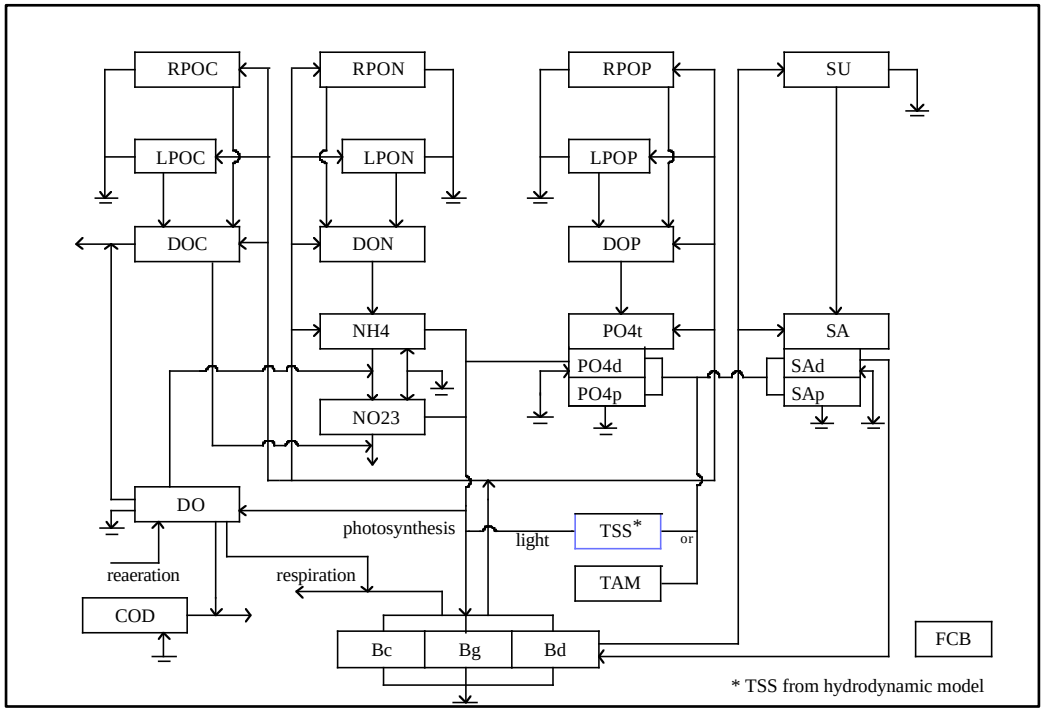

Figure 2. Box and arrow diagram showing the EFDC water quality state variables and the mass flows between them. See Table 1 for the constituent names and abbreviations

Temporal and spatial variations in additional state variables (e.g. temperature, x-, y-, and z-direction velocity) were simulated with the water-column hydrodynamic model. A predictive sediment diagenesis sub-model was also used to simulate the time-varying exchange of particulate organic matter settling from the water column and the benthic fluxes of inorganic nutrients and dissolved oxygen between the benthos and the water column (DiToro 2001, Craig 2018).

A version of the EFDC code was developed by Dynamic Solutions International, LLC (DSILLC) that simplifies the modeling process and provides links to a pre-processing and post-processing software called EFDC Explorer. Model setup, data input, and post-processing of model results can be performed with the EFDC Explorer graphical user interface. The model runs and post-processing of model results can also be done with programs such as MATLAB and Python. This project utilized the DSILLC version of the EFDC code. The pre-processing and post-processing was done with EFDC Explorer 8.4 and MATLAB scripts developed by the project team.

Recent reports of modeling lake hydrodynamics and water quality were reviewed in preparation for developing the Jordan Lake model (Table 2). These reports provided technical support for the selection of the numerous model parameters, many of which are not explicitly identifiable for Lake Jordan. They also provided guidance for conducting hydrodynamic and water quality model calibrations and selecting appropriate calibration targets. Local (in-state) model reports were also reviewed for consistency with previously reported input data and model results.

Table 2. Recent Water Quality Modeling Reports Used as a Basis for this Study

Report and Reference	Subject	Specific areas considered
Tenkiller Ferry Lake EFDC Water Quality Model (Michael Baker 2015)	EFDC model of hydrodynamics and water quality	Water balance calibration, water quality model parameters, sediment diagenesis model setup
3-D Hydrodynamic and Water Quality Model of Lake Thunderbird, Oklahoma (Dynamic Solutions 2013)	EFDC model of hydrodynamics and water quality	Water balance calibration, water quality model parameters, sediment diagenesis model setup
3-D Modeling of Hydrodynamics and Transport in Narragansett Bay (Abdelrhman 2015)	EFDC model of hydrodynamics and water quality	Water balance calibration, water quality model parameters, sediment diagenesis model setup
Integration of a benthic sediment diagenesis module into the 2D hydrodynamic and water quality model – CE-QUAL-W2 (Zhang, Sun et al. 2015)	sediment diagenesis model integration into CE-QUAL-W2	Sediment diagenesis model theory and results for transient (seasonal) periods
Falls Lake Nutrient Response Model (Falls Lake Technical Advisory Committee 2009, Lin and Li 2011)	EFDC model of hydrodynamics and water quality	Consistency with local/regional data inputs and results
High Rock Lake Hydrodynamic and Nutrient Response Models (Tetra Tech 2016)	EFDC model of hydrodynamics and water quality	Consistency with local/regional data inputs and results
Jordan Lake Nutrient Response Model (Tetra Tech 2002, Tetra Tech 2003)	EFDC model of hydrodynamics and water quality	Consistency with local/regional data inputs and results
Puget Sound Dissolved Oxygen Modeling Study: Development of an Intermediate Scale Water Quality Model (Khangaonkar, Long et al. 2012)	FVCOM/ E-QUAL-ICM model of hydrodynamics and water quality	Water balance calibration and water quality model parameter selection, calibration
Total Maximum Daily Load Evaluation for Lake Lanier in the Chattahoochee River Basin for Chlorophyll a (Georgia Department of Natural Resources-Environmental Protection Division 2017)	EFDC model of hydrodynamics and water quality	Water balance calibration, water quality model parameters, sediment diagenesis model setup

2.2 Description of Jordan Lake Basin

Jordan Lake is a physically unique lake with distinct characteristics. Some unique features include the sharp variations in depths across the lake area, a deep and narrow section along the Haw River Arm, and a shallow and broad section along the New Hope Arm. The Haw River contributes the most flow into the lake, accounting for about 70 to 90 percent of the total annual flow (NC DWQ 2007). At normal operating conditions (216 feet MSL), Jordan Lake has an area of 13,940 acres. Another significant characteristic is the existence of a large area that alternates between wet and dry conditions depending on the water level in the lake (Tetra Tech 2002). As water level increases due to high inflows and precipitation, there is a significant increase in the wet area of the lake in comparison to the normal pool level. Additionally, the influence of causeways and natural constrictions restrict flow between sections of the lake. The influence of constrictions and causeways across the lake caused by the Mount Carmel Church Road, U.S. 64 Highway, NC 751 Road and Farrington Road are included in this project using EFDC's masking feature that simulates thin flow barriers between adjoining model cells (Tetra Tech 2007, Craig 2018).

2.3 Previous Modeling of Jordan Lake

The previous modeling study performed by Tetra Tech (2002 (Tetra Tech 2002)) concluded that algal growth in Jordan Lake is boosted by high levels of nitrogen and phosphorus input and recycling (Tetra Tech 2002). Tetra Tech studied Jordan Lake's response to nutrient loadings with a linked system combining a hydrodynamic model generated by using Environmental Fluid Dynamics Code (EFDC) which served as input to a water quality model generated by the Water Quality Analysis Simulation Program (WASP) (Hamrick 1992, Ambrose, Wool et al. 1993). The model was calibrated and validated to observed data between the time periods 1992-2001 (Tetra Tech 2003).

2.4 Model Grid and Bathymetry

The first step in the model setup is the definition of the model grid. The grid should provide a good approximation of the actual physical dimensions (morphometry) of the water body. EFDC is set up to use a curvilinear-orthogonal grid in the horizontal plane that is stretched to provide an approximate representation of the curvature of the actual water body. Vertical structure is represented by specifying a fixed or varying number of vertical subdivisions for each horizontal grid cell. CVLGrid, which is a grid generating preprocessor program alongside EFDC Explorer modeling package and Google Earth are used to construct the horizontal model grid. Bathymetric data obtained from sonar sampling in the lake by Collaboratory partners and LIDAR data obtained from North Carolina Flood Risk Information System (FRIS) were used to update the bottom elevation in the grid cells (Figure 3). Horizontal projection for the XY data used to define shoreline and grid coordinates is UTM Zone 17 as meters. The Jordan Lake model grid contains 407 horizontal grid cells, with cell sizes varying from 178 m to 1105 m. Depth of the water column was represented with vertical layers using the SGZ vertical layering option, with the model grid having seven minimum active vertical layers and 25 maximum vertical layers to account for the effects of seasonal stratification. The SGZ (also known as a z-grid) vertical

layering option was developed by DSI to deal with pressure gradient errors that occur in models that have steep changes in bed elevation (Craig 2018). The developed model grid was validated using the Volume Elevation relationship reported by US Army Corps of Engineers.

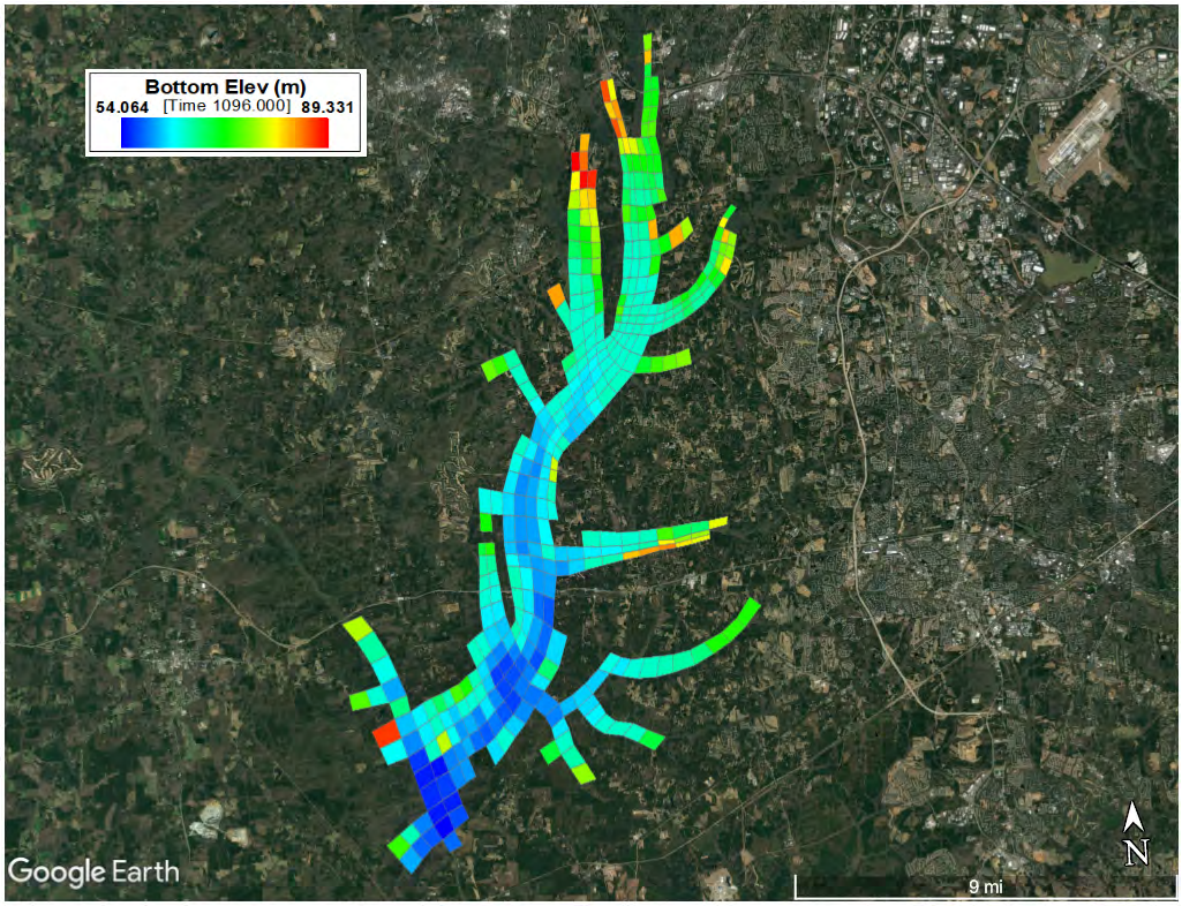

Figure 3. Color contours of bottom elevations (m) for the 407 cells in the Jordan Lake model grid.

The lateral cell grid and bathymetric data represent the geometry of Jordan Lake previously reported by (USACE 2019) by the Volume Elevation and Area Elevation curves (Figures 4 and 5). Additional spatial data was obtained from North Carolina Flood Risk Information System (FRIS) and was combined with the bathymetry data to update grid portions beyond the lake's shoreline at normal pool elevation to better match the USACE data (Figures 4 and 5).

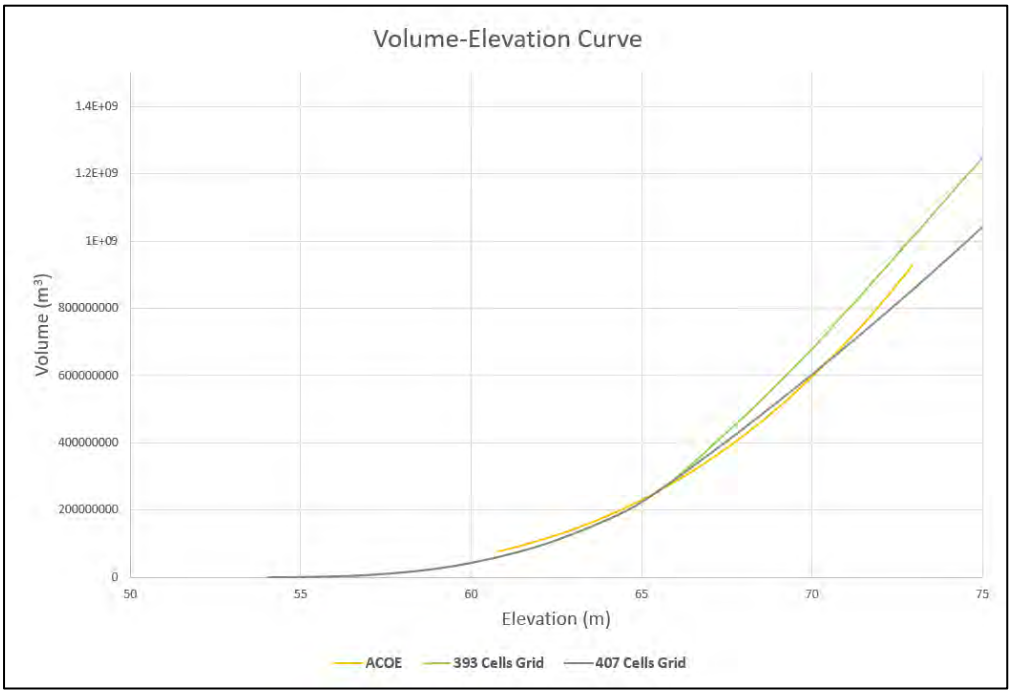

Figure 4. Jordan Lake volume-elevation curve.

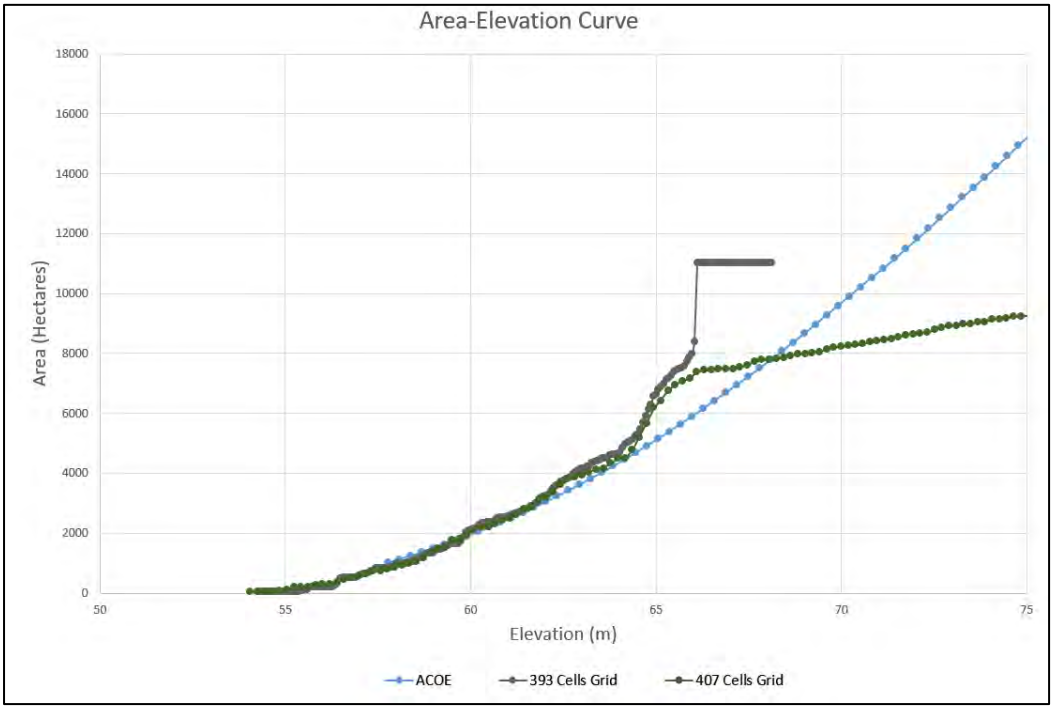

Figure 5. Jordan Lake area-elevation curve

The influence of causeway/bridge constrictions on inter-segment flow are also included in the model through use of the MASK option in EFDC. This option inserts a thin (no-flow) barrier between adjacent cells (Craig 2018) and was used to represent the constrictions and causeways at the Mount Carmel Church Road, U.S. 64 Highway, NC 751 Road and Farrington Road (Figure 6). The final Jordan Lake model grid contains 407 horizontal grid cells with 7 minimum active vertical layers and 25 maximum vertical layers using the sigma-zed (SGZ) vertical layering option.

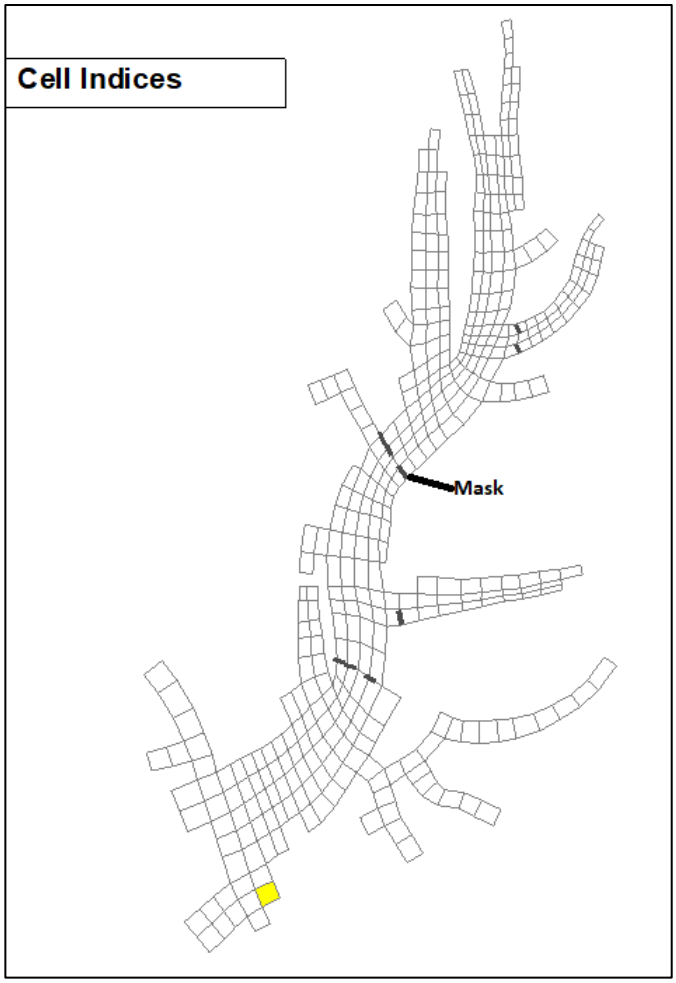

Figure 6. Mask location on Jordan Lake 407 cell model grid.

Another characteristic of Jordan Lake is the presence of areas that wet or dry depending upon the water level in the lake. The model utilizes the wetting/drying option with the wet depth specified as 0.1 meters and dry depth as 0.06 meters. Model cells that contain water at normal pool are shown in blue in Figure 7, while cells that are dry at normal pool are shown in grey.

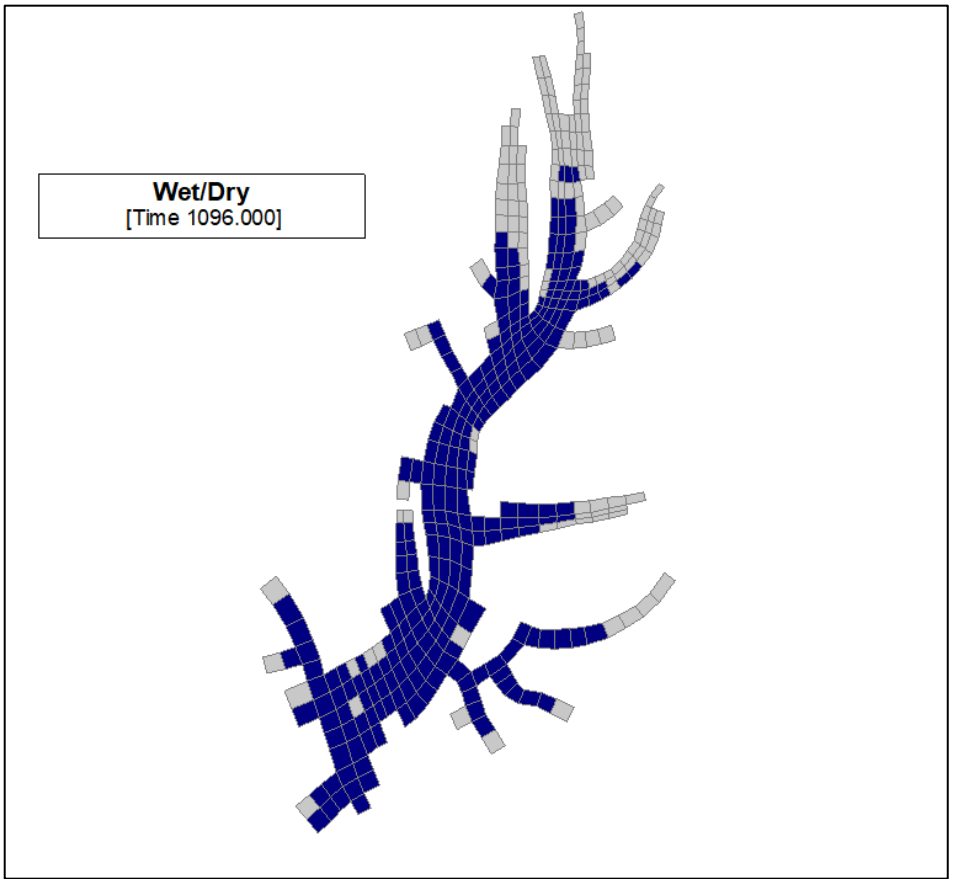

Figure 7. Jordan Lake wet and dry model cells.

2.5 Monitoring Data Used for Model Setup and Calibration

2.5.1 Data Sources

Model input data sets and observed data sets used for calibration and validation, and model scenario testing were developed using observed data gathered from various agencies (Table 3). Time series data including flow rates, flow temperature and pollutant loading from the drainage areas, withdrawals from water supply intakes and releases at the dam, meteorological and wind forcing data, and atmospheric and benthic deposition of nutrients were obtained for the model period 2014 to 2018. Flow input data were obtained from US Geological Survey (USGS) gages and US Army Corps of Engineers, meteorological and wind forcing data were obtained from North Carolina State Climate Office (NCSCO) and National Oceanic and Atmospheric Administration (NOAA). Atmospheric deposition of nutrients were obtained from National Atmospheric Deposition Program (NADP) and Clean Air Status and Trends Network (CASTNET) for nitrogen with phosphorus estimated from annual average N/P ratios for atmospheric deposition of N and P (Willey and Kiefer 1993). Benthic deposition of nutrients for the flux specified simulations were obtained using limited sampling data from Collaboratory partners and model results for sediment fluxes from other lake models that included sediment diagenesis (Dynamic Solutions 2013, Abdelrhman 2015, Michael Baker 2015). Water

temperature time series were derived from measured water temperatures at NCDEQ water quality stations. Time histories of nutrient loading were derived with a WRTDS watershed model (Hirsch and De Cicco 2015) model developed for the Jordan Lake watershed (Del Giudice, Aupperle et al. 2019).

Table 3. EFDC Input Files and Data Sources.

EFDC Input Filename	Description of Data Contained in File	Data Sources
QSER.INP	Flow time series data at flow specified model boundaries and point source locations	US Geological Survey (Haw River, creeks), US Army Corps of Engineers (water treatment plant, dam outflows)
ASER.INP	Meteorological time series data (air temp, dewpoint temp, relative humidity, short-wave solar radiation, precipitation, cloud cover)	North Carolina State Climate Office (NCSCO) and National Oceanic and Atmospheric Administration (NOAA)
TSER.INP	Temperature time series data at all model boundaries and point source inputs	North Carolina Department of Environmental Quality (NC DEQ) and US Geological Survey
WSER.INP	Wind time series data for magnitude and direction	North Carolina State Climate Office (NCSCO) and National Oceanic and Atmospheric Administration (NOAA)
DXDY.INP	Horizontal cell lengths, widths, depths, bottom roughness	Collaboratory Partners (Bathymetry), North Carolina Flood Risk Information System (FRIS) and US Army Corps of Engineers (Lake elevation at the start of each model phase)
LXLY.INP	Horizontal cell size location, orientation relative to E-W, N-S direction	Google Earth (UTM Zone 17) and CVLGrid (Craig 2018)
WQBENMAP.INP, BENFLUX.INP	Map of benthic nutrient and DO flux zones, specification of NO3, NH4, PO4, and DO flux time histories by zone (flux specified runs only)	Calibrated values w/ information from Collaboratory Partners (NO3 and DO benthic flux measurements), and recent lake model studies (Table 2)
TEMP.INP	Initial condition for temperature for every model cell and layer	created with a model spinup run, using the EFDC restart option
CWQSRXX.INP (XX indicates constit. number)	Time series concentration boundary condition at flow specified boundaries	Collaboratory partners (TN and TP loading), DWR data on N speciation, MATLAB script used to create files as described in Cape Fear Model Report (Bowen, Negusse et al. 2009)

An extensive water quality monitoring dataset was available to support the model. Water quality data is available at eighteen stations (Table 4) across the lake. The data was collected by the NC

Division of Water Resources and made available to this study as a Microsoft Access database. Water quality parameters from the database that were used for this study included temperature profiles, and grab samples analyzed for nitrate, ammonia, total phosphorus, Kjeldahl nitrogen, chlorophyll a, and dissolved oxygen. Stations were present in all regions of the lake (Figure 8).

Table 4. Monitoring Stations Used to Calibrate the Jordan Lake Model.

No.	Description	Station	Latitude in degrees	Longitude in degrees
1	Jordan Lake Dam	Dam	35.6548	-79.0672
2	Jordan Lake above Stinking Creek Near Pittsboro, NC	CPF055C	35.6913	-79.0791
3	Jordan Lake in Haw River Bay Arm Upstream	CPF055C1	35.6988	-79.0820
4	Jordan Lake in Haw River Bay Arm NE	CPF055C2	35.6955	-79.0761
5	Jordan Lake in Haw River Bay Arm NW	CPF055C3	35.6932	-79.0830
6	Jordan Lake in Haw River Bay Arm SE	CPF055C4	35.6899	-79.0756
7	Jordan Lake in Haw River Bay Arm SW	CPF055C5	35.6867	-79.0841
8	Jordan Lake in Haw River Arm Bay Downstream	CPF055C6	35.6822	-79.0780
9	Jordan Lake in Middle of Haw River Arm	CPF055D	35.6725	-79.0772
10	Jordan Lake above Dam Near Moncure, NC	CPF055E	35.6600	-79.0700
11	Jordan Lake Downstream Crooked Creek, New Hope Arm	CPF081A1B	35.8365	-78.9763
12	Jordan Lake @ Mouth of New Hope Creek	CPF081A1C	35.8162	-78.9868
13	Jordan Lake @ Mouth of Morgan Creek Near Farrington	CPF086C	35.8215	-78.9974
14	Jordan Lake In Upstream	CPF086CUPS	35.8382	-79.0014
15	Jordan Lake, Downstream Morgan, New Hope Creek Arm	CPF086D	35.8095	-78.9974
16	Jordan Lake Near Farrington, NC	CPF086F	35.7970	-79.0108
17	Jordan Lake at Buoy #9 Near Merry Oaks, NC	CPF087B3	35.7652	-79.0260
18	Jordan Lake @ Mouth White Oak Creek Near Seaforth, NC	CPF087D	35.7386	-79.0242
19	Jordan Lake Near Mouth Beaver Creek Near Merry Oaks, NC	CPF0880A	35.6965	-79.0436

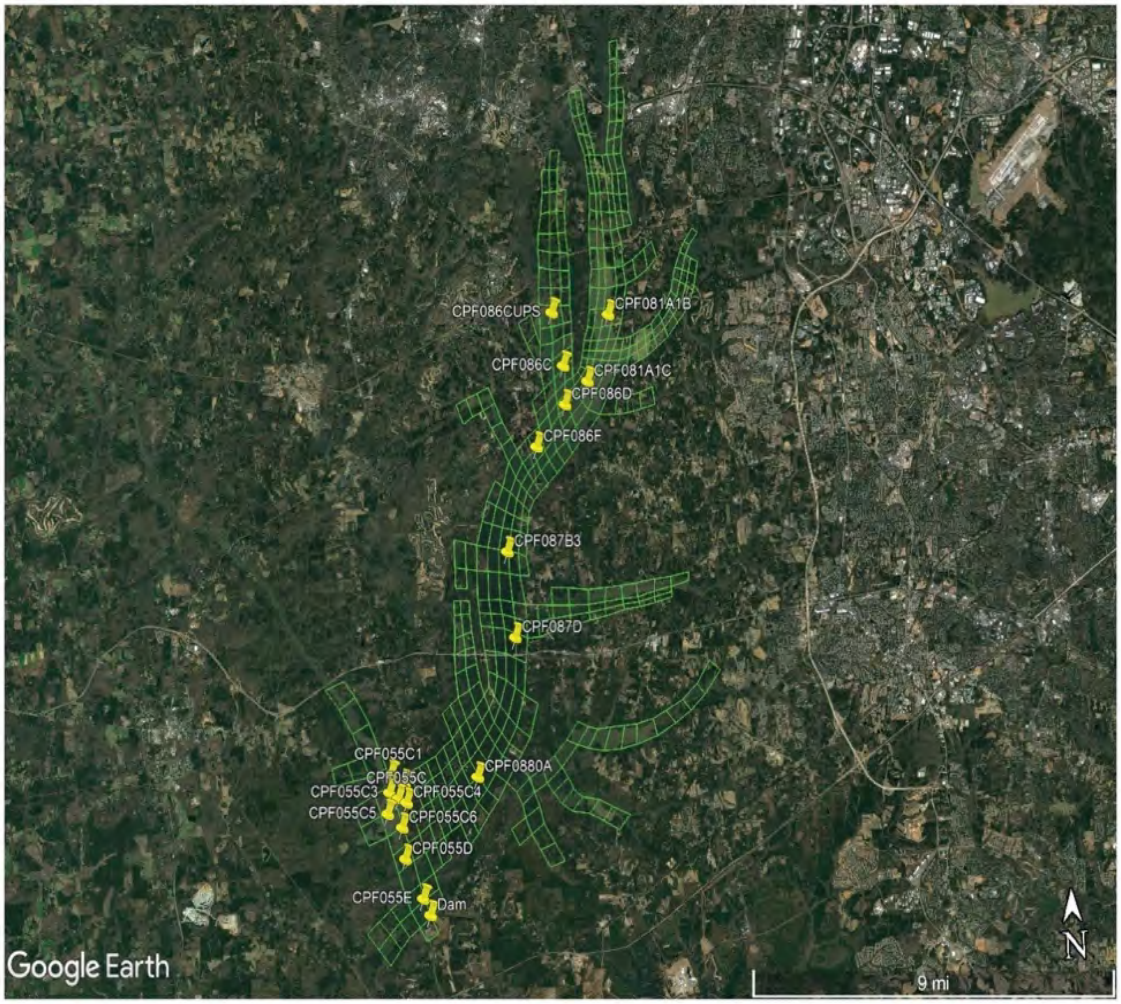

Figure 8. Locations of 18 Jordan Lake Monitoring Stations Sampled by the NC Division of Water Resources. The newly developed 407 cell EFDC model grid is also shown.

2.5.2 Data for Nutrient Response, Flow, and Temperature Models

In the Jordan Lake nutrient response model, chlorophyll a data are used as a measure of the cumulative abundance of the three state variables (cyanobacteria, diatoms, and green algae) collectively representing the phytoplankton biomass. The spatial and temporal dynamics in the data are used to calibrate the algal growth kinetic parameters in the model. North Carolina also uses chlorophyll a as a numeric water quality criteria (NC Division of Water Resources 2017). The current approved regulatory text for the State's chlorophyll a criteria, located at 15A NCAC 02B .0211(4), states:

Chlorophyll-a (corrected): not greater than 40 ug/l for lakes, reservoirs, and other waters subject to growths of macroscopic or microscopic vegetation not designated as trout waters, and not greater than 15 ug/l for lakes, reservoirs, and other waters subject to growths of macroscopic or microscopic vegetation designated as trout waters (not applicable to lakes or reservoirs less than 10 acres in surface area).

A waterbody is considered impaired if there is a 90% confidence that more than 10% of the photic zone average chlorophyll measurements area above the regulatory limit, in this case 40 ug/L (NCDWR 2018).

Based upon a review of the chlorophyll a monitoring data collected over the five-year (2014-2018) model time period, every one of the eighteen monitoring stations exceeded the 40 ug/L more than 10% of the time (Table 5). The 90th percentile (the value exceeded exactly 10% of

Table 5. Analysis of 2014 – 2018 Photic Zone Chl a Measurements at selected stations within four regions of Jordan Lake.

Lake Region	Station	Number of Chl a samples	Chl a median concentration (µg/L)	90th percentile Chla a concentration (µg/L)	Reduction needed for 90th percentile Chl a concentration at 40 µg/L
Haw River	CPF055C	74	29.0	63.7	37%
	CPF055D	72	25.0	44.9	11%
	CPF055E	73	28.0	44.0	9%
Above Causeways	CPF081A1C	74	57.5	90.4	56%
	CPF086C	74	58.5	89.0	55%
	CPF086F	74	52.5	81.7	51%
Between Causeways	CPF087B3	74	34.0	52.4	24%
	CPF087D	74	29.5	53.0	25%
Below Causeways	CPF0880A	74	28.0	42.0	5%
Jordan Lake	All 18 Stations	1004	36.0	72.0	44%

the time) photic chlorophyll a concentration for all eighteen stations considered collectively (1004 measurements total) for the 2014-2018 time period was 72.0 ug/L (Table 5). A reduction of 44% would be needed to lower the 90th percentile chlorophyll a concentration to the regulatory limit of 40 ug/L.

Frequently sampled stations in each of the four regions of the lake also had 90th percentile chlorophyll a concentrations above the criteria value, but the magnitude of the exceedances varied significantly from region to region. The one station in the below causeways region of the New Hope Creek arm of the lake exceeded the 90th percentile by only 5% (74 samples total). In the above causeways region of the New Hope Creek arm of the lake, all three stations exceeded the 40 ug/L by more than 50% (Table 5). The other two regions of the lake (Haw River, between

causeways had exceedance levels between these two extremes. Model calibration was divided into two phases: hydrodynamic and water-quality calibration. In both cases, model predictions were compared to observed data collected at 18 NC DWR monitoring stations (see Table 4 for list of stations, Figure 8 for a map of stations).

Observations of water surface elevations were available at the dam and were compared to model predictions over each model time period. These observed data were collected by the Army Corps of Engineers, who also provided outflow data at the dam and the Cary Water Treatment Plant.

Inflows from eight ungaged watersheds were estimated by prorating the daily unbalanced outflow (i.e., the difference between dam outflow and sum of gaged inflows) based on their respective drainage areas.

Regressions between measured air temperatures and stream water temperatures were developed to estimate ungaged water temperatures at water quality stations. Maximum and minimum daily air temperatures for the weather station at Chapel Hill (USC00311677 CHAPEL HILL 2 W, NC US) from 2008 to 2018 inclusive were retrieved. Measured air temperatures were processed by (a) replacing maximum and minimum air temperatures less than 32 deg F with 32.5 deg F, (b) averaging these maximum and minimum values for each day, and finally (c) calculating an average value for each day as the average of the current day and the two previous days. These final averages were regressed against the measured water temperatures at each water quality station, where approximately 220 daily water temperature measurements over the period 2008 to 2016 are available. The regression equations are 2nd order polynomials with non-zero y intercepts. The three regression constants a, b, and c (corresponding to the equation: $y = ax^2 + bx + c$ where x = air temperature and y = water temperature) were used to estimate water temperatures for the simulation period (2014-2018) based on corresponding measured air temperatures. Temperature profile data from the eighteen DWR monitoring stations were compared to corresponding model predictions for each model time period.

2.5.3 Nutrient Loading Analysis

A nutrient loading analysis based on the model's input files was used to quantify the relative nutrient load contributions from the external and internal sources of pollutants to the lake for the model period 2014 - 2018. The external sources include the surface water inputs, and wet and dry atmospheric deposition, while the internal sources include the benthic fluxes of inorganic nutrients across the sediment-water interface of the lake. A flow analysis was also used to quantify the inflow and outflow contributions to the lake for the model period as rates (m^3/day). The Haw River accounts for over 75% of the inflows while the dam outflow accounts for over 95% of the outflows for the model period (Figures 9 a & b). The nutrient loading analysis indicated that majority of nutrients entered the lake from the Haw River arm, and these nutrients

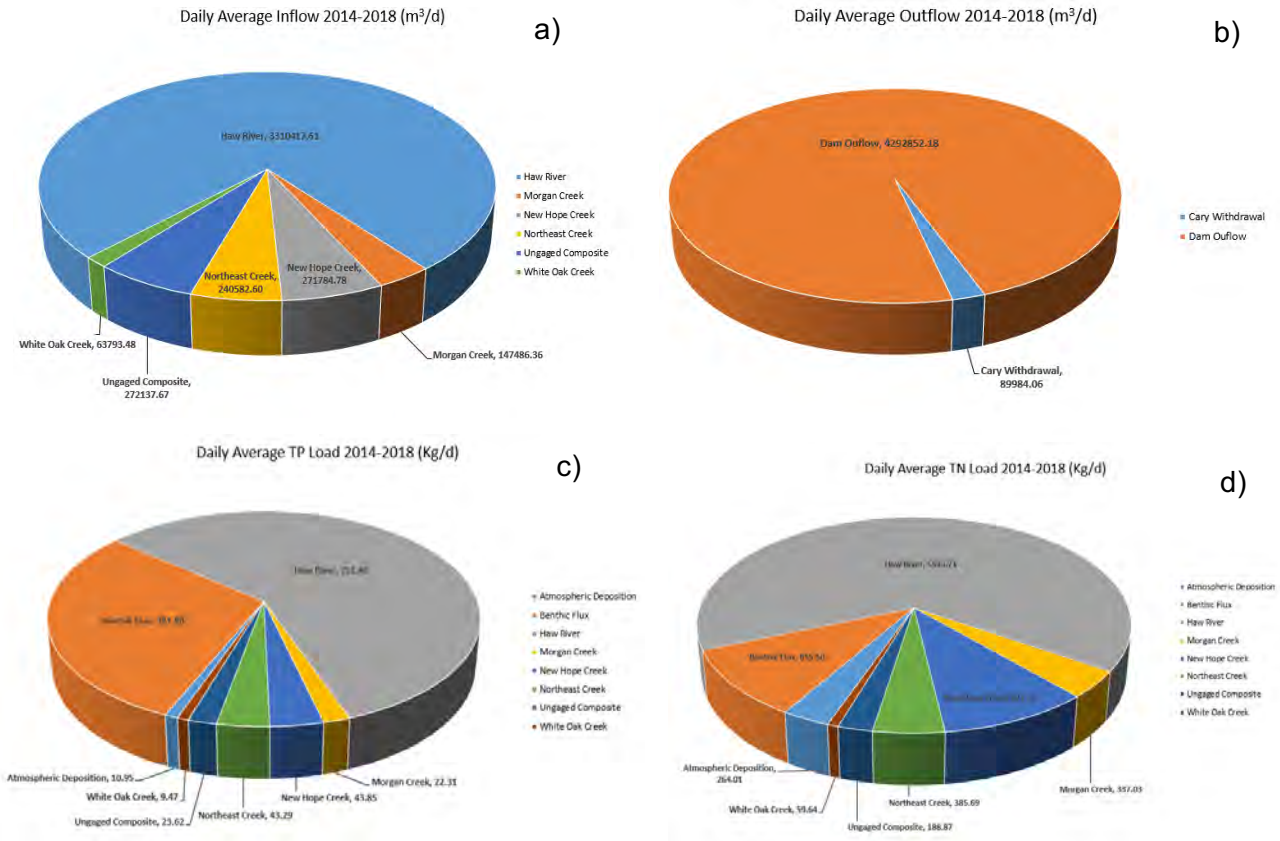

Figure 9. Pie charts showing 2014-2018 daily average inflows (a), daily average outflow (b), daily average total phosphorus (TP) load (c), and daily average total nitrogen (TN) load for Jordan Lake, NC

entered majorly in organic forms that were not immediately bioavailable. The Haw River arm accounted for over 65% of total nitrogen and 55% of total phosphorus loads into the lake (Figures 9 c & d). Benthic sediments were a significant source of bioavailable nutrients, providing more than 40% of phosphate and 85% of ammonia to the lake (Figures 10 a & b).

Benthic sediments also acted as a major sink for the particulate fraction of organic nutrients, nitrate (Figure 10 c & d), and dissolved oxygen. Atmospheric deposition was a relatively minor source of nutrients to the lake, accounting for less than 5% of the total nitrogen. Through dye tracer studies, it was observed that only a small fraction of nutrient inputs from the Haw River arm moved up into the upper reaches of the New Hope Creek arm of the lake on a long-term basis. However, some high flow events did transport Haw River water throughout the lake, but these high flow events did not contribute significantly to the flushing of the New Hope Creek arm or to the nutrient loading in these areas. The majority of nitrate to the New Hope Creek arm of the lake (Figure 10 d) is provided by the local surface water sources (Morgan, New Hope, Northeast, and other smaller creeks). For certain inorganic forms of nitrogen and phosphorus, benthic sediments were the major supply source to the water column in the New Hope arm of the lake, providing more than 75% of the phosphate and 90% of ammonia (Figures 11 a & b).

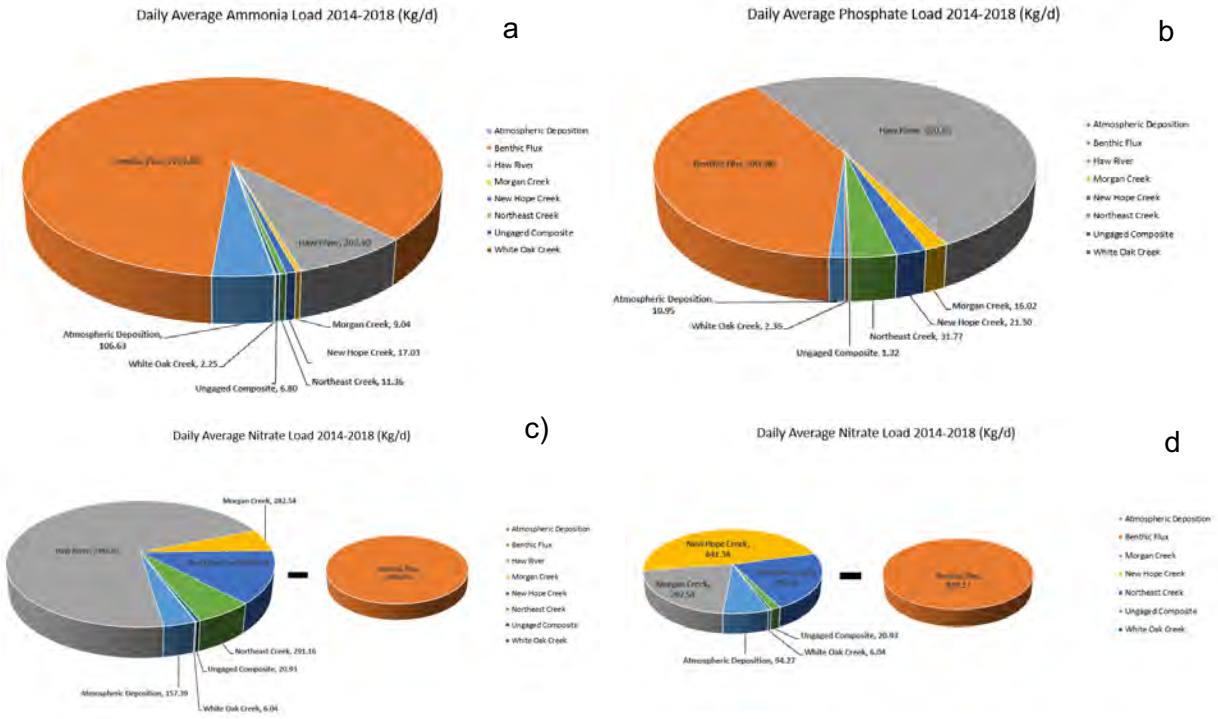

Figure 10. Pie charts showing 2014-2018 daily average ammonia load (a), daily average phosphate load (b), and the daily average nitrate load (c) for Jordan Lake NC. Panel d shows the daily average nitrate load for the New Hope Creek arm of the lake.

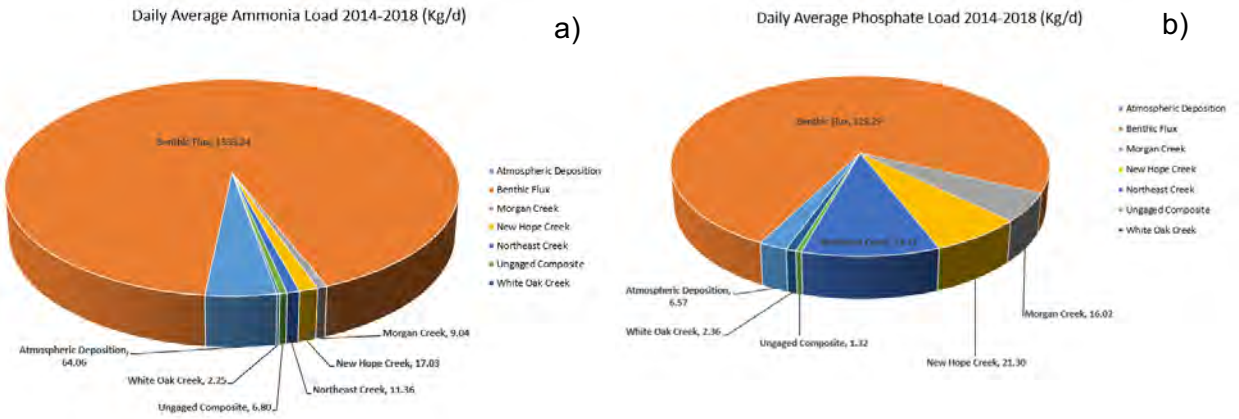

Figure 11. Pie charts showing the 2014-2018 daily average ammonia (a) and phosphate (b) load into the New Hope Creek arm of Jordan Lake, NC.

3. SPECIFICATION OF MODEL INPUT FILES

The EFDC lake model requires the specification of external boundary data to execute the hydrodynamic and water quality simulations. Time series data including flow, water temperature, and pollutant loading from the drainage areas, withdrawals from water supply intakes and releases at the dam, meteorological and wind forcing data, and atmospheric and benthic deposition of nutrients were assembled for the model period 2014 to 2018.

EFDC simulations for the model time period 2014 to 2018 are implemented in 3 phases: 2014-2015, 2016, and 2017-2018. Initial conditions must be specified for lake surface elevation and temperatures. The elevations are set at the start of each year from ACOE project data with the assumption that the lake surface is level, while the bed temperatures are set to vary spatially and in time.

3.1 Riverine Inputs

3.1.1 Flow Specification

Flows to and from the lake are provided in the QSER.INP file. Fifteen inputs and outputs were specified in the Jordan Lake model domain to represent 13 tributaries, one outflow as withdrawal for water supply and the outflow at the dam. Inflow data was obtained from USGS gages for 5 stations, Haw River near Bynum USGS Gage 02096960, Morgan Creek USGS Gage 02097517, New Hope Creek USGS Gage 02097314, Northeast Creek USGS Gage 0209741955 and White Oak Creek USGS Gage 0209782609. This data was adjusted to account for additional drainage area from the gage stations to the inflow mouth into the lake. Outflow data was also obtained for the dam using the Haw River at Moncure USGS Gage 02098206. Additionally, to represent ungaged inflows into the lake, a flow balance was estimated using all gaged inflows, rainfall, all outflows and evaporation. The flow balance was computed to minimize the difference between measured versus modeled lake water levels over time. The resulting ungaged composite flow was distributed to 8 boundary inflow locations to represent the remaining tributary inflow. A summary of all flows is given in Table 6 with the boundary locations in the model grid shown in Figure 12.

Table 6: Specification of External Flow Series

Name	Description	Data Source
QSER1	Haw R. @ Jordan Lake	USGS Gage 02096960, Haw River at Bynum
QSER2	Morgan Ck. @ Jordan L.	USGS Gage 02097517, Morgan Creek
QSER3	New Hope Ck. @ Jordan L.	USGS Gage 02097314, New Hope Creek
QSER4	Northeast Ck. @ Jordan L.	USGS Gage 0209741955, Northeast Creek
QSER5	White Oak @ Jordan L.	USGS Gage 0209782609, White Oak Creek
QSER6	Ungaged, Lake Segment 4, west	Ungaged Composite
QSER7	Outflow @ Dam	USGS 02098206, Haw River at Moncure
QSER8	Ungaged, Lake Segment 3, west	Ungaged Composite
QSER9	Ungaged, Lake Segment 3, east	Ungaged Composite
QSER10	Ungaged, Lake Segment 2, west	Ungaged Composite
QSER11	Ungaged, Lake Segment 2, east	Ungaged Composite
QSER12	Ungaged, Lake Segment 1	Ungaged Composite
QSER13	Cary Withdrawal	USACOE Operational Records
QSER14	Ungaged, Lake Segment 4, east	Ungaged Composite
QSER15	Ungaged, Lake Segment 4, north	Ungaged Composite

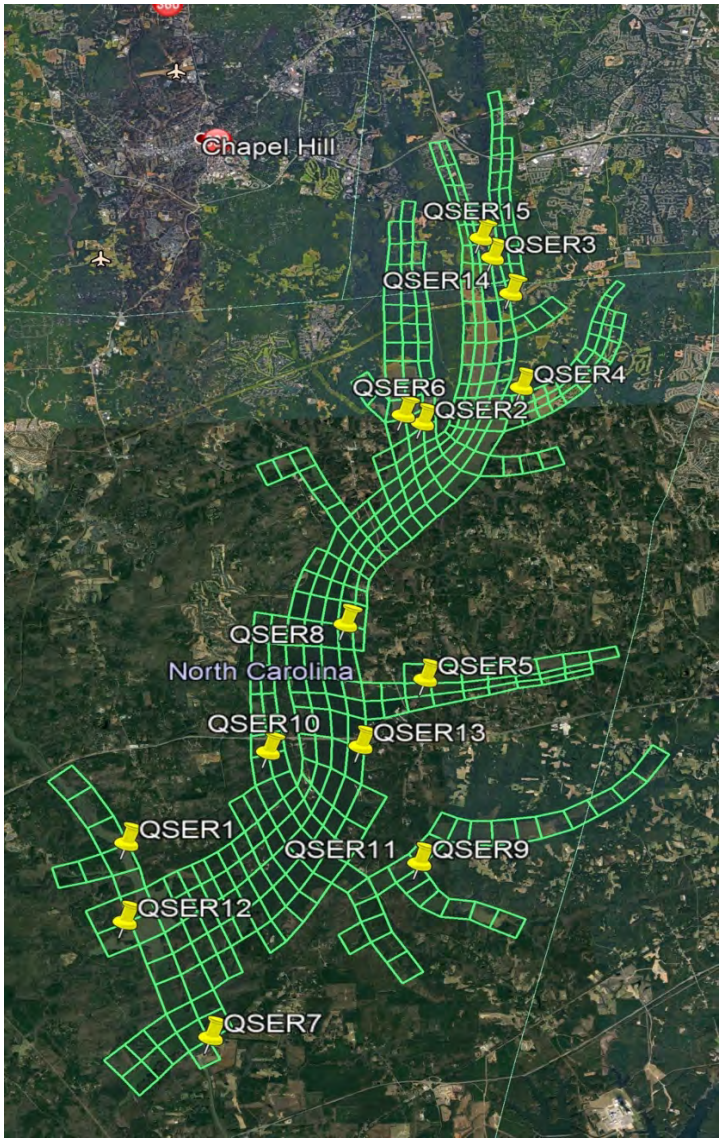

Figure 12. Model flow boundary locations.

3.1.2 Temperature and Concentration Specification

Each tributary inflow contributes heat energy, and thus the temperature balance in the lake is dependent on these inflow temperatures. Water temperature data was obtained from 5 NC WQ stations for 2008-2016, B4050000 Haw River below Jordan Dam near Moncure, B2100000 Haw River near Bynum, B3660000 Northeast Creek near Nelson, B3040000 New Hope Creek near Blands, B3900000 Morgan Creek near Farrington. The regression equations described in Section 2.5.2 were used to estimate water temperatures at water inflow boundaries to the Lake model for the simulation period from 2014 to 2018. The time history for these data are specified in the TSER.INP file.

The water quality lake model requires the definition of water quality loading time series for each of the external flow series entering the lake (Table 6). The lake model consists of time series

concentration input for the parameters listed in Table 7. The water quality model is driven by these parameters consisting of three algal groups, nine organic matter constituents (three each of organic nitrogen, organic phosphorus, and organic carbon), three 3 inorganic nutrients (NOx, NH4, PO4), and dissolved oxygen. Nutrient fractionation estimates for the model were based upon calculated long-term averages of tributary concentrations that were determined on a monthly basis. A transformation matrix approach was used to estimate the concentration time history of each constituent needed by the model (see Appendix 1). Ungaged watershed inputs were estimated based on a proration of data from representative gaged watershed (White Oak Creek). The time history for these data are specified in the CWQSR.INP files.

Table 7: State variables for water quality model

Description	Units
Cyanobacteria	mg/L
Diatoms	mg/L
Green Algae	mg/L
Refractory POC	mg/L
Labile POC	mg/L
Dis Org Carbon	mg/L
Ref Part Org Phosphorus	mg/L
Lab Part Org Phosphorus	mg/L
Dis Org Phosphorus	mg/L
Total Phosphate	mg/L
Ref Part Org Nitrogen	mg/L
Lab Part Org Nitrogen	mg/L
Dis Org Nitrogen	mg/L
Ammonia Nitrogen	mg/L
Nitrate Nitrogen	mg/L
Dissolved Oxygen	mg/L

3.2 Point Source Outflow

Outflow data was also obtained for the Cary/Apex Water Treatment Plant intake from USACE website for Lake Jordan (https://epec.saw.usace.army.mil/jord.htm).

3.3 Benthic Inputs

Nutrient fluxes to and from the underlying sediment in a water body influence the nutrient levels in the water column. Benthic exchange sampling data at six lake locations, above the causeways, between the causeways, below the causeways and along Haw River arm by Collaboratory partners are used in driving the sediment model. The EFDC water quality model provides three

options for defining the sediment-water interface fluxes for nutrients and dissolved oxygen. The options are: (1) externally forced spatially and temporally constant fluxes; (2) externally forced spatially and temporally variable fluxes; and (3) internally coupled fluxes simulated with the sediment diagenesis model. The water quality state variables that are controlled by diffusive exchange across the sediment-water interface include phosphate, ammonia, nitrate, silica, chemical oxygen demand and dissolved oxygen. Option 3 provides the cause-effect predictive capability to evaluate how water quality conditions might change with the implementation of alternative load reduction or management scenarios. However, Option 2 was selected for the Jordan Lake model as Option 3 required a calibrated water column model of 5 years simulation time with sediment nutrient fluxes included. Numerous model iterations at very short time steps would be necessary to achieve calibration. Therefore, a water column organic matter calibration based on an Option 2 sediment diagenesis model was selected as it provided for rapid, reliable results that are consistent with calibration targets in the water column. A review of model results for sediment fluxes from other EFDC models that included sediment diagenesis combined with the limited benthic exchange data obtained from Collaboratory partners were used as a guide to estimate time series for spatially and temporally variable fluxes in the Jordan Lake model. Sediment flux spatial variability has been attributed to characteristics of the water quality zones (i.e., lacustrine, riverine, or transition) and sediment particle size distribution (sand, silt, clay). Temporal variability is mainly attributed to seasonal temperature trends. All flux time series (for NO3, NH4, PO4, and SOD) exhibit an annual maximum near mid-summer for the reports cited. The time history for these data are specified in the BENFLUX.INP file.

3.4 Meteorological Inputs

The lake model requires information on meteorological conditions in the modeled region. The time history for these data are specified in the ASER.INP and WSER.INP files. The required data includes atmospheric pressure, air temperature, relative humidity, precipitation, evaporation rate, solar radiation, cloud cover, wind speed, and wind direction. The data utilized for the model are obtained from the Raleigh Durham (RDU) International Airport Station (WBAN 13722) through North Carolina State Climate Office (NCSCO) and National Oceanic and Atmospheric Administration (NOAA) for the model period 2014 to 2018.

- Daily precipitation data obtained from RDU are assigned as a rate in inches per hour for the model time period. The EFDC model has an option to include a conversion factor to handle various rainfall units.
- Dry bulb temperature and wet bulb temperatures are obtained from RDU in degree Fahrenheit and converted to degree Celsius for the model period.
- Atmospheric pressure data were obtained from NOAA for RDU in inches of mercury and converted to millibars for the model period.
- Wind speed in miles per hour (mph) and wind direction in degrees were obtained from NCSCO for RDU. Wind speed was converted to meters per second (m/s) and wind direction was utilized in degrees but converted in the direction the wind is blowing from and applied the lake model.

- Cloud cover values are calculated from sky condition codes and NOAA sky cover rating (from 0-8) obtained for RDU weather station. Sky condition codes and NOAA sky cover ratings were converted to a W2 cloud cover (from 0-10), with zero indicating clear skies and ten indicating cloudy skies (Table 8) for the model period. This method has been utilized in previous water quality models to estimate cloud cover (Bowen and Harrigan 2017).
- Solar Radiation is calculated from cloud cover data using the method from CE-QUAL-W2, version 3 (Cole and Wells 2006) adapted into a MATLAB Code. The values are obtained in watts per meter square (Watts/m^2) and applied to the model domain.
- Evaporation was calculated by the program. EFDC Explorer contains options for calculating evaporation via different methods. The option to compute evaporation utilizing the EFDC original method was selected for this model.
- Atmospheric deposition has been observed to be an important source of inorganic nutrients to a water body (NC DWR, 2016). Atmospheric deposition is represented in the EFDC model with separate source terms for dry deposition and wet deposition. Dry deposition is defined by a constant mass flux rate (as g/m^2day) for constituents that settles as dust during a period of no rainfall. Wet deposition is defined by a constant concentration (as mg/L) of a constituent in rainfall and it utilizes the time series of precipitation assigned in the ASER.INP file for input to the hydrodynamic model. The Jordan Lake model is driven by specification of constant wet and dry atmospheric deposition of ammonia as nitrogen, and nitrate as nitrogen obtained through 2018 from the National Atmospheric Deposition Program (NADP) National Trends Network (NTN) from Finley Farm station NC41, and Clean Air Status and Trends Network (CASTNET) Site ID RTP 101 located in Research Triangle Park, Durham, NC. Since phosphorus deposition data was unavailable for the CASNET and NADP sites, dry and wet deposition of Phosphate was estimated by CASTNET and NADP data for nitrogen with annual average N/P ratios for atmospheric deposition of N and P from Willey and Kiefer (1993).

Table 8. Sky condition observations and corresponding W2 cloud cover input.

Condition	CODE	NOAA Sky Cover (out of 8)	W2 Cloud Cover (out of 10)
Clear Sky	CLR	0	0
Few Clouds	FEW	1 — 2	1.25
Scattered Clouds	SCT	3 — 4	4.38
Broken	BKN	5 — 7	7.5
Variable	VV	8	10
Overcast	OVC	8	10

4. CALIBRATION

Model calibration was undertaken in two phases: hydrodynamic and water-quality calibration. In both cases, the lake's model parameters are varied in order to produce the best agreement between model predictions and observed data collected at 18 NC DWR monitoring stations and stage observations by USACE at the dam. These stations are described in Table 9, with their locations in the model grid shown in Figure 13. This section describes the steps taken for the hydrodynamic calibration of Jordan Lake. For the hydrodynamic model, predictions from the model are calibrated to observations for water level and water temperature for both bottom and surface layers. Water quality calibration will focus on chlorophyll-a, nutrients, and dissolved oxygen. Calibration was accomplished first using only the hydrodynamic model, comparing model predicted water surface elevations and temperatures to corresponding values from the monitoring stations. Once the hydrodynamic model is calibrated, water quality calibration can be conducted. The major goal of calibration for this model was to minimize mean error between observations and predictions while achieving the highest coefficient of determination (i.e. R^2).

Table 9: Monitoring stations for model calibration.

No.	Description	Station	Lat.	Long.
1	Jordan Lake Dam	Dam	35.6548	-79.0672
2	Jordan Lake above Stinking Creek Near Pittsboro, NC	CPF055C	35.6913	-79.0791
3	Jordan Lake in Haw River Bay Arm Upstream	CPF055C1	35.6988	-79.0820
4	Jordan Lake in Haw River Bay Arm NE	CPF055C2	35.6955	-79.0761
5	Jordan Lake in Haw River Bay Arm NW	CPF055C3	35.6932	-79.0830
6	Jordan Lake in Haw River Bay Arm SE	CPF055C4	35.6899	-79.0756
7	Jordan Lake in Haw River Bay Arm SW	CPF055C5	35.6867	-79.0841
8	Jordan Lake in Haw River Arm Bay Downstream	CPF055C6	35.6822	-79.0780
9	Jordan Lake in Middle of Haw River Arm	CPF055D	35.6725	-79.0772
10	Jordan Lake above Dam Near Moncure, NC	CPF055E	35.6600	-79.0700
11	Jordan Lake Downstream Crooked Creek, New Hope Arm	CPF081A1B	35.8365	-78.9763
12	Jordan Lake @ Mouth of New Hope Creek	CPF081A1C	35.8162	-78.9868
13	Jordan Lake @ Mouth of Morgan Creek Near Farrington	CPF086C	35.8215	-78.9974
14	Jordan Lake In Upstream	CPF086CUPS	35.8382	-79.0014
15	Jordan Lake, Downstream Morgan, New Hope Creek Arm	CPF086D	35.8095	-78.9974
16	Jordan Lake Near Farrington, NC	CPF086F	35.7970	-79.0108
17	Jordan Lake at Buoy #9 Near Merry Oaks, NC	CPF087B3	35.7652	-79.0260
18	Jordan Lake @ Mouth White Oak Creek Nr Seaforth, NC	CPF087D	35.7386	-79.0242
19	Jordan Lake Near Mouth Beaver Creek Nr Merry Oaks, NC	CPF0880A	35.6965	-79.0436

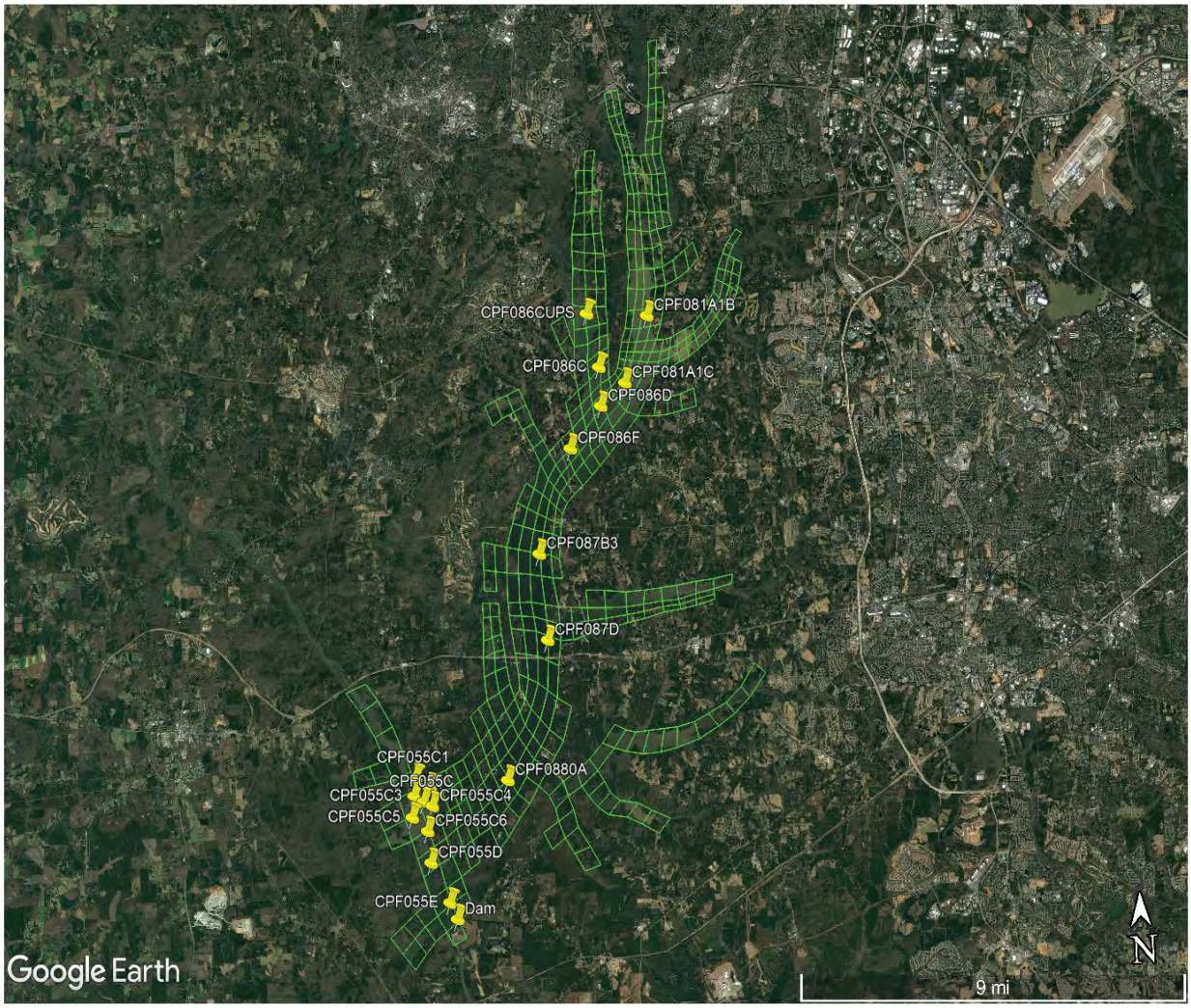

Figure 13. DWR Monitoring Stations

4.1 Description of the Calibration Time Period

The Jordan Lake EFDC model was run over a five-year time period (January 1, 2014 – December 31, 2018). The five-year time period was split into three separate model runs for purposes of model calibration and verification. Two two-year time periods (2014-2015 and 2017-2018) were used for model calibration. A one-year time period (January 1, 2016 – December 31, 2016) was used once the model was calibrated for the purpose of model verification. For each of the model runs, the model was initiated from cold start conditions using specified initial conditions. The initial water surface was determined iteratively to provide an acceptable fit between observed and predicted water surface elevations.

4.2 Hydrodynamic Model Calibration

The processes involved in the hydrodynamic calibration of the lake model are discussed in two parts, water surface elevation calibration, and temperature calibration. For each of these model versus data comparison, both statistical measures of calibration performance are used with additional graphical comparisons of model fit. As explained in the following sections, model calibration was performed by considering a number of these graphical and quantitative several measures of model fit.

4.2.1 Modeled and Observed Water Surface Elevations

Hydrodynamic calibration began by comparing model predictions to observed water surface elevations data by the USACE at the dam. Daily stage data are compared to model predictions for the time period 2014 to 2018. Initial simulation using the 393 cells grid showed that model prediction of elevation was higher than observed data for most of the model time period as shown in a time history comparison (Figure 14) and a scatter plot of observed vs. predicted water surface elevations (Figure 15).

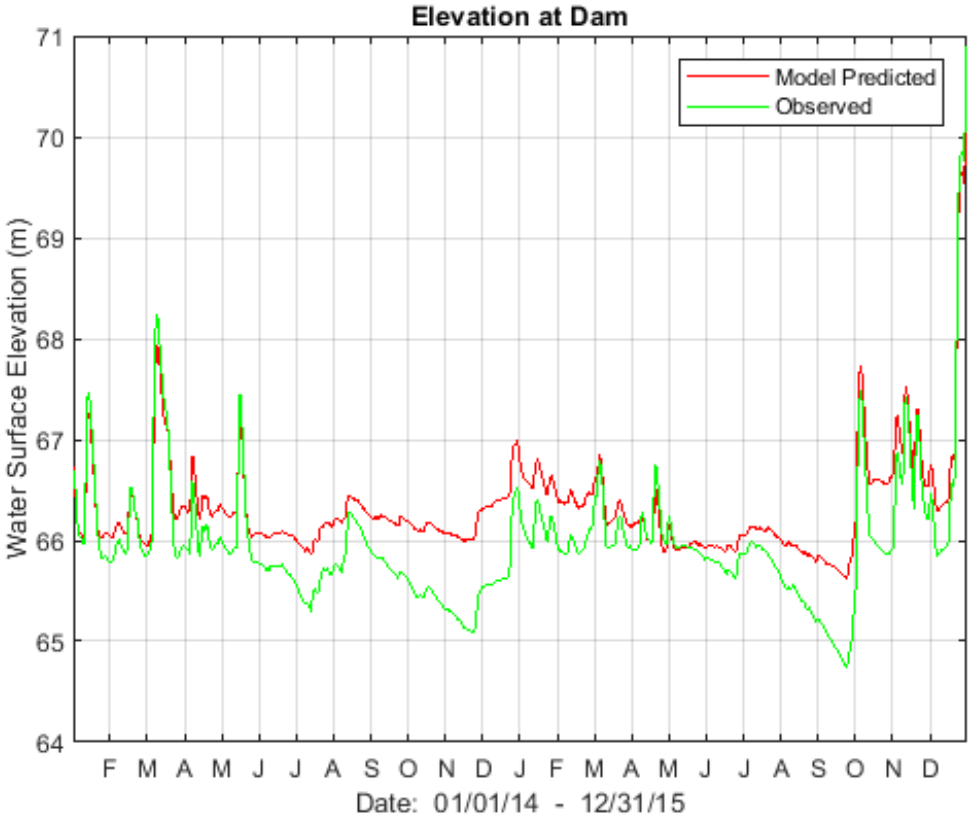

Figure 14. Modeled vs observed water surface elevations using the 393 cell grid model.

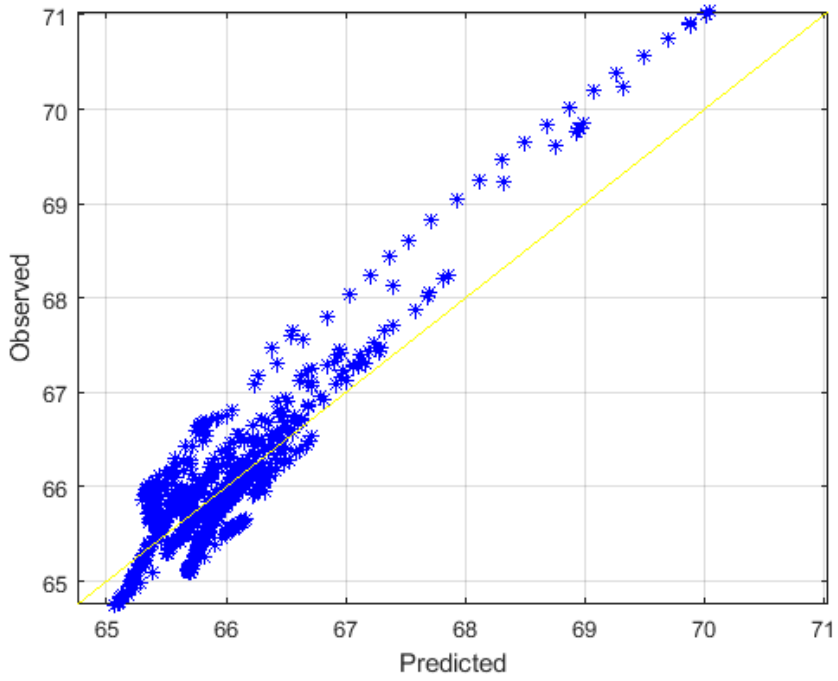

Figure 15. Scatter plot of modeled vs observed water surface elevation (2014-2015).

Factors such as grid adjustment, bathymetric update with LIDAR data, adjustment of ungaged inflows using the flow balance method, and changing the dam outflow from USACE records to USGS gage 02098206 at Moncure were considered to improve the match between modeled and observed water surface elevations with the 407 cells grid (Figures 16 - 20). The final grid provided an acceptable match with the coefficient of determination values (R^2) above 80% for all modeled years. The mean model error was -0.09 m, 0.08m and -0.05 for 2014-2015, 2016, and 2017-2018 models, respectively. The root mean square errors were 0.38, 0.26, and 0.44 meters for 2014-2015, 2016, and 2017-2018 models, respectively. These corresponded to less than 1% of the mean value for all three model phases. Other statistical comparisons of modeled prediction to observed data are shown in Table 10.

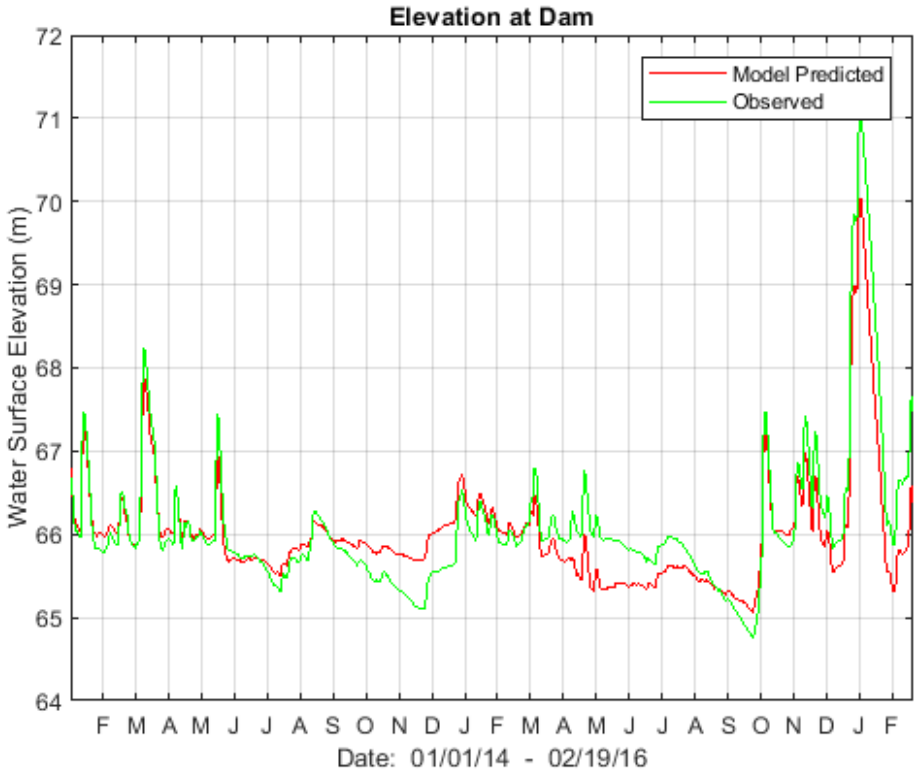

Figure 16. Modeled vs observed water surface elevation (2014-2015).

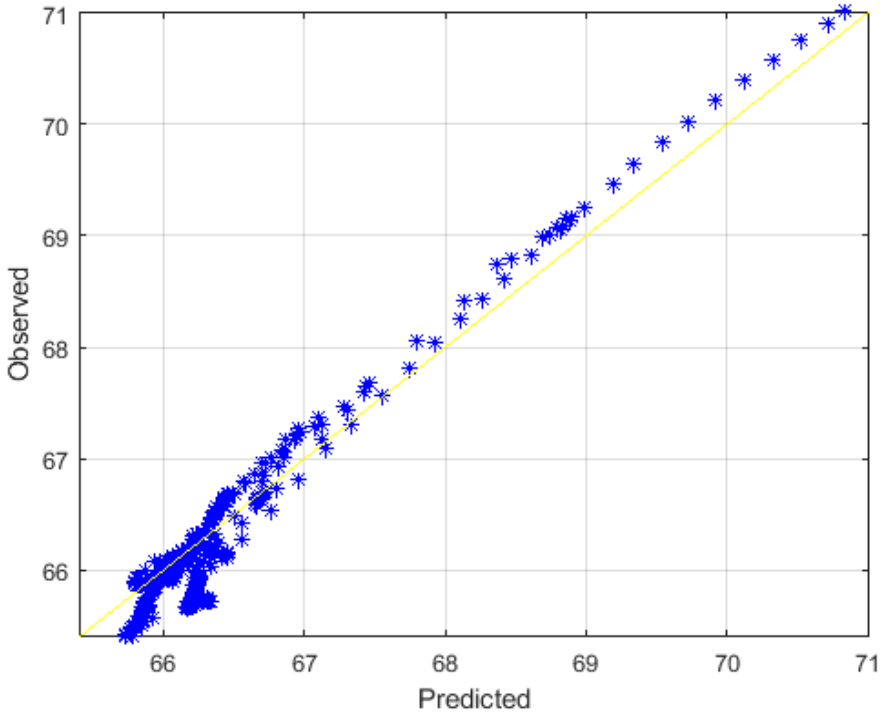

Figure 17. Scatter plot of modeled vs observed water surface elevation (2016).

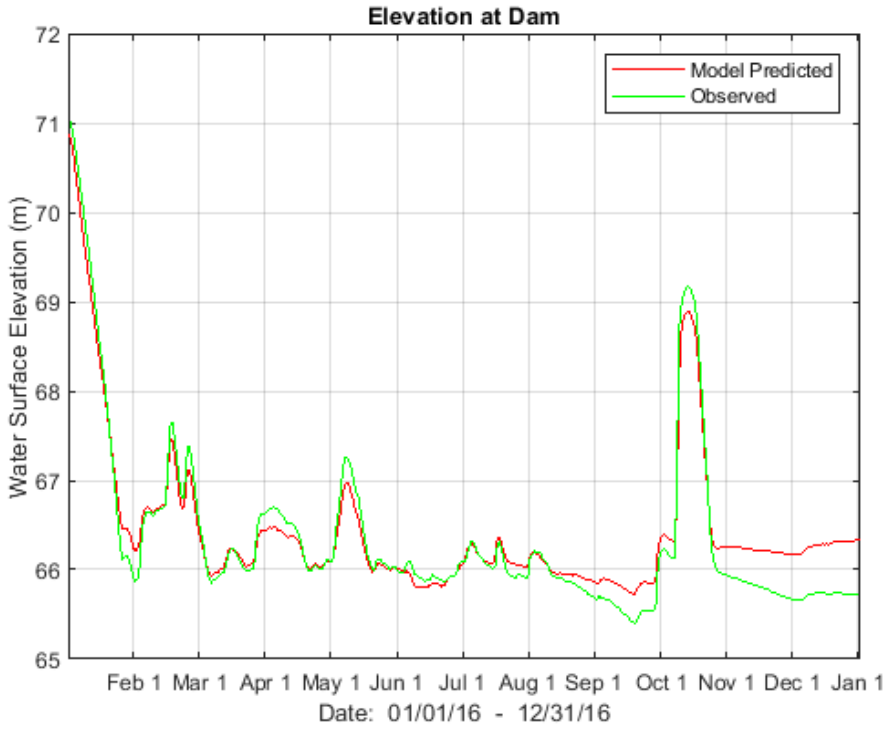

Figure 18. Modeled vs observed water surface elevation (2016).

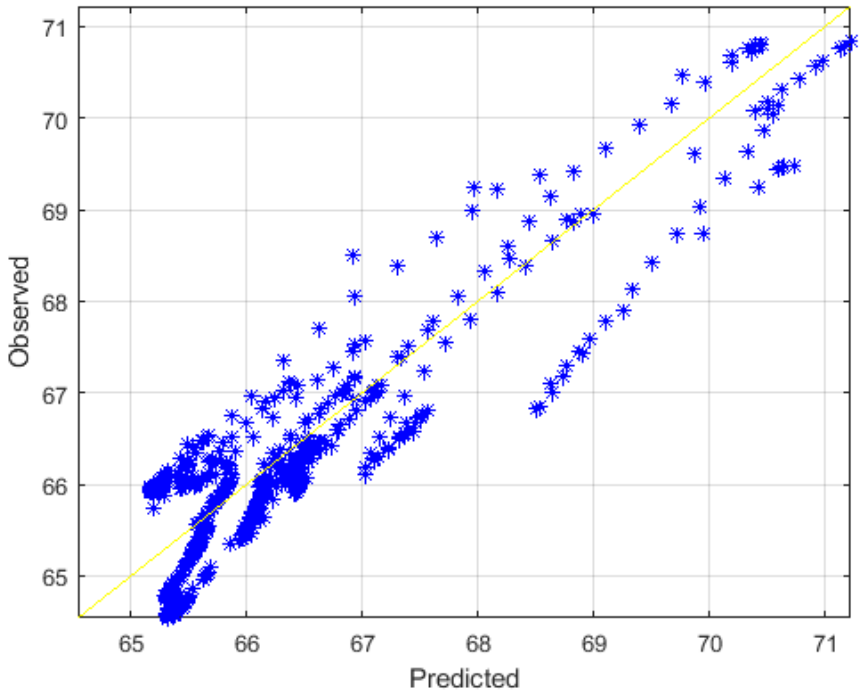

Figure 19. Scatter plot of modeled vs observed water surface elevation (2017-2018).

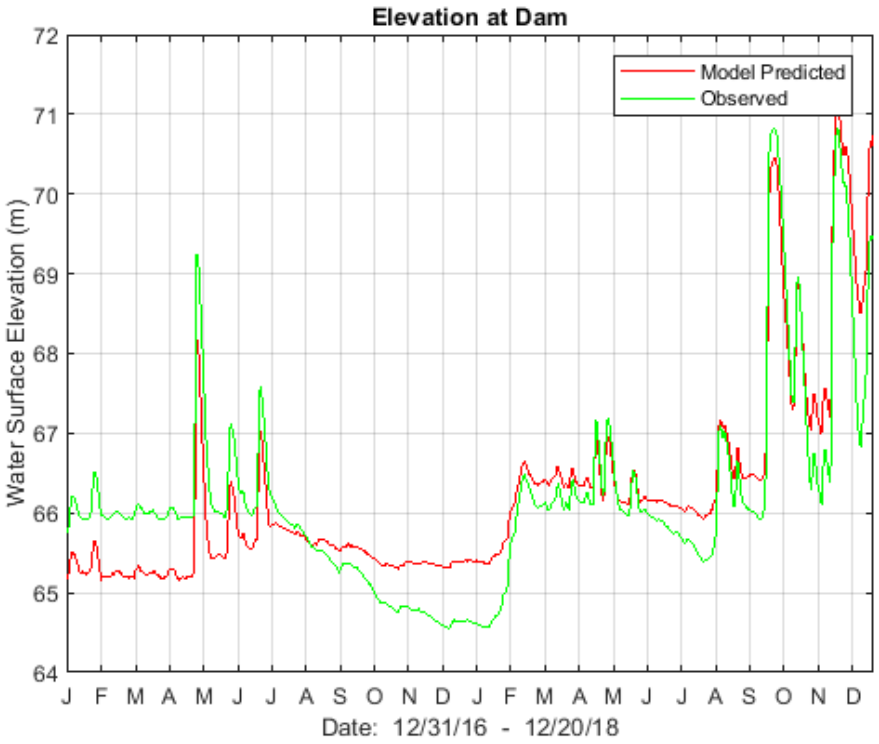

Figure 20. Modeled vs observed water surface elevation (2017-2018).

Table 10: Statistical comparison of modeled vs observed water surface elevation

Calibration Statistic	Time Period			Units
	2014-2015	2016	2017-2018	
Mean Error (predicted – observed)	-0.09	0.08	-0.05	m
Normalized Mean Error	-0.10%	0.10%	-0.10%	%
Root Mean Square Error	0.38	0.26	0.44	m
Normalized Root Mean Square Error	0.60%	0.40%	0.70%	%
Mean Absolute Error	0.28	0.19	0.37	m
Normalized Mean Absolute Error	0.40%	0.30%	0.60%	%
Correlation R^2	85%	95%	91%	%
Number of Model/Data Comparisons	779	365	717	-
Model Efficiency	82%	93%	88%	%

Over both the two time periods used for model calibration (2014-2015 and 2017-2018) and the one time period used for model validation (2016) the mean error of water surface elevations is low and does not suggest a trend (positive or negative) in the error with respect to the time period of the model (Table 10). The normalized mean error is also low, and a minor negative or positive trends in the error with respect to the time period are indicated. The root mean square error, which does not reveal positive or negative trends in the error, is low for all three model periods. The normalized root mean square error is also low for all three model periods. The correlation coefficients indicate that measured and modeled water surface elevations are highly correlated for all model periods. Consideration of water surface elevation time histories (Figure 21) is essential to understanding the goodness of fit between measured and modeled water levels. The largest errors are associated with time periods when the lake water level apparently has been drawn down and when peak water level events occur due to high inflows. Accurate modeling of water level drawdowns is problematic as these periods were not directly related to gaged and estimated (ungaged) inflows, outflow at the dam, and water supply withdrawals used in the model. Accurate modeling of peak water level events is also problematic as they are very sensitive to the timing of inflows and outflows that are applied as daily averages in the model.

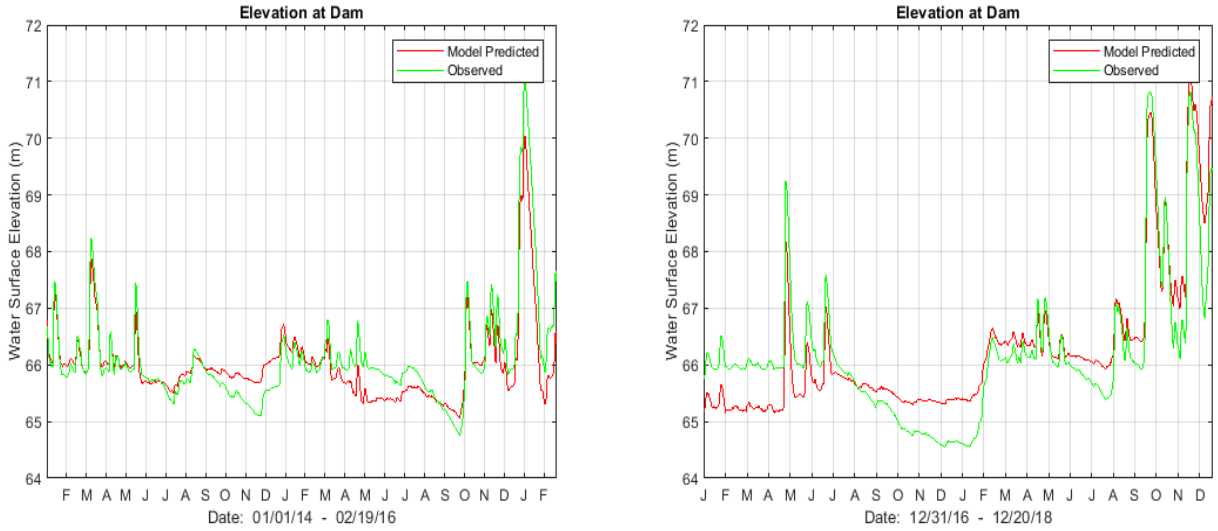

Figure 21. Time history comparisons of observed and model predicted water surface elevations at the Jordan Lake dam for the 2014-2015 model time period (left panel) and the 2017-2018 time period (right panel).

4.3 Temperature Model Calibration

All statistical measures of calibration performance for temperature calibration (Table 11) such as mean error, root mean square error, and goodness of fit measures (correlation R^2 and model efficiency) indicate the agreement between measured and modeled water temperatures is good to very good. The time history comparisons for the surface and bottom water layers (Figure 22) are also in good agreement with the measured temperatures at a representative location (station CPF055E) for the two periods used for model calibration. The model results are consistent with observed water temperature for both well-mixed winter conditions and summer stratified conditions. Scatter plots of observed vs. model predicted temperature (Figures 23) indicate the limited scatter and low bias across the full range of predicted and observed temperatures. A more complete set of observed vs. model predicted temperature time histories are available in Appendix 2.

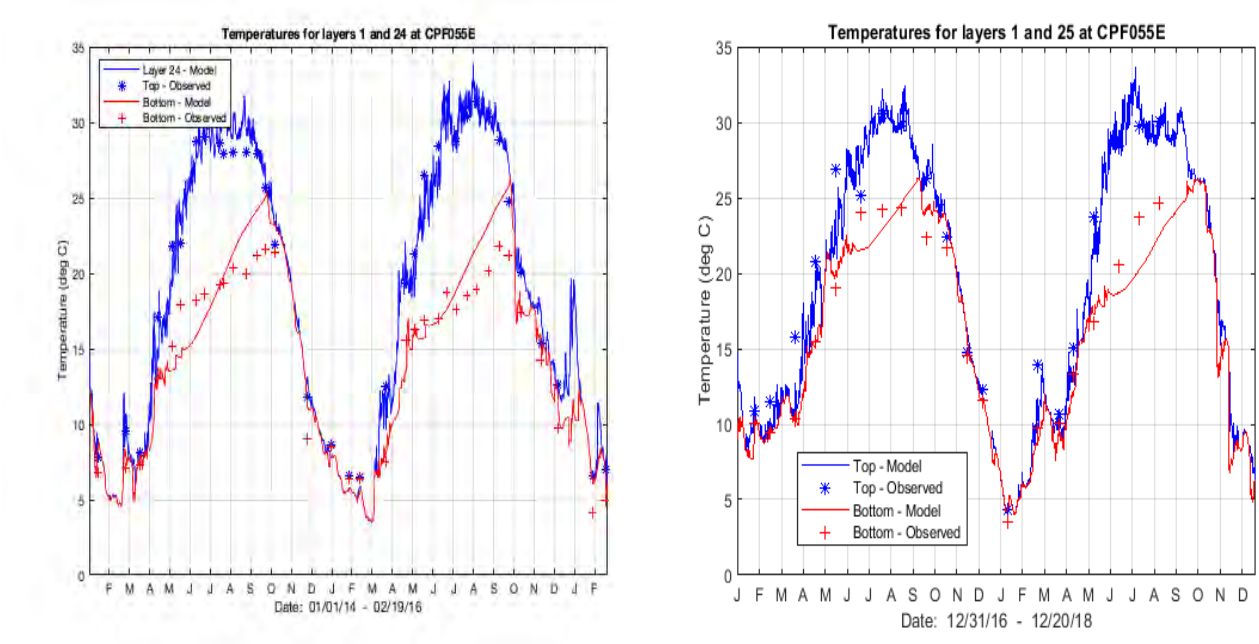

Figure 22. Time history comparisons of observed and model predicted surface and bottom temperatures at station CPF055E for the 2014-2015 model time period (left panel) and the 2017-2018 time period (right panel).

Table 11. Statistical comparison of modeled vs. observed water temperatures

Parameter	Time Period			Units
	2014-2015	2016	2017-2018	
Mean Error (predicted – observed)	0.17	-0.3	-0.8	°C
Normalized Mean Error	1%	-2%	-4%	%
Root Mean Square Error	2.11	1.56	2.07	°C
Normalized Root Mean Square Error	11%	9%	11%	%
Correlation R^2	94%	97%	96%	%
Number of Model/Data Comparisons	1144	370	398	-
Model Efficiency	94%	97%	93%	%

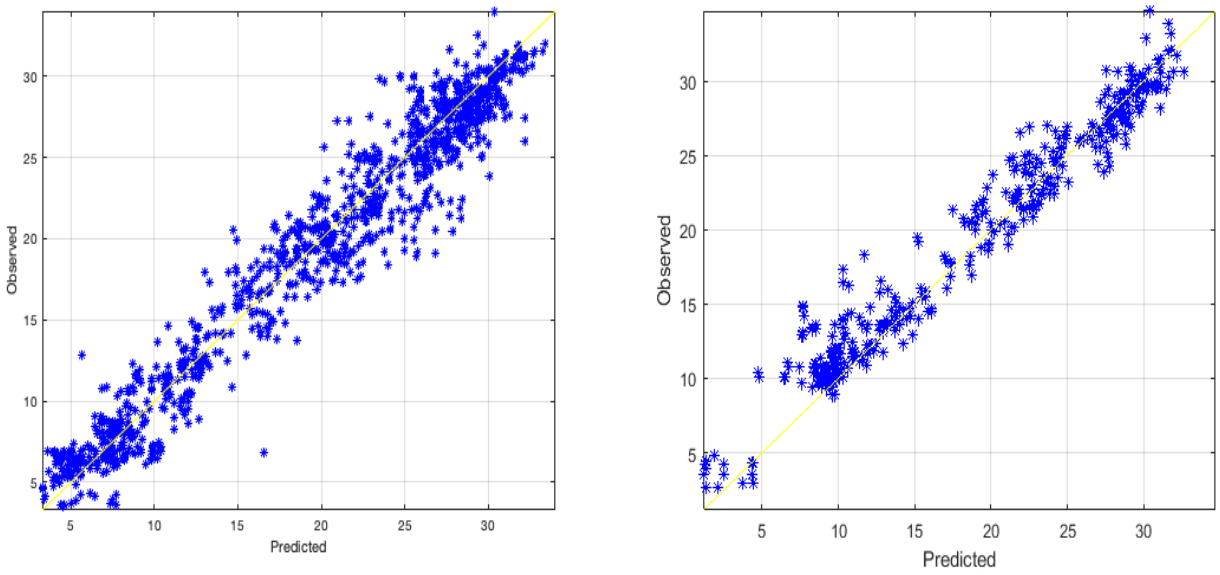

Figure 23. Scatter plot of observed and model predicted temperatures at all monitoring stations in Jordan Lake, NC for the 2014-2015 (left) and 2017-2018 (right) model time periods

4.4 Water Quality Model Calibration

Since the numeric criteria for chlorophyll a examines the magnitude of infrequently occurring high chlorophyll a values (i.e. what is the chlorophyll a value that is exceeded exactly 10% of the time), it is important the distribution of model predicted chlorophyll a concentrations closely match that of the observed values. Said another way, it is more important the model accurately predicts the magnitude and frequency of high chlorophyll values than it accurately predicts exactly where and when those high values occur. For this reason, the primary objective of the chlorophyll a calibration was to match well the frequency distribution of observed values. Other quantitative calibration measures such as mean error, root mean square error and correlation R^2 were considered as well, but were given a lower importance during calibration.

During calibration, cumulative distribution functions (CDFs) of model predicted and observed chlorophyll a data were examined for approximately 200 separate model runs for both the 2014-2015 and 2017-2018 model time periods to select kinetic parameters related to algal growth and nutrient dynamics. Kinetic parameters that were considered during calibration include maximum algal growth rates for each algal group, temperature, nutrient, and light dependence of algal growth, carbon to chlorophyll ratio for algal organic matter, algal respiration and predation rates, benthic nutrient fluxes of nitrate, phosphate, and ammonia, background light attenuation, and chlorophyll and organic matter specific light attenuation. The CDFs were based on concurrent measured and modeled chlorophyll a concentrations for all eighteen monitoring stations taken over the two model time periods. The CDFs for the calibrated model matched well that of the observed values for both model time periods (Figure 24). The 90th percentile value was slightly

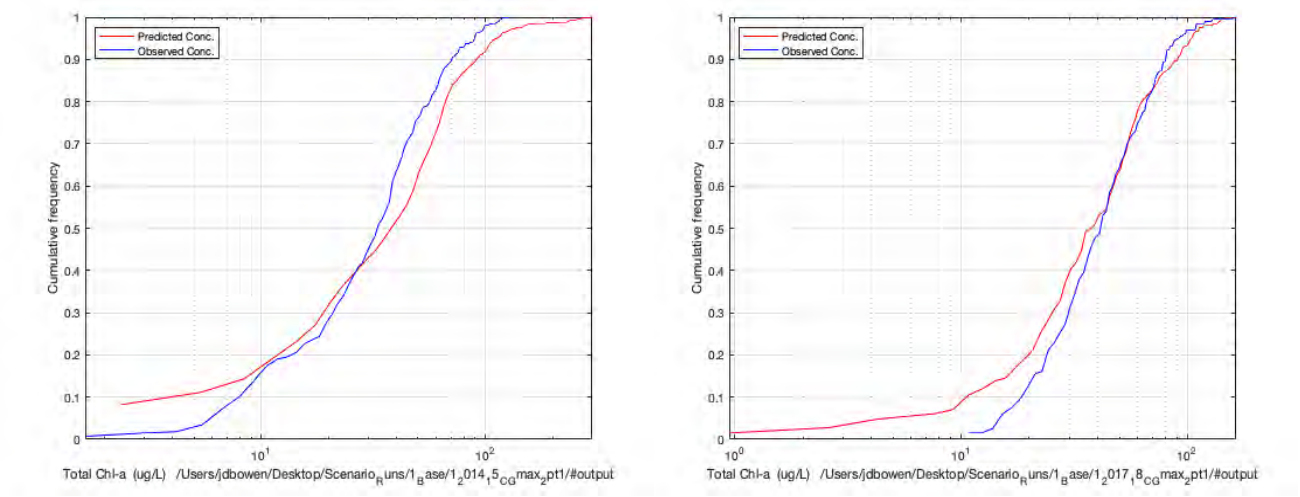

Figure 24. Cumulative distribution functions of observed and model predicted chlorophyll a concentration at all 18 monitoring stations in Jordan Lake, NC for the 2014-2015 (left) and 2017-2018 (right) model time periods

overpredicted for both time periods by about 20%. Median values (50th percentile) matched more closely the observed chlorophyll a concentration, while the model underpredicts the lower end of the chlorophyll a distributions (Figure 24). Time history comparisons of one representative station in the New Hope arm of the lake (station CPF087D) and one station in the Haw River arm of the lake (CPF055D) shows the large magnitude of seasonal variation in the chlorophyll a concentrations (Figure 25) observed in the lake during the 2014-2015 model time

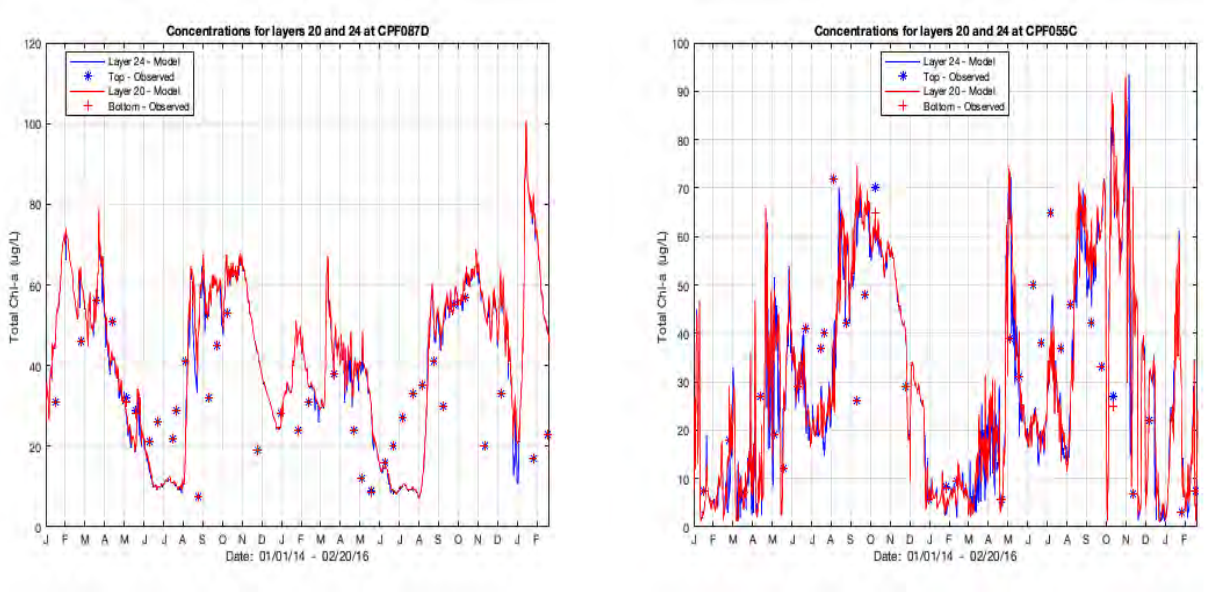

Figure 25. Time history comparison of observed and model predicted chlorophyll a concentrations at monitoring stations CPF087D and CPF055C for the 2014-2015 model time period.

period. The 2017-2018 temporal patterns in chlorophyll a concentrations at these stations were qualitatively similar. The model does a good job overall in predicting the chlorophyll magnitudes but misses in some cases the timing of the minimum and maximum values. Model predicted chlorophyll a concentrations can vary widely at a station over a short time period, particularly in the Haw River arm of the lake. This is likely due to variations in inflow that move the peak chlorophyll a concentrations upstream and downstream.

The statistics for chlorophyll a modeling calibration in Table 12 (mean error, normalized mean error, normalized mean error, correlation coefficient) should be considered along with the time histories (Figure 25) in order to understand the magnitude of some of the statistical errors which may seem high, but are also a reflection of the short-term transient nature of the measured and modeled concentrations. The validation time period (2016) had similar calibration performance to the two time periods used for model calibration. The level of calibration performance achieved is typical of models of algal growth in highly dynamic, long residence time systems. The model was considered to be sufficiently calibrated to the observed chlorophyll a for the purposes of investigating the effects of nutrient load reductions on chlorophyll a concentrations.

Table 12. Statistical comparison of modeled vs. observed chlorophyll a concentration

Parameter	Time Period			Units
	2014-2015	2016	2017-2018	
Mean Error (predicted – observed)	0.06	0.10	-0.03	log µg/L
Normalized Mean Error	4.1%	6.8%	-1.9%	%
Root Mean Square Error	0.41	0.40	0.27	log µg/L
Normalized Root Mean Square Error	29%	28%	17%	%
Correlation R^2	27%	26%	28%	%
Number of Model/Data Comparisons	898	366	334	-

The statistics for total phosphorus and nitrate nitrogen for the calibrated water quality model are also presented as cumulative distribution functions (CDFs) for the 2014-2015 model time period (Figure 26). Total phosphorus was used for model vs. data comparison since no orthophosphate data were available. For calibrating algal growth models, orthophosphate is preferred because of its bioavailability to phytoplankton. Total phosphorus is a cumulative measure of inorganic, organic, and particle associate forms of phosphorus, and is therefore less desirable for model calibration. Like the chlorophyll a concentration, the CDFs were based on all concurrent measured and modeled total P and nitrate concentrations. The CDFs are indirect measures of both the magnitude and timing of the calibrated models for these nutrients. They were considered to be acceptable for both periods. The modeled trends for both nutrients are adequate. Total P is underpredicted at the lower range concentration and overpredicted at the higher range, while nitrate N was underpredicted throughout the range of data, but was not grossly overestimated. The 2017-2018 model calibration run produced total P and nitrate CDFs that were qualitatively similar to that shown for the 2014-2015 model time period.

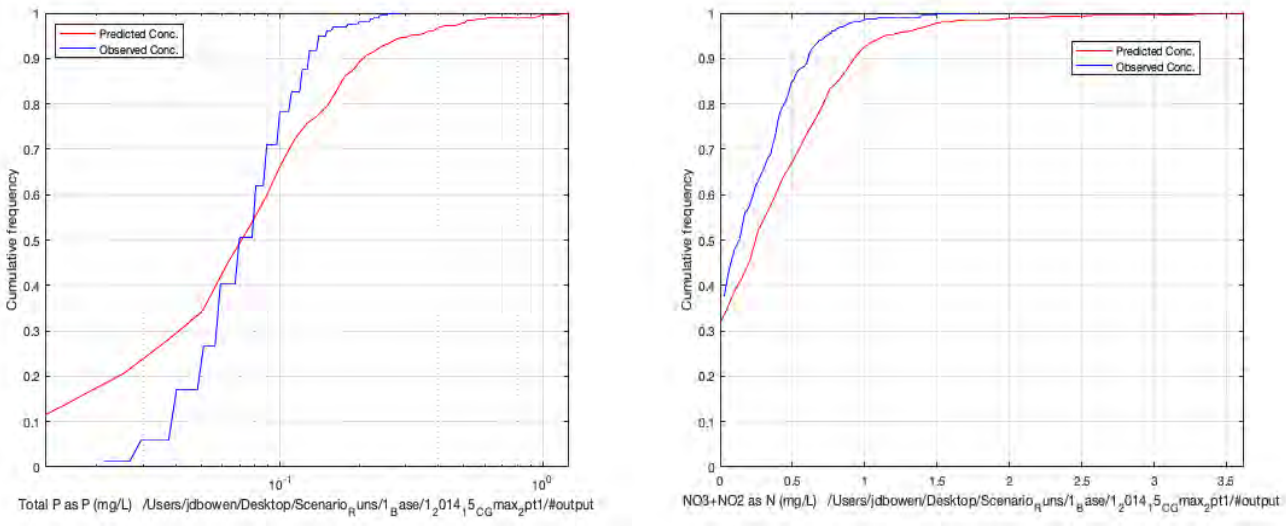

Figure 26. Cumulative frequency distributions of observed and model predicted total phosphorus (mg/L, left) and nitrate nitrogen (mg/L, right) concentrations at all 18 monitoring stations in Jordan Lake, NC for the 2014-2015 model time period.

5. MODEL EVALUATION

5.1 Model Verification

A one-year time period (January 1, 2016 – December 31, 2016) was used for model verification. The calibrated model was run using the parameter values determined using the two other model time periods (2014 - 2015, 2017 – 2018). Statistical measures of calibration performance were calculated in an identical fashion to that done during calibration using the other two time periods. These statistical measures of calibration performance for water surface elevation (Table 10), temperature (Table 11) and chlorophyll-a (Table 12) were found to be nearly identical for the 2016 verification time period as they were for the two time periods used for model calibration (2014-2015, 2017-2018), which indicates that the calibrated model can adequately simulate conditions in years other than the one for which it was calibrated.

5.2 Analysis of Simulated Dye Releases

The age of water is unique to each water parcel that enters the Jordan Lake model domain. Water age is defined as the time a water parcel has spent since entering the domain at one of its boundaries. Inherent to the time scale of water age is the recognition of spatial heterogeneity: parcels at different locations within a waterbody have different ages at any given time. Water age as a function of time and location in Jordan Lake was calculated based upon the simulation of a dye study release using the hydrodynamic model. Qi, Lu et al. (2016) describes this approach in which a conservative tracer is discharged to the lake. Two advection-dispersion equations for concentration are derived: one for the tracer and another for water age. The water age at any specific location and time is defined as the ratio of water age concentration to tracer concentration. Water age differs from flushing time (or retention time) in that flushing time is a bulk parameter that quantifies the general exchange characteristics of a waterbody without identifying their spatial distribution. On the other hand, water age can be combined with constituent concentrations that also vary with location and time to develop a comprehensive analysis of constituent fate and transport.

The distribution of water age within the model domain at any given simulation time represents the transient effects of flow boundary locations (inflow and outflow), structures within the lake (i.e., causeways), and water quality zones, which are defined by local flow conditions (water depth and width) and water temperature. Water ages were found to be most dependent on the proximity of a given location to inflow boundaries and the time-dependent magnitude of the lake inflows (Table 13). Water age at station CPF055D is strongly influenced by inflow from the Haw River as indicated by the significant decrease in water age corresponding to the high inflow event occurring in late September/early October (Figures 27 and 28). Similarly, water age at CPF087B3 (Figure 29) is influenced by inflow from the New Hope arm of the lake including New Hope Creek, which also contributed high flows during the same period (Figure 28). Water age at CPF0880A (Figure 30) is likely influenced by inflows from a smaller tributary, Beaver Creek, and the Haw River. Its response is similar to that as CPF055D with longer maximum water age.

Table 13. Estimates of Water Age at Selected DWR Monitoring Stations of Jordan Lake, NC for the May 2015-Oct 2015 Model Time Period.

Station	Water Age Range (days) for 05/01/2015 to 10/31/2015
CPF055D	1-188
CPF086C	1-93
CPF086F	1-108
CPF087B3	1-170
CPF0880A	1-209

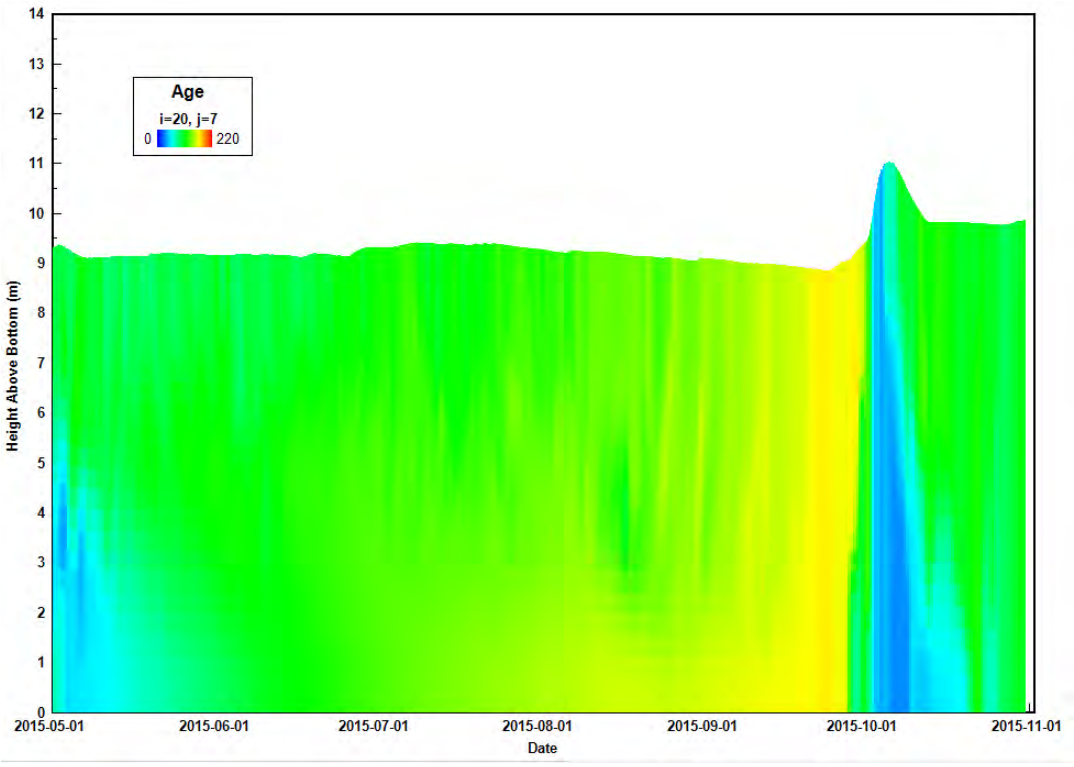

Figure 27. Water age model estimates (days) at station CPF055D for May 1 to Oct 31, 2015

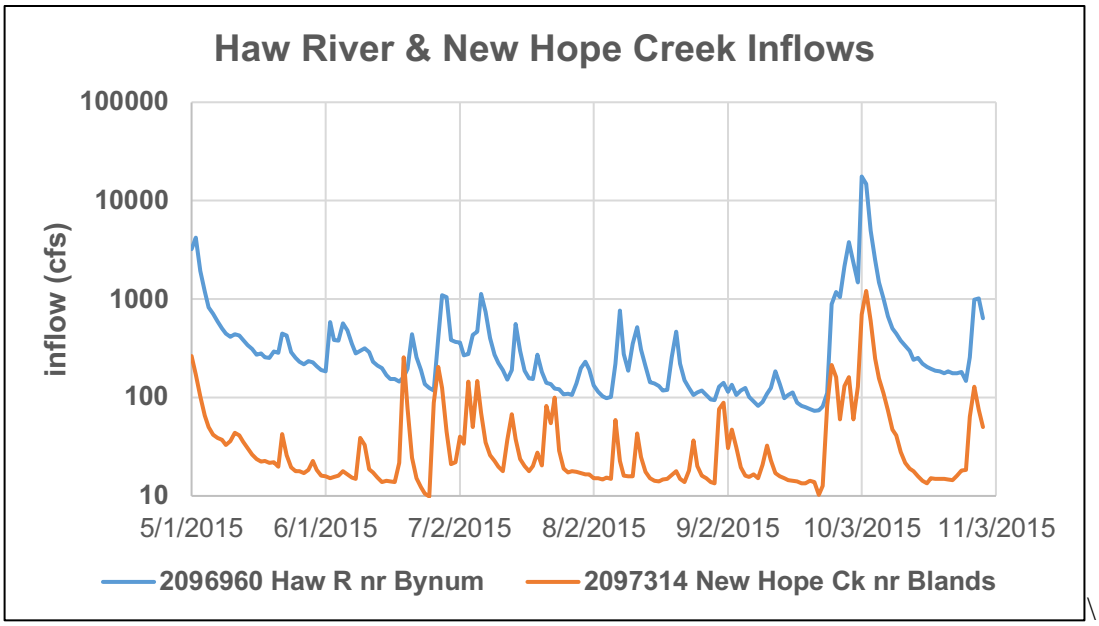

Figure 28. Inflows at USGS Gaging Stations 02096960 Haw River and 02097314 New Hope Creek

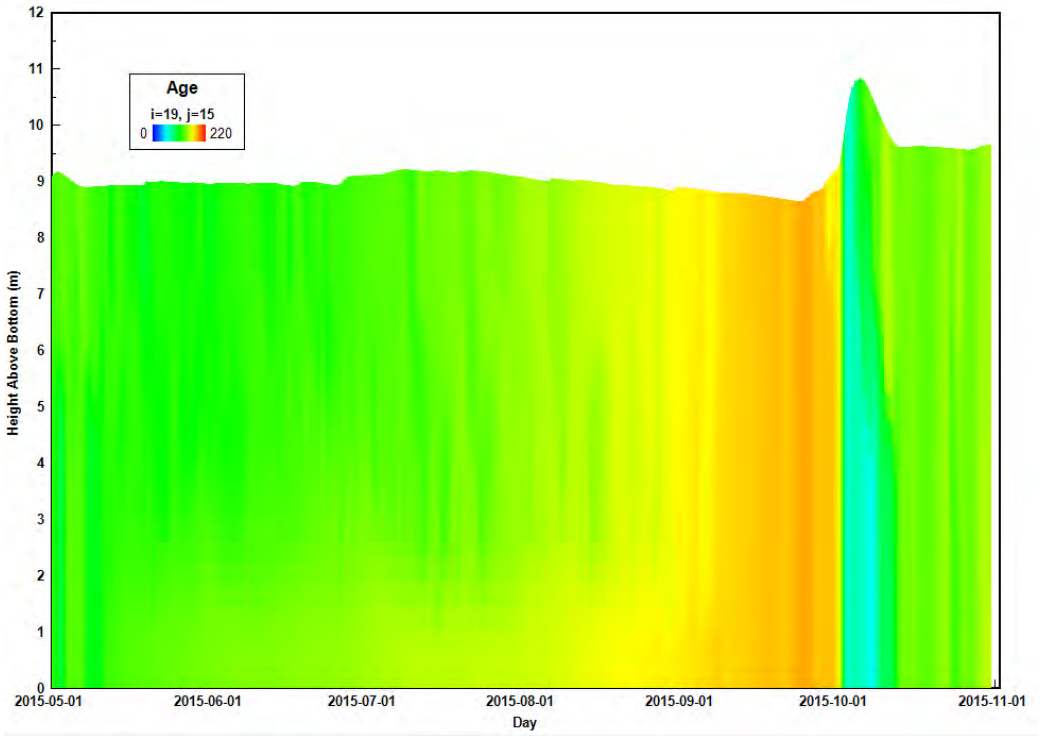

Figure 29. Water age model estimates (days) at station CPF0880A for May 1 to Oct 31, 2015.

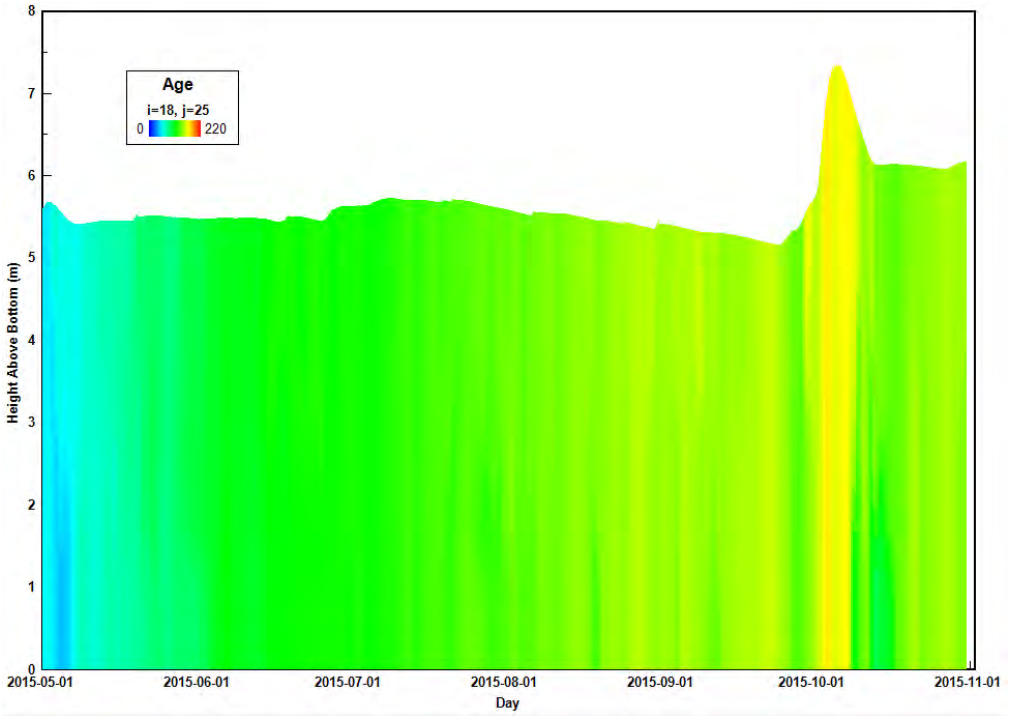

Figure 30. Water age model estimates (days) at station CPF087B3 for May 1 to Oct 31, 2015.

Previous works cite 5 days and 418 days as the average hydraulic retention times for the Haw River and the New Hope arm of Jordan Lake, respectively (NCDEHNR 1992). Loftis, Saunders et al. (1976) reported travel time of less than one day for the Haw River inflow, and greater than a physical test duration of 120 days for the New Hope inflow. Del Giudice, Aupperle et al. (2019) reported flushing rates (inverse of water residence time) that ranged from 0.2-1.5 per month for Segment 1 (furthest north), 0.1-0.5 per month for Segment 2 (north of U.S. 64), 0.1-0.5 per month for Segment 3 (south of U.S. 64), and 1.0-5.0 for Segment 4 (furthest south) for the period from 1983 to 2018. These times estimates reflect averaging over space and time, whereas the water age estimates are specific for both location and time.

A second simulated dye release was done to reveal the extent to which inflow from the Haw River mixes with waters in each of the four water quality regions of the lake (Table 14). Three of the regions are in New Hope Creek arm of the lake (above causeways, between causeways, below causeways), while the fourth region is the western arm of the lake along the old Haw River bed. As expected, the contributions from the Haw decreased significantly moving uplake (upstream) from the Haw River region through each region in the New Hope Creek arm of the lake and eventually into to the Morgan Creek and New Hope arms of the lake (Table 14). At the same time, the results indicated that the Haw contribution was still potentially measurable

Table 14. Time-average simulated dye concentrations at locations across four Jordan Lake regions. Higher concentrations indicate a higher contribution from Haw River inflow. The average concentration for a region is based upon all stations within that region.

Jordan Lake Region	Station	Time-Average Contribution from Haw River Water (%)	
		2014-2015	2017-2018
Haw River	CPF055C	100%	100%
	CPF055D	100%	100%
	CPF055E	100%	100%
	Average	**93.5%**	**93.1%**
Above Causeways	CPF086C	0.0%	1.0%
	CPF086D	0.8%	2.8%
	CPF086F	1.0%	3.2%
	Average	**0.0%**	**1.2%**
Between Causeways	CPF087B3	12.0%	20.1%
	CPF087D	20.1%	30.0%
	Average	**16.0%**	**25.0%**
Below Causeways	CPF0880A	59.2%	70.4%
	Average	**59.2%**	**70.4%**

throughout each region of the lake, but makes up only a very small fraction of the input to the upper and between causeways regions (< 2% and 25% Haw River water respectively). These results are also consistent with the residence time model described previously, which showed much longer residence times, and hence lower amounts of flushing in the New Hope Creek arm of the lake.

6. SCENARIO TESTING

6.1 Description of Base and Scenario Cases

To test the sensitivity of the Jordan Lake system to nutrient load reduction, incoming loads of both organic and inorganic forms of nitrogen and phosphorus were reduced independently over a range of values from 10% to 50%. The load reductions were accomplished by reducing concentrations of the appropriate model state variables at the inflow boundaries by the given percentages. For the organic fractions, reductions were made in the concentrations of the labile particulate and dissolved nitrogen and phosphorus state variables, but not in the refractory particulate fraction. These relatively inert state variables were held constant because it was assumed that treatment operations would be less effective on the inert matter compared to the more reactive labile particulate and dissolve fractions.

6.2 Nutrient Load Reductions with Constant Dry Deposition and Benthic Fluxes

Wet and dry deposition of nutrients and benthic flux rates were held constant for the first set of nutrient load reductions (Table 15). A total of twenty-five load reduction cases were considered, with N and P reductions from zero to forty percent. For each load reduction case, an alternate set of the flow boundary concentration files (CWSRXX.INP files) were developed and run with the calibrated model for the 2014-2015 and 2017-2018 model time periods. The model results were analyzed to determine the reduction in the 25th, 50th, 75th, and 90th percentile chlorophyll a concentration for all eighteen monitoring stations as compared to the corresponding base case. For each case the fraction of chlorophyll a concentrations above the regulatory limit of 40 ug/L was also determined.

Both nitrogen and phosphorus load reductions reduced chlorophyll a concentrations, but to a different extent. Over the range of N and P reduction scenarios from 0% to 40%, chlorophyll a concentrations decreased by 0% to 17% (Table 15). In general nitrogen reductions of a particular percentage were more effective in reducing chlorophyll concentrations than the corresponding phosphorus load reduction. Since the chlorophyll reductions were modest in all cases (0% - 17%), not surprisingly, the frequency of exceedance of the 40 ug/L water quality criteria value were always significantly above 10% (Table 15). Even the case with largest decrease in loading (-40% N, -40% P) produced a chlorophyll a reduction (-17%) that was far from the 40-50% needed to bring the lake into compliance with the water quality criteria for chlorophyll a (see Table 3).

Table 15. Average reduction in model predicted chlorophyll a concentration at 18 locations from the 2014-2015 and 2017-2018 base case runs for various nutrient load reduction scenarios (upper table) and the fraction of model predicted values exceeding the chlorophyll a water quality criteria value of 40 μg/L (lower table).

Change in N loading					Chl a Reduction (μg/L)	
-40%	-30%	-20%	-10%	0%		
-12%	-9%	-6%	-3%	0%	0%	Change
-13%	-10%	-7%	-3%	-1%	-10%	in
-15%	-12%	-9%	-5%	-3%	-20%	P
-16%	-13%	-10%	-7%	-5%	-30%	Loading
-17%	-14%	-12%	-10%	-7%	-40%	

Change in N loading					% Chl a Above 40 μg/L	
-40%	-30%	-20%	-10%	0%		
39%	41%	43%	44%	45%	0%	Change
38%	40%	42%	43%	44%	-10%	in
37%	39%	41%	43%	44%	-20%	P
36%	38%	40%	42%	43%	-30%	Loading
35%	37%	39%	41%	42%	-40%	

6.3 Nutrient Load Reductions with and without Haw River Inputs

The earlier analysis of simulated dye releases showed that very little of the water that enters the lake via the Haw River makes it up into the upper part of the New Hope Creek arm of the lake. This characteristic of Jordan Lake suggests that reductions in nutrient loading from the Haw River arm are likely to be minimally effective in reducing chlorophyll a concentrations outside of the Haw River arm of the lake. A set of load reductions considered this lake characteristic. Five runs that reduced N and P loading from 10% to 50% in all incoming surface waters were compared to five corresponding cases without reductions in the N and P loading from the Haw River (Table 16). As expected, eliminating the Haw River N & P load reductions lead to only a minor change in the reduction in chlorophyll a concentrations. Eliminating the Haw River loading had more of an effect when all eighteen monitoring stations were considered. When the analysis was limited to stations in the New Hope Creek arm of the lake, there was very little difference between cases with and without reductions in Haw River loading (Table 16).

Table 16. Average reduction in model predicted chlorophyll a concentration at 18 locations from the 2014-2015 and 2017-2018 base case runs for various nutrient load reduction scenarios with and without reductions in Haw River inputs (upper table) and the fraction of model predicted values exceeding the chlorophyll a water quality criteria value of 40 µg/L (lower table).

Change in N and P Loading					Chl a Reduction
-50%	-40%	-30%	-20%	-10%	
-23%	-17%	-13%	-9%	-3%	With Haw Reduction, all stations
-12%	-8%	-8%	-4%	-3%	w/o Haw Reduction, all stations
-22%	-17%	-13%	-9%	-4%	With Haw Reductions, New Hope Creek arm only
-19%	-16%	-12%	-8%	-4%	w/o Haw Reductions, New Hope Creek arm only

Change in N and P Loading					% Chl a Above 40 ug/L
-50%	-40%	-30%	-20%	-10%	
32%	35%	38%	41%	43%	With Haw Reduction, all stations
40%	41%	42%	43%	44%	w/o Haw Reductions, all stations

6.4 Nutrient Load Reductions with and without Removal of Causeways

Another distinctive characteristic of Jordan Lake is the presence of four causeway bridges over the New Hope Creek arm of the lake. The four bridges (Hwy 64, Farrington Road (N & S), and Beaver Creek Road) greatly diminish the cross-sectional area available for up and downstream flow in the lake. Removal of one or more these bridges could potentially increase the flushing in the New Hope Creek arm of the lake, and therefore improve water quality. The hydrodynamic model used for this research (EFDC) is ideally suited to considering this effect, as it has a "masking" feature that allows for thin "no-flow" boundary between adjoining model cells. Masks were used to represent the four causeways in the calibrated model. Removal of the masks removes the no-flow boundary, and therefore allows for a simulation of the effect of eliminating the causeways. To study the "causeway removal" effect, five additional model runs, with N & P load reductions from 10% to 50% were run and analyzed as described previously. There was a measurable, but slight difference seen between the with and without causeways cases (Table 17). Removal of the causeways only very slightly improved water quality in the lake. Nitrogen and phosphorus load reductions from 0% to 50% reduced chlorophyll a concentrations by 3% to 23% for the with causeway cases, and 4% to 24% for the without causeway cases. These results suggest that the limited flushing and very high chlorophyll a concentrations in the New Hope Creek arm of the lake are not a result of the flow restrictions posed by the presence of the four causeways.

Table 17. Average reduction in model predicted chlorophyll a concentration at 18 locations from the 2014-2015 and 2017-2018 base case runs for various nutrient load reduction scenarios with and without removal of causeways (upper table) and the fraction of model predicted values exceeding the chlorophyll a water quality criteria value of 40 µg/L (lower table).

Change in N and P Loading					Chl a Reduction (% from base case)
-50%	-40%	-30%	-20%	-10%	
-24%	-18%	-13%	-8%	-4%	Cases w/o Causeways
-23%	-17%	-13%	-9%	-3%	Cases w/ causeways

Change in N and P Loading					% Chl a Above 40 ug/L	
-50%	-40%	-30%	-20%	-10%	0%	
33%	37%	41%	45%	48%	49%	w/o Causeways

6.5 Nutrient Load Reductions with Predictive Sediment Diagenesis

One result of the loading analysis was that benthic cycling of nutrients was a major contributor to the water column's supply of bioavailable nitrogen and phosphorus. Particularly in the New Hope Creek arm of the lake, the loading of inorganic nutrients to the water column was principally from the benthic sediments (75% of phosphate, 90% of ammonia, see Figure 11) . With this fact in mind, it is not surprising that the reductions in chlorophyll concentrations were relatively insensitive to nutrient load reductions (e.g. 40% N & P load reduction reduced chlorophyll a by 17%, see Table 16).

It is possible, however, that long-term reductions in nutrient loading could eventually produce a change in the benthic flux of inorganic nutrients. As phytoplankton biomass is reduced with load reduction, settling of that organic matter would be reduced, which might eventually feedback to a reduced benthic flux of nutrients. To investigate this possibility, long-term simulations of nutrient load reductions were run using the predictive sediment diagenesis model available in the particular version of the model (EFDC+) used for this study (Craig 2018). EFDC+ is an updated and enhanced version of the original EFDC model (Tetra Tech 2007) that includes among other improvements the predictive sediment diagenesis model originally developed by Di Toro and Fitzpatrick for the Chesapeake Bay water quality model (Di Toro and Fitzpatrick 1993).

To accomplish the long-term simulation, the 2014-2015 calibrated model was run repeatedly with a 50% N and P load reduction. At the end of the two-year simulation, the ending sediment conditions were saved to a file and used to initialize the sediment conditions for the next two-year simulation. The model was run this way a total of nine times, for a total simulation time of eighteen years. For each run having the time varying sediment organic matter composition and the 50% N & P load reduction, the reduction in chlorophyll a concentrations was determined as in the previous scenario test runs. Over the eighteen year time period, the reduction in

chlorophyll concentrations did increase from 23% initially to 45% in the last two years of the simulation (Table 18), The change in chlorophyll a concentration reductions was most pronounced in the early years, and seem to plateau after approximately ten years (Table 18).

Table 18. Average reduction in model predicted chlorophyll a concentration at 18 locations for the 2014-2015 model time period for a 50% load reduction in N & P for various time periods using time-varying sediment organic matter compositions.

Effect of 50% N & P load reductions for the following time periods									Chl a Reduction (% from base case)
0-2 years	2-4 years	4-8 years	6-8 years	8-10 years	10-12 years	12-14 years	14-16 years	16-18 years	
-23%	-27%	-33%	-41%	-43%	-44%	-45%	-45%	-45%	

7. SUMMARY, DISCUSSION, AND CONCLUSIONS

The nutrient load reduction scenario analysis was designed to simulate the effects of a wide range of possible reductions in both nitrogen and phosphorus loading. Considering this broad range of possibilities with their resulting reductions in chlorophyll a concentrations, a few conclusions emerge. The first has to do with the magnitude of the decreases in chlorophyll a concentrations. Overall, the decreases in chlorophyll a were relatively modest considering the significant reductions in nutrient loading that were considered. For instance, a 50% N and P load reduction initially produced only an initial 23% decrease in chlorophyll a concentrations (Table 15 or 16), which increased to 45% eventually (Table 18), but this level was produced only after more than a decade of sustained load reductions. A second conclusion relates to the magnitude of the needed algal biomass reductions to meet numeric water quality criteria. The analysis of 2014-2018 chlorophyll a monitoring data in Jordan Lake (Table 5) showed that at least a 45% biomass reduction would be needed to lower chlorophyll a concentrations enough so that Jordan Lake meets current numeric water quality criteria for chlorophyll a. Taken together, these two results, one based on the analysis of monitoring data, and the second based upon results from the model, suggest that Jordan Lake needs significant load reductions (approximately 50%) in nitrogen and phosphorus over a long period time to meet water quality criteria. The model also suggests that reductions in loading to the Haw River arm of the lake will not improve water quality conditions in the New Hope Creek arm of the lake.

Water quality calibration relied upon existing data for the most part. Collaboratory partners provided many important new pieces of information on the lake that greatly aided the modeling project. Unfortunately there was some missing information in the water quality monitoring dataset provided by NC DWR that would have been useful for this modeling effort. In particular, there was no information available in either the watershed data or the lake data on phosphorus fractionation. Datasets used to support model efforts of this sort usually include orthophosphate measurements since this is the bioavailable fraction taken up phytoplankton during photosynthesis. Nitrogen fractionation into ammonia, Kjeldahl, and nitrate nitrogen was available and was helpful in creating model input files and for calibration purposes. Future modeling efforts in Jordan Lake would benefit greatly from adding orthophosphate measurements in the lake and the watershed.

A surprising challenge in this modeling effort was the simulation of water surface elevations. Considerable effort was expended during the project on the estimation of the flow hydrograph for the ungaged portion of the Jordan Lake watershed. The simple scaling approach based upon watershed area for estimating watershed hydrographs produced unacceptably large errors in the water surface elevation time histories at the dam. A review of previous modeling work on Jordan Lake (Tetra Tech 2002, Tetra Tech 2003) and other recent modeling work using the EFDC+ model for lake water quality simulation (Dynamic Solutions 2013, Michael Baker 2015) indicated that the problems we experienced are not unique. The earlier Jordan Lake model and the more recent Tenkiller reservoir model significantly improved the fit to observed water surface elevations by increasing the outflows at the dam. We chose not to make any adjustment

to the measured outflow hydrodraph at the dam, and instead only adjusted the inflow hydrograph to the lake. This decision limited our ability to fit the model predicted elevations to the observed data. It is our judgement that this was a reasonable approach given the focus of this work on eutrophication issues rather than concerns more directly related to lake water depths.

Another challenging aspect of the modeling effort related to the predictive sediment submodel. The version of the Di Toro and Fitpatrick (Di Toro and Fitzpatrick 1993) sediment diagenesis model used for this study (Craig 2018) proved difficult to run, primarily due to numerical instability issues. To prevent numerical instabilities, the maximum model time step was decreased to five seconds, rather than the 100 second values that could be used for a model using the standard EFDC specified spatially and temporally varying benthic fluxes. Shortening the model time step by a factor of twenty increased computer model run times by a similar amount so that a two year run took closer to forty hours rather than two hours. This greatly complicated and lengthened model calibration and scenario testing in cases using the predictive sediment model. To get the work done within the available time, we therefore followed an approach that used both modeling approaches for the benthic sediment submodel, depending upon the available time and the modeling needs. We ended up not being able to do some model analyses that we had planned and have used in previous work (Bowen and Harrigan 2017, Bowen and Harrigan 2018). In future work we plan to continue to explore approaches to calibration and model testing in circumstances where a predictive sediment diagenesis model is needed.

8. REFERENCES

Abdelrhman, M. (2015). "Three-Dimensional Modeling of Hydrodynamics and Transport in Narragansett Bay." Narragansett, Rhode Island: US Environmental Protection Agency, Office of Research and Development, EPA.

Ambrose, R. B., et al. (1993). "The water quality analysis simulation program, WASP5, Part A: Model documentation." Environmental Research Laboratory, US Environmental Protection Agency, Athens, GA.

Bowen, J. and N. Harrigan (2018). "Water Quality Model Calibration via a Full-Factorial Analysis of Algal Growth Kinetic Parameters." Journal of Marine Science and Engineering **6**(4): 137.

Bowen, J. and N. B. Harrigan (2017). Comparing the impact of organic versus inorganic nitrogen loading to the Neuse River Estuary with a mechanistic eutrophication model, NC WRRI.

Bowen, J. D., et al. (2009). Development and Use of a Three-Dimensional Water Quality Model to Predict Dissolved Oxygen Concentrations in the Lower Cape Fear River Estuary, North Carolina. Charlotte, NC, University of North Carolina at Charlotte.

Cole, T. M. and S. A. Wells (2006). "CE-QUAL-W2: A two-dimensional, laterally averaged, Hydrodynamic and Water Quality Model, Version 3.5."

Craig, P. M. (2018). User's Manual for EFDC_Explorer8.4: A Pre/Post Processor for the Environmental Fluid Dynamics Code. May, 2018, EFDC_Explorer8.4 Version 180509, Dynamic Solutions- International (DSI), Seattle, WA 98020.

Del Giudice, D., et al. (2019). "Jordan Lake Reservoir Model Report." North Carolina Policy Collaboratory.

Di Toro, D. M. and J. J. Fitzpatrick (1993). Chesapeake Bay sediment flux model, Hydroqual Inc Mahwah NJ.

DiToro, D. M. (2001). Sediment Flux Modeling. Wiley Interscience, New York, NY.

Dynamic Solutions, L. (2013). "Final Lake Thunderbird Report for Nutrient, Turbidity, and Dissolved Oxygen TMDLs, prepared for Oklahoma Department of Environmental Quality, Water Quality Division, Oklahoma City, OK." 306.

Falls Lake Technical Advisory Committee (2009). Falls Lake Nutrient Response Model Final Report, prepared for Modeling & TMDL Unit, Division of Water Quality, North Carolina Department of Environment and Natural Resources**:** 145.

Georgia Department of Natural Resources-Environmental Protection Division (2017). Final Total Maximum Daily Load Evaluation for Lake Lanier in the Chattahoochee River Basin for Chlorophyll a, submitted to U.S. Environmental Protection Agency Region 4, Atlanta, GA**:** 130.

Hamrick, J. M. (1992). A three-dimensional environmental fluid dynamics computer code: theoretical and computational aspects, Virginia Institute of Marine Science, College of William and Mary.

Hirsch, R. M. and L. A. De Cicco (2015). User guide to Exploration and Graphics for RivEr Trends (EGRET) and data retrieval: R packages for hydrologic data. Techniques and Methods 4-A10. Reston, VA**:** 104.

Khangaonkar, T., et al. (2012). Puget Sound Dissolved Oxygen Modeling Study: Development of an Intermediate Scale Water Quality Model, Washington State Department of Ecology Publication No. 12-03-049, PNNL-20384 Rev 1, prepared for U.S. Department of Energy Contract DE-AC05-76RL01830**:** 166.

Lin, J. and J. Li (2011). "Nutrient response modeling in falls of the Neuse Reservoir." Environmental management **47**(3): 398-409.

Loftis, B., et al. (1976). B. Everett Jordan Lake Water-quality Study, US Department of Defense, Department of the Army, Corps of Engineers ….

Michael Baker, J., Inc., Aqua Terra Consultants, and Dynamic Solutions, LLC, (2015). Setup, calibration, and validation for Illinois River Watershed Nutrient Model and Tenkiller Ferry Lake EFDC Water Quality Model, prepared for the U.S. EPA, Region 6, Dallas, TX**:** 351.

NC Division of Water Resources (2017). Surface Water Quality Standards History Document: Chlorophyll a. Raleigh, NC, NC Division of Water Resources**:** 2.

NC DWQ (2007). B. Everett Jordan Reservoir, North Carolina Phase I Total Maximum Daily Load. Prepared by: NC Department of Environment and Natural Resources Division of Water Quality, 1617 Mail Service Center Raleigh, NC 27699-1617. September 20, 2007.

NCDEHNR (1992). North Carolina Lake Assessment Report 92-02, NC Dept of Environment, Health, and Natural Resources, Divsion of Environmental Management.

NCDWR, N. C. D. o. W. R. (2018). 2018 303(d) LISTING AND DELISTING METHODOLOGY, Approved by the North Carolina Environmental Management Commission on March 8, 2018. N. C. D. o. E. Quality. Raleigh, NC.

Qi, H., et al. (2016). "Water age prediction and its potential impacts on water quality using a hydrodynamic model for Poyang Lake, China." Environmental Science and Pollution Research **23**(13): 13327-13341.

Tetra Tech (2002). Jordan Lake Nutrient Response Model. Prepared for the Jordan Lake Project Partners by Tetra Tech, Inc., Research Triangle Park, NC. Nov. 13, 2002.

Tetra Tech (2003). B. Everett Jordan Reservoir Nutrient Response Model Enhancement. Prepared for the North Carolina Division of Water Quality by Tetra Tech, Inc., Research Triangle Park, NC. Final - September 2003.

Tetra Tech (2007). "The Environmental Fluid Dynamics Code." User Manual, US EPA Version **1**: 231.

Tetra Tech, I. (2016). High Rock Lake Hydrodynamic and Nutrient Response Models, draft report under EPA Contract (Sept 2012), report finalized by North Carolina Division of Water Resources (Oct 2016)**:** 94.

Tetra Tech Inc. (2003). B. Everett Jordan Lake Nutrient Response Model Enhancement. Research Triangle Park, NC.

USACE (2019). "B. Everett Jordan - Cape Fear River Basin Data Retrieval." from https://epec.saw.usace.army.mil/jord.htm.

Willey, J. D. and R. H. Kiefer (1993). "Atmospheric Deposition in Southeastern North Carolina: Composition and Quantity." The Journal of the Elisha Mitchell Scientific Scociety **109**(1): 1-19.

Zhang, Z., et al. (2015). "Integration of a benthic sediment diagenesis module into the two dimensional hydrodynamic and water quality model–CE-QUAL-W2." Ecological modelling **297**: 213-231.

Appendix 1. Creating Constituent Time Series at Inflow Model Boundaries

EFDC requires specification of the complete time history of all model constituents at each inflow model boundary. For this Jordan Lake model, thirteen model boundaries were considered inflow boundaries with a corresponding flow time history that was also specified in the QSER.INP file. There were a total of fifteen model boundaries, two of which were outflow boundaries (Jordan Lake Dam, Cary Water Treatment Plant specified as QSER7 and QSER13). Six concentration time histories were used to specify these thirteen inflowing model boundaries, as follows:

1. Haw River: QSER1
2. Morgan Creek: QSER2
3. New Hope Creek: QSER3
4. Northeast Creek: QSER4
5. White Oak Creek: QSER5
6. Ungaged watersheds discharging directly to Jordan Lake: QSER6, QSER8, QSER9, QSER10, QSER11, QSER12, QSER14, QSER15

There were eight ungaged watersheds that drained directly to Jordan Lake. One of these was in the Haw River arm of the lake (QSER12). Three additional ungaged watersheds were in the region above the Farrington Road causeway (QSER6, QSER14, QSER15) draining to Jordan Lake from the west, north, and east. Two other ungaged watersheds (QSER10, QSER11) drained to the Jordan Lake region below the Highway 64 causeway from the west and east. The remaining two ungaged watersheds (QSER8, QSER9) drained to the region of Jordan Lake between these two causeways from the west and east respectively.

The six concentration time histories were developed from water quality monitoring data collected by the North Carolina Department of Environmental Quality (NC DEQ) in the Jordan Lake watershed at five locations (Haw River, Morgan Creek, New Hope Creek Northeast Creek, White Oak Creek). The ungaged watersheds used the White Oak Creek data to specify the concentration time history information. A total of twenty-one concentration time history files (cwqsr1.inp to cwqsr21.inp), one for each EFDC water quality state variable, were created for the full model time history (January 1, 2014 – December 31, 2018) at a daily time frequency. In each of these twenty-one files were all six concentration time history for that particular water quality state variable.

A multi-step calculation procedure was used to create the concentration time histories. First, the time history data at the available watershed stations were collected and assembled into an Excel spreadsheet. For each of the five locations, these data were estimated at a daily frequency:

1. Total Nitrogen (mg/L as N)
2. Total Phosphorus (mg/L as P)
3. Ammonia Nitrogen (mg/L as N)
4. Nitrite + Nitrate Nitrogen (mg/L as N)
5. Organic Nitrogen (mg/L as N)

A sixth parameter, dissolved oxygen, was also estimated on a daily frequency for each of the five time histories using the available temperature data, with the assumption that the inflowing waters were fully saturated with dissolved oxygen.

Daily data were available for only two of the five constituents (total nitrogen, total phosphorus). These data were estimated as a daily load by the WRTDS watershed model created for the Jordan Lake (Del Giudice, Aupperle et al. 2019). Daily concentrations were calculated from the daily loads using the daily flow for that watershed. The other three nitrogen concentrations (ammonia, nitrite+nitrate, organic nitrogen) were estimated on a daily basis by developing monthly estimates of nitrogen fractionation. The fractionation estimates relied on the watershed data for a nineteen year time period (2000-2018). Using all the available data, monthly average values of total nitrogen, total phosphorus, ammonia fraction, nitrite+nitrate fraction, and organic nitrogen fraction were calculated.

The monthly nitrogen fractions were similar for four (Haw River, Morgan Creek, New Hope Creek, Northeast Creek, Figures A1.1 – A1.4) all of the watersheds except the White Oak Creek watershed (Figure A1.5). These four watersheds were found to have a nitrogen fractionation pattern that is typical for watersheds containing domestic wastewater treatment plant inputs. For these watersheds, most of the nitrogen was in the nitrite + nitrate fraction. The ammonia fraction had some seasonality, but was always less than 10%. The organic fraction also showed some seasonality, with higher values in the spring months and lower values in the fall months. The organic fraction in the Haw River (Figure A1.1) was generally higher than the three watersheds in the New Hope Creek arm of the lake (Figure A1.2, A1.3, A1.4). Total nitrogen concentrations were also lower for the Haw River station as compared to the three stations in the New Hope Creek arm of the lake (data not shown).

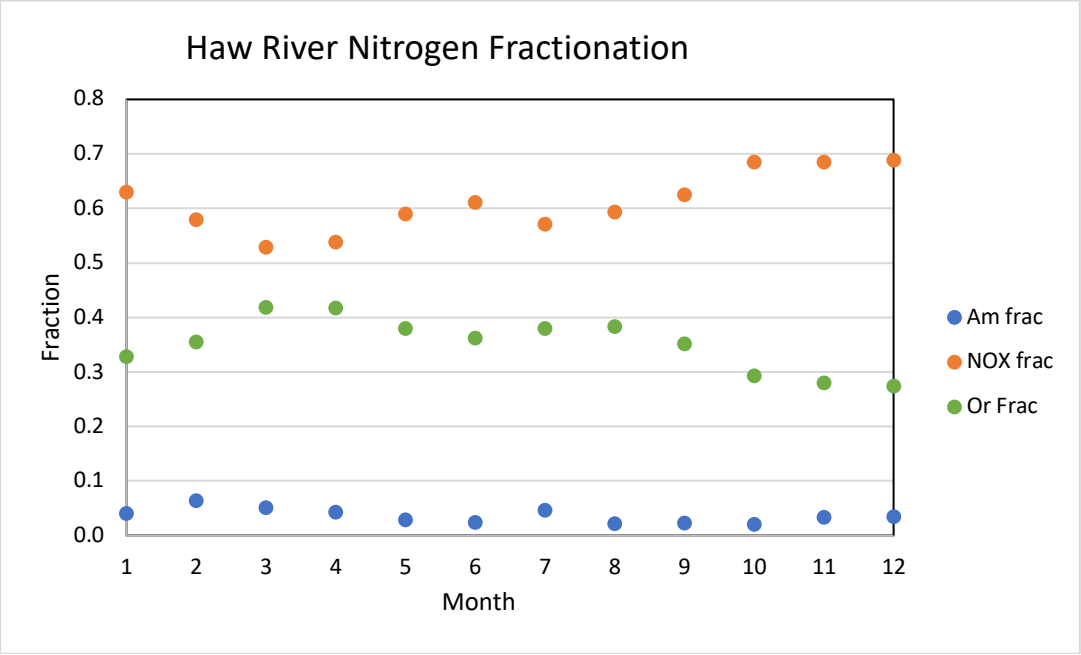

Figure A1.1. Calculated Average Monthly Haw River Nitrogen Fractionation

The one watershed without a wastewater treatment plant input, White Oak Creek (Figure A1.5) had a nitrogen fractionation that was significantly different than the other watersheds. In the White Oak Creek watershed, the nitrogen was primarily in the organic fraction. Like the other watersheds, the ammonia fraction was always less than 10% in all months (Figure A1.5). There was some seasonality in the nitrate + nitrite fraction, with highest values in the winter and spring months. For all months the nitrate + nitrite fraction was less than 20%, which is significantly less than seen in the other four stations (Figures A1.1 – A1.4).

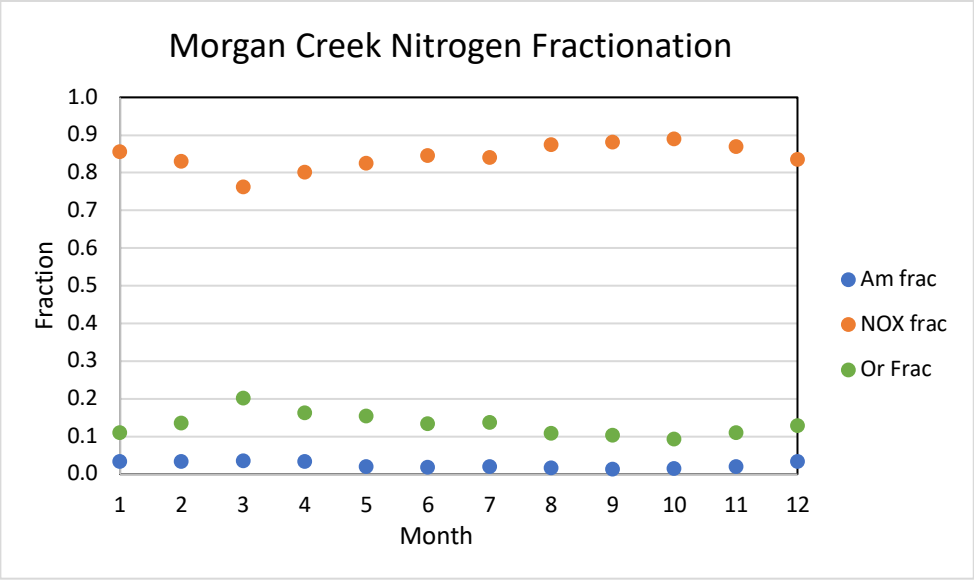

Figure A1.2. Calculated Average Monthly Morgan Creek Nitrogen Fractionation

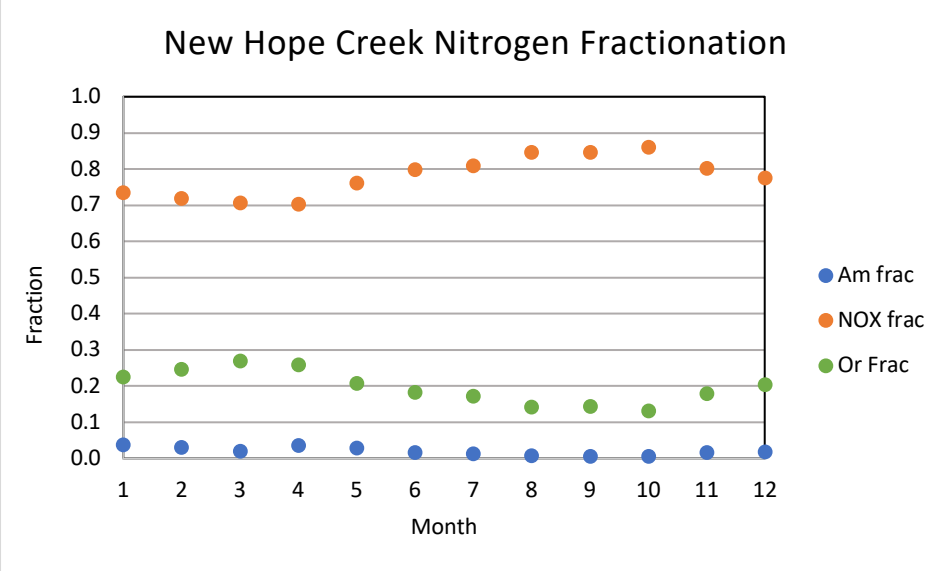

Figure A1.3. Calculated Average Monthly New Hope Creek Nitrogen Fractionation

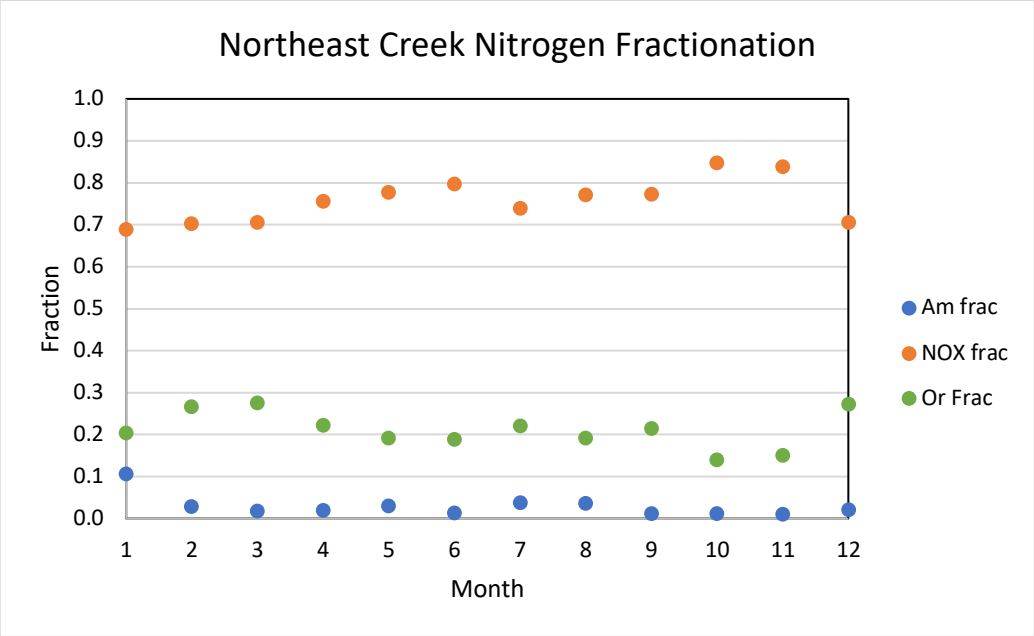

Figure A1.4. Calculated Average Monthly Northeast Creek Nitrogen Fractionation

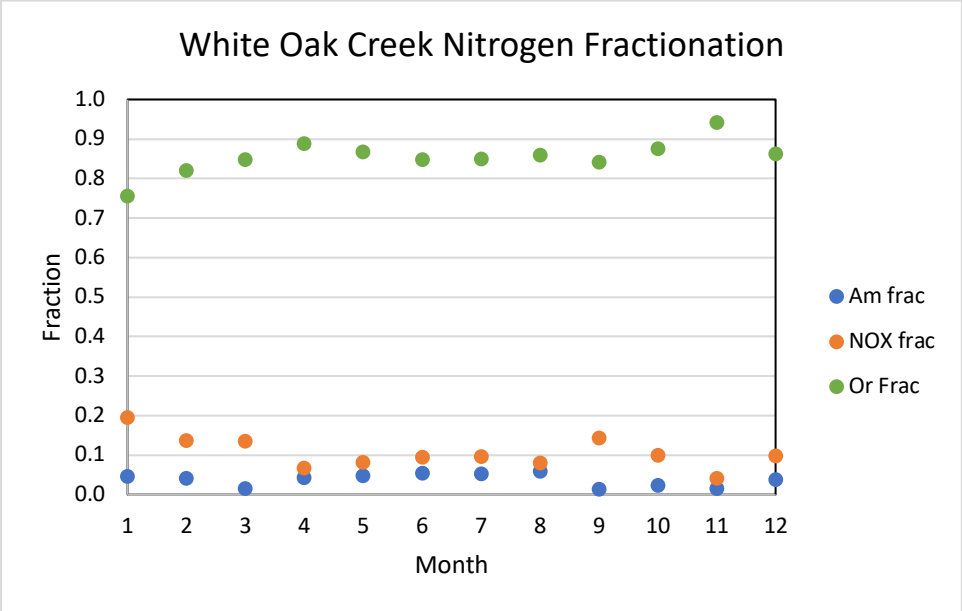

Figure A1.5. Calculated Average Monthly White Oak Creek Nitrogen Fractionation

Monthly average total nitrogen and total phosphorus concentrations were also calculated for each of the five watersheds using all of the available data in the Jordan Lake watershed from 2000 – 2018. The four watersheds having domestic wastewater inputs (Haw River, Morgan Creek, Northeast Creek, New Hope Creek) had significantly higher total P values than that for White Oak Creek, which does not have a wastewater input (Figure A1.6). Total phosphorus values

were higher for the three watersheds in New Hope Creek arm of the lake (Morgan Creek, New Hope Creek, Northeast Creek). The total nitrogen concentrations show a similar pattern, with significantly lower values in White Oak Creek than the other four watersheds, and somewhat lower values for the Haw River than the other three watersheds in the New Hope Creek arm of the lake that receive domestic wastewater inputs (data not shown).

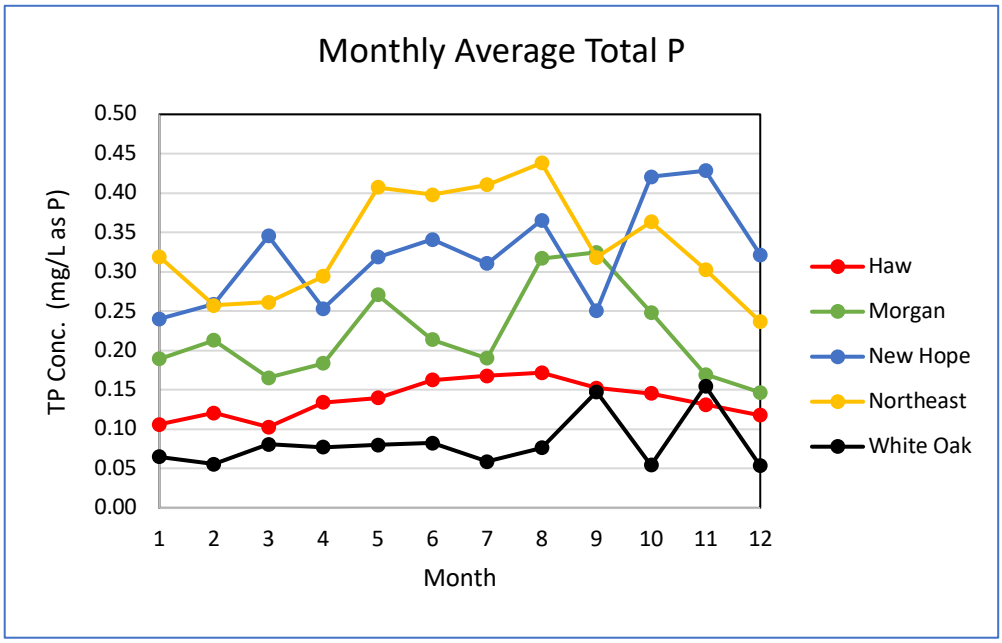

Figure A1.6. Monthly calculated total P concentrations (mg/L) for the five watersheds used to quantify concentration time series for the Jordan Lake model.

The remaining water quality constituents were estimated using the following assumptions:

- organic matter fractions for carbon, nitrogen, and phosphorus were assumed to be evenly split between the labile particulate, refractory particulate, and dissolved constituents
- a background concentration of 0.01 mg/L was used for the three algal constituents
- the organic phosphorus concentration for all three constituents (labile particulate, refractory particulate, dissolved) was calculated from the organic nitrogen fraction using the Redfield N/P ratio
- the organic carbon concentration for all three constituents (labile particulate, refractory particulate, dissolved) was calculated from the organic nitrogen fraction using the Redfield N/C ratio
- soluble reactive phosphorus (total phosphate) was assumed to be equal to the total phosphorus minus organic phosphorus
- the background ultimate carbonaceous oxygen demand was assumed to be 2.0 mg/L
- all concentrations were adjusted if necessary to be greater or equal to zero

Time history tables for all constituents (21 columns) were then calculated using matrix multiplication from the six daily time histories (TN, TP, Ammonia N, NOx N, Organic N, DO),

using a 6x21 transformation matrix that was calculated using the assumptions shown above (Figure A1.7). The figure has been rotated to maximize the font size.

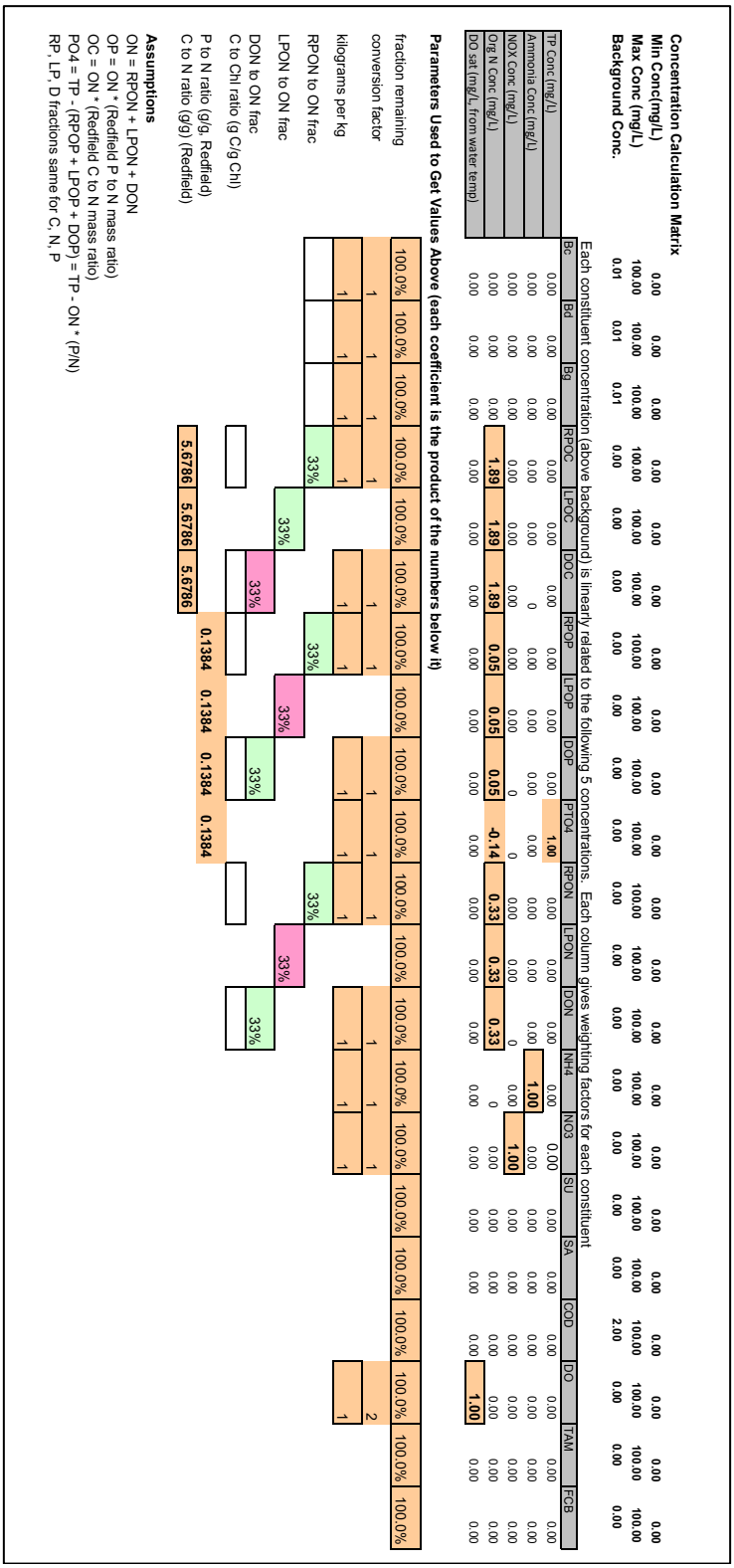

Figure A1.7. Transformation Matrix Used to Develop the Concentration Time Histories for the Base Case of the Jordan Lake Model

The transformation matrix approach was used to create six daily time histories for all twenty-one EFDC water quality model constituents. A Matlab script (make_CWQSR.m) was then used to take the data from the six Excel sheets and then write the information into the twenty-one files needed (cwqsr01.inp to cwqsr21.inp) needed by EFDC. The Matlab code is provided below.

```
function make_CWQSR();
% make_PS_conc.m
% reads a spreadsheet w/ Point Source Concentration information
% and makes the concentration input files  cwqrs##.inp files

% set the project name
project = { 'Jordan Lake Model' };

%set day 0 date (jday 0.0 is at 12:00 AM on this date)
jday0 = '01/01/2011';

% set the constituent names
constit = get_constit_names();

if ispc
    slc = '\';
else
    slc = '/';
end

% load the saved filename and path
load make_CWQSR

disp('choose a spreadsheet with the point source info');

[xlfile, xlpath] = uigetfile([xlpath,'*.xlsx'], 'Pick a spreadsheet w/ the
point source info');

disp(['Existing number of layers =  ',int2str(num_lay)]);
opn = 'y';
while ~strcmp(opn,'y') & ~strcmp(opn,'n')
    opn = input('Do you want to use the existing number of layers? (y or n):
','s');
end
if strcmp(opn,'n')
   %set qser output filename
   num_lay = input('Enter the number of layers:  ');
end
% concentrations are uniform vertically
lyrs(1:num_lay) = 1.0;

save make_CWQSR xlpath xlfile num_lay

opn = 'y';
while ~strcmp(opn,'y') & ~strcmp(opn,'n')
    opn = input('Do you want to use the list of point sources set in the
script? (y or n):  ','s');
end
if strcmp(opn,'y')
```

```
   %set the sheets to include
   incl_sheet = {'PS 1, Haw R.';'PS 2, Morgan Ck.';'PS 3, New Hope Ck.';'PS
4, Northeast Ck.' ; ...
                 'PS 5, White Oak Ck.';'PS 6, Ungaged Watersheds'};
   choose_sheets = false;
else
    choose_sheets = true;
end

% now get the list of sheets in spreadsheet
[status,sheets] = xlsfinfo([xlpath,xlfile]);

if choose_sheets
  disp('these are the sheets available, choose the number to select one');

  for i = 1: length(sheets)
    disp([int2str(i),' = ',char(sheets(i))]);
  end

    num_PS = input('How many point sources to include?  ');
    sheetnum(1:num_PS) = 0;
    for i = 1:num_PS
        while sheetnum(i) < 1 | sheetnum(i) > length(sheets)
            sheetnum(i) = input('Choose a sheet number:  ');
        end
    end
else
    num_PS = size(incl_sheet,1);
    % look for each point source in spreadsheet
    for i = 1:num_PS
        j = 1 ;
        while ~strcmp(char(incl_sheet(i)),char(sheets(j))) & j<
size(sheets,2)
            j = j+1;
        end
        if strcmp(char(incl_sheet(i)),char(sheets(j)))
            sheetnum(i) = j;
        else
            disp([' cant find this point source in spreadsheet:
',char(incl_sheet(i))]);
            disp(' fix and rerun')
            return
        end
    end
end

% read first sheet to get the number and list of constituents
sheet = char(sheets(sheetnum(1)));
%read the spreadsheet data
[numg1,tex1] = xlsread([xlpath,xlfile],sheet);
num_con = size(tex1,2) - 1;
disp([int2str(num_con),' constituents in spreadsheet']);
if num_con ~= 21
  disp(' number of constituents should be 21, fix and rerun');
  return
end
```

```
% now read all the sheets
for i = 1:num_PS
  %set the sheet to read
  sheet = char(sheets(sheetnum(i)));
  %read the spreadsheet data
  [numg,tex] = xlsread([xlpath,xlfile],sheet);
  num_rows(i) = size(numg,1); num_cols(i) = size(numg,2);
  PS_vals(1:num_rows(i),1:num_cols(i),i)=numg;
  disp(['Sheet=',sheet,', read ',int2str(size(numg,1)),' lines from
spreadsheet']);
end

% set the format for printing layer information
if num_lay == 8
      l_form = '%6.3f %6.3f %6.3f %6.3f %6.3f %6.3f %6.3f %6.3f\r\n';
elseif num_lay == 16
      l_form = '%5.3f %5.3f %5.3f %5.3f %5.3f %5.3f %5.3f %5.3f %5.3f %5.3f
%5.3f %5.3f %5.3f %5.3f %5.3f %5.3f %5.3f %5.3f\r\n';
elseif num_lay == 25
      l_form =['%4.2f %4.2f %4.2f %4.2f %4.2f %4.2f %4.2f %4.2f %4.2f %4.2f
%4.2f %4.2f %4.2f %4.2f %4.2f %4.2f %4.2f ', ...
                  '%4.2f %4.2f %4.2f %4.2f %4.2f %4.2f %4.2f %4.2f
%4.2f %4.2f\r\n'];
else
        disp('need a format for this number of layers, fix and rerun');
end
file_dir = [xlpath,xlfile(1:strfind(xlfile,'.')-1),slc];
if ~exist(file_dir)
    mkdir(file_dir);
    disp(['creating folder ',file_dir]);
end
% now make all the point source files
disp(' point source files being saved to specified folder');
for i= 1: num_con
  fileout = sprintf('%scwqsr%2.2i.inp',file_dir,i);
  %open the output filename
  fout = fopen(fileout,'w');
  % set the headers for this file
  header1 = setheader(constit(i),project,jday0,xlfile);

  %write the header at the top of the file
  for r=1:size(header1,1)
        fprintf(fout,'%s\r\n',char(header1(r)));
  end
  for j = 1: num_PS
     % print the header for this point source and the layer information
     fprintf(fout,' 1  %i  86400.0   0.0   1.0000   0.0   0
!%s\r\n',num_rows(j),char(sheets(sheetnum(j))));
     fprintf(fout,l_form,lyrs);
     % print the time history for this point source and this constituent
     conc_data = [PS_vals(1:num_rows(j),1,j)' ; PS_vals(1:num_rows(j),1+i,j)'
];
     fprintf(fout,'%9.4f %10.4f\r\n',conc_data);
  end
  fclose(fout);
end

disp(['finished creating ',int2str(num_con),' files']);
```

```
end

function constit = get_constit_names()

%set the constituent names for the first line of the header in cwqsr##.inp
constit = { ...
    'C  cwqsr01.inp, Cyanobacteria (mg/l as C)' ; ...
    'C  cwqsr02.inp, Diatoms (mg/l as C)' ; ...
    'C  cwqsr03.inp, Green Algae (mg/l as C)' ; ...
    'C  cwqsr04.inp, Refractory POC (mg/l)' ; ...
    'C  cwqsr05.inp, Labile POC (mg/l)' ; ...
    'C  cwqsr06.inp, Dis Org Carbon (mg/l)' ; ...
    'C  cwqsr07.inp, Ref Part Org Phosphorus (mg/l)' ; ...
    'C  cwqsr08.inp, Lab Part Org Phosphorus (mg/l)' ; ...
    'C  cwqsr09.inp, Dis Org Phosphorus (mg/l)' ; ...
    'C  cwqsr10.inp, Total Phosphate (mg/l)' ; ...
    'C  cwqsr11.inp, Ref Part Org Nitrogen (mg/l)' ; ...
    'C  cwqsr12.inp, Lab Part Org Nitrogen (mg/l)' ; ...
    'C  cwqsr13.inp, Dis Org Nitrogen (mg/l)' ; ...
    'C  cwqsr14.inp, Ammonia Nitrogen (mg/l)' ; ...
    'C  cwqsr15.inp, Nitrate Nitrogen (mg/l)' ; ...
    'C  cwqsr16.inp, Part Biogenic Silica (mg/l)' ; ...
    'C  cwqsr17.inp, Dis Available Silica (mg/l)' ; ...
    'C  cwqsr18.inp, Chemical Oxygen Demand (mg/l)' ; ...
    'C  cwqsr19.inp, Dissolved Oxygen (mg/l)' ; ...
    'C  cwqsr20.inp, Total Active Metal (mg/l)' ; ...
    'C  cwqsr21.inp, Fecal Coliform (MPN/100ml)'};

end

function header1 = setheader(constit,project,jday0,xlfile)
%SETHEADER sets the headers for the make_QSER script

% set last line of header
last_line = sprintf('C  JDAY 0.0 is at midnight on %s',jday0);

%set the header at the top of the point source file
header1= {char(constit); ['C  Project ID:  ',char(project),', Concentration
Spreadsheet:  ',xlfile] ; ...
'C'; ...
'C  ISTYP  MCSER(NS,8)  TCCSER(NS,8)  TACSER(NS,8)  RMULADJ(NS,8)
ADDADJ(NS,8)'; ...
'C'; ...
'C  if istyp.eq.1 then read depth weights and single value of CSER'; ...
'C'; ...
'C  (WKQ(K),K=1,KC)'; ...
'C'; ...
'C  TCSER(M,NS,8)   CSER(M,NS,8)  !(mcser(ns,8) pairs for ns=8,ncser(8)
series)'; ...
'C'; ...
'C  else read a value of CSER for each layer'; ...
'C'; ...
'C  TCSER(M,NS,8)   (CSER(M,K,NS,8),K=1,KC) !(mcser(ns,8) pairs)'; last_line
};

end
```

Appendix 2. Observed vs. Model Predicted Temperature Time Histories

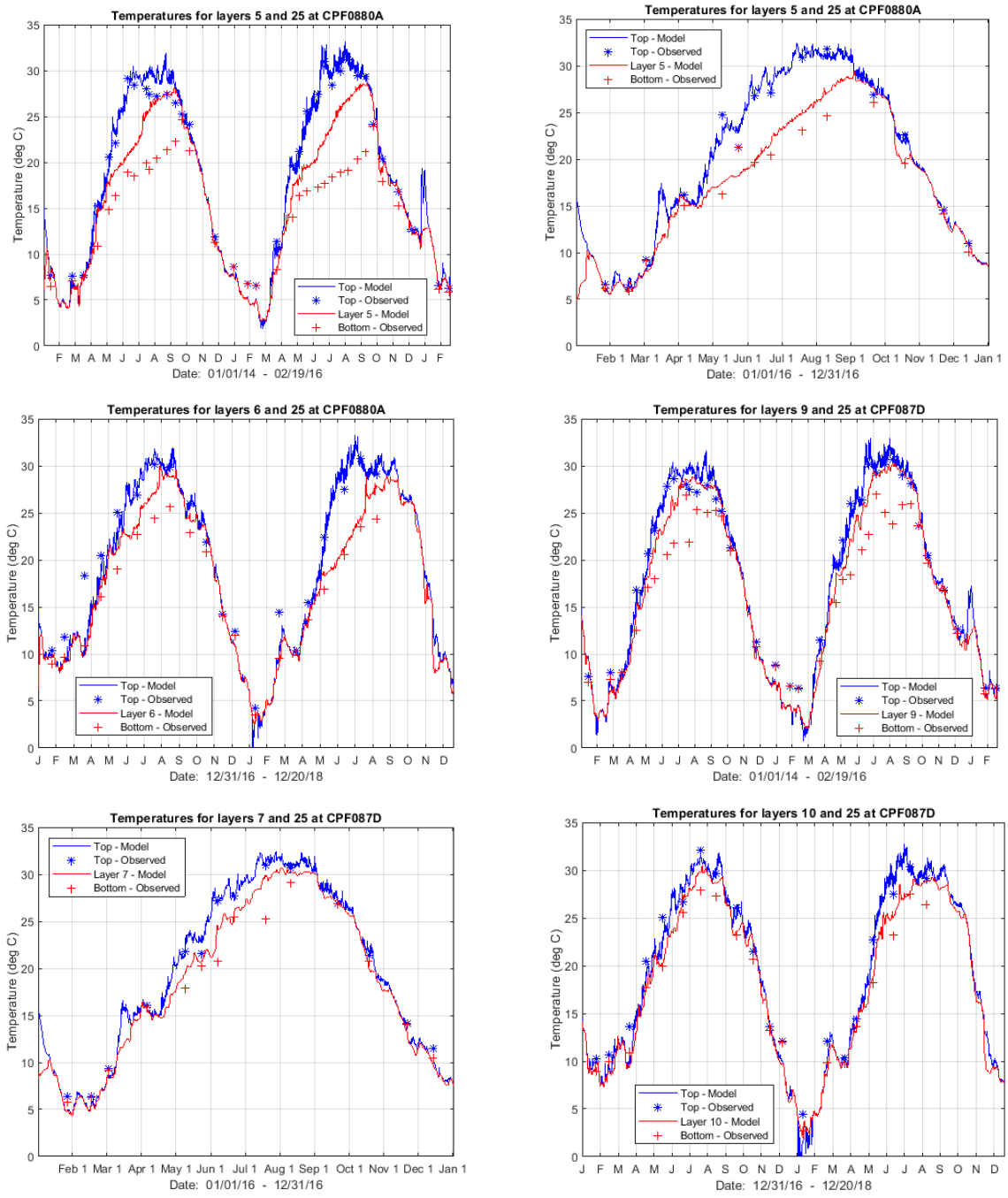

Figure A2.1. Top and bottom (blue and red), observed (symbols) and model predicted (solid lines) temperature time histories for three model time periods (Jan. 2014 - Feb. 2015, Jan. 2016 – Dec. 2016, Jan. 2017 – Dec. 2018) at stations CPF088A and CPF087D.

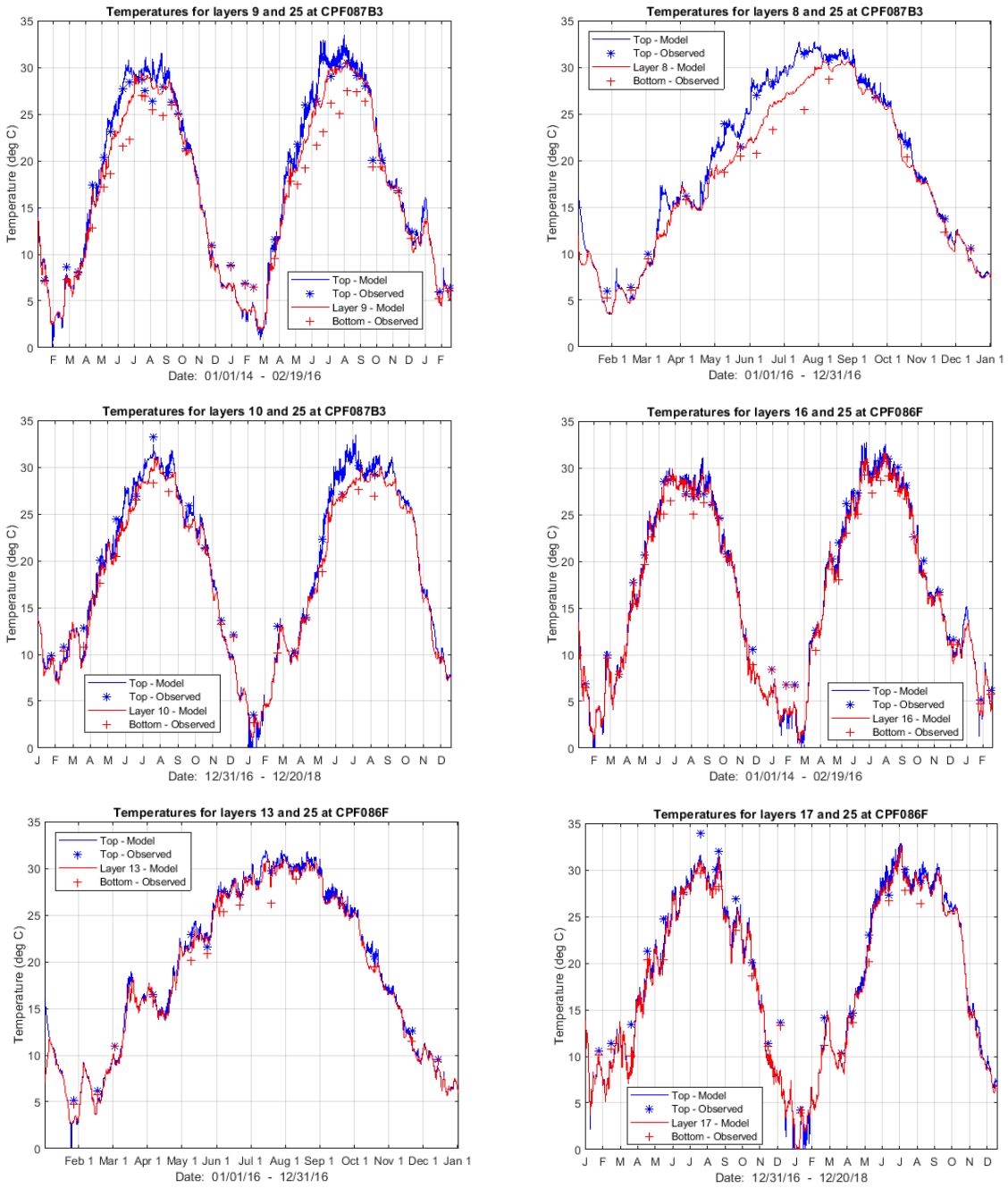

Figure A2.2. Top and bottom (blue and red), observed (symbols) and model predicted (solid lines) temperature time histories for three model time periods (Jan. 2014 - Feb. 2015, Jan. 2016 – Dec. 2016, Jan. 2017 – Dec. 2018) at stations CPF087B3 and CPF086F.

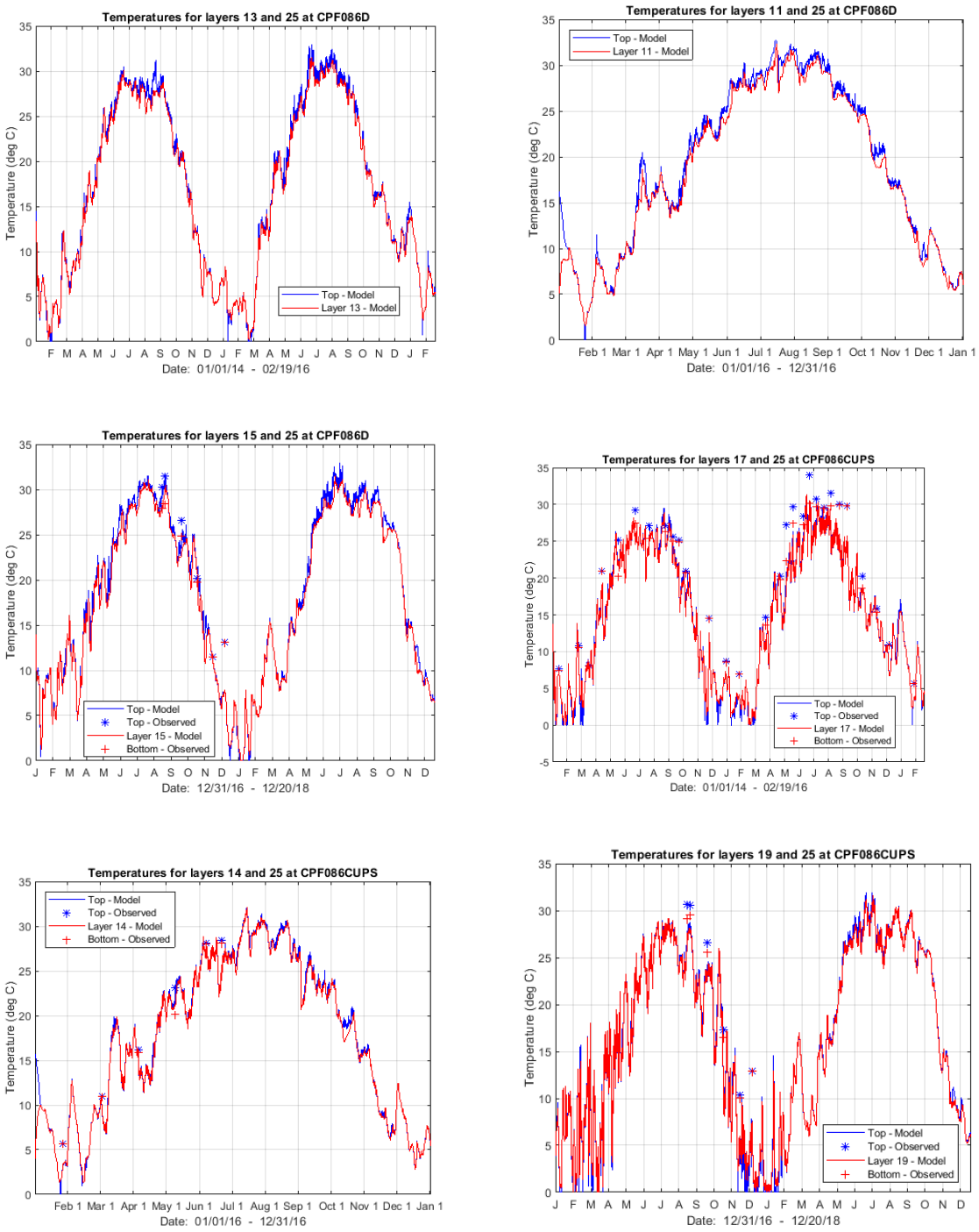

Figure A2.3. Top and bottom (blue and red), observed (symbols) and model predicted (solid lines) temperature time histories for three model time periods (Jan. 2014 - Feb. 2015, Jan. 2016 – Dec. 2016, Jan. 2017 – Dec. 2018) at stations CPF086D and CPF086CUPS.

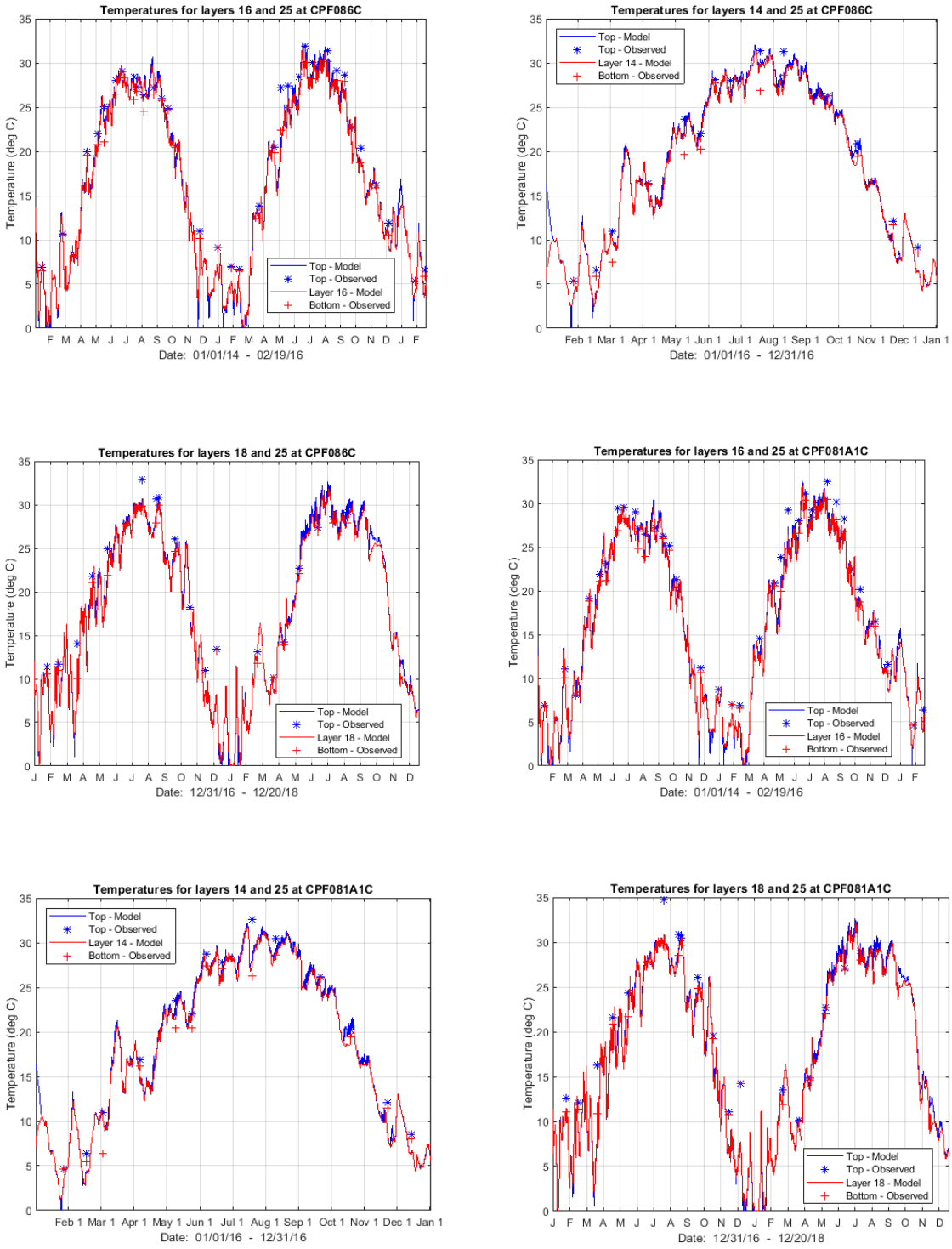

Figure A2.4. Top and bottom (blue and red), observed (symbols) and model predicted (solid lines) temperature time histories for three model time periods (Jan. 2014 - Feb. 2015, Jan. 2016 – Dec. 2016, Jan. 2017 – Dec. 2018) at stations CPF086C and CPF081A1C.

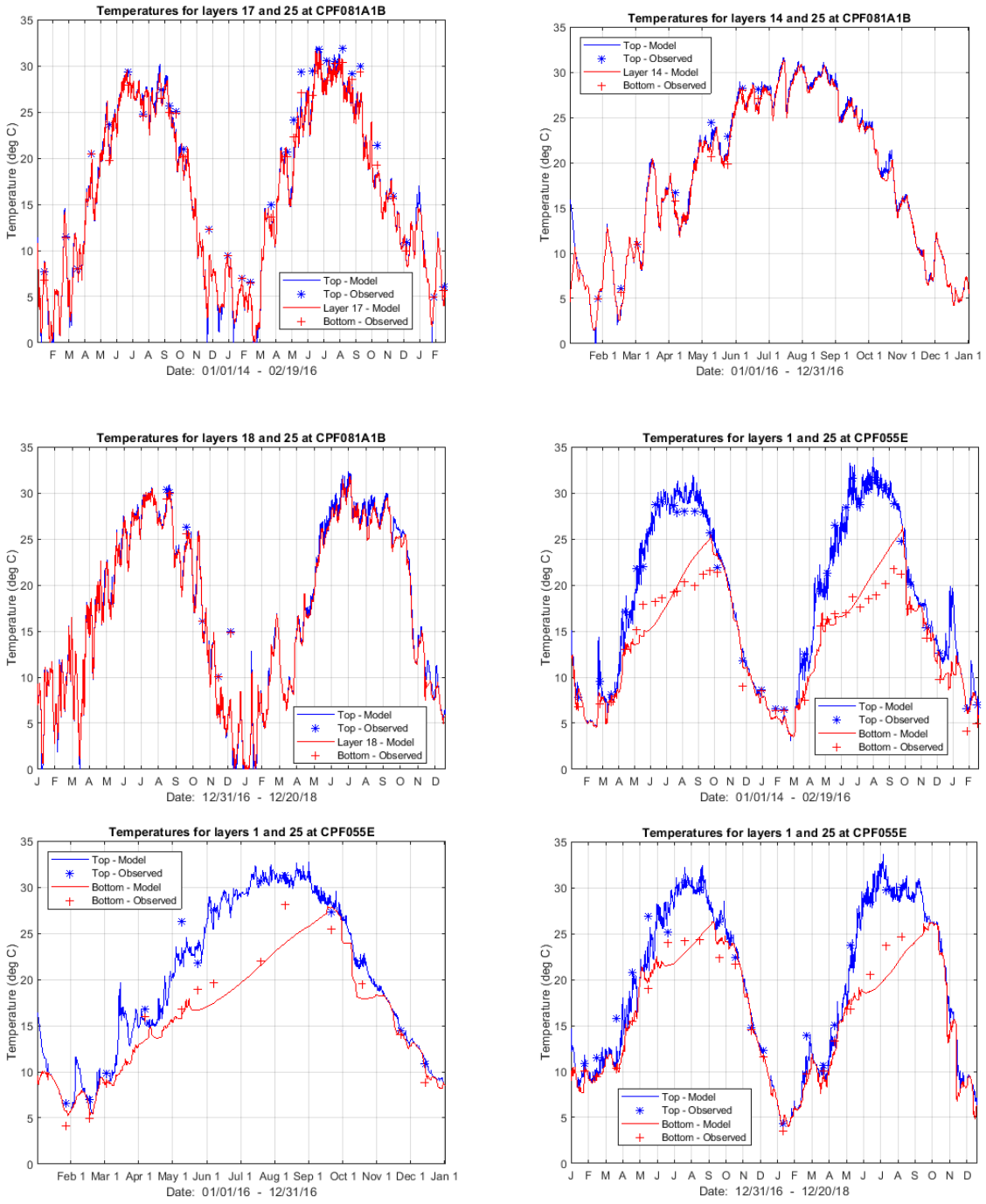

Figure A2.5. Top and bottom (blue and red), observed (symbols) and model predicted (solid lines) temperature time histories for three model time periods (Jan. 2014 - Feb. 2015, Jan. 2016 – Dec. 2016, Jan. 2017 – Dec. 2018) at stations CPF081A1B and CPF055E.

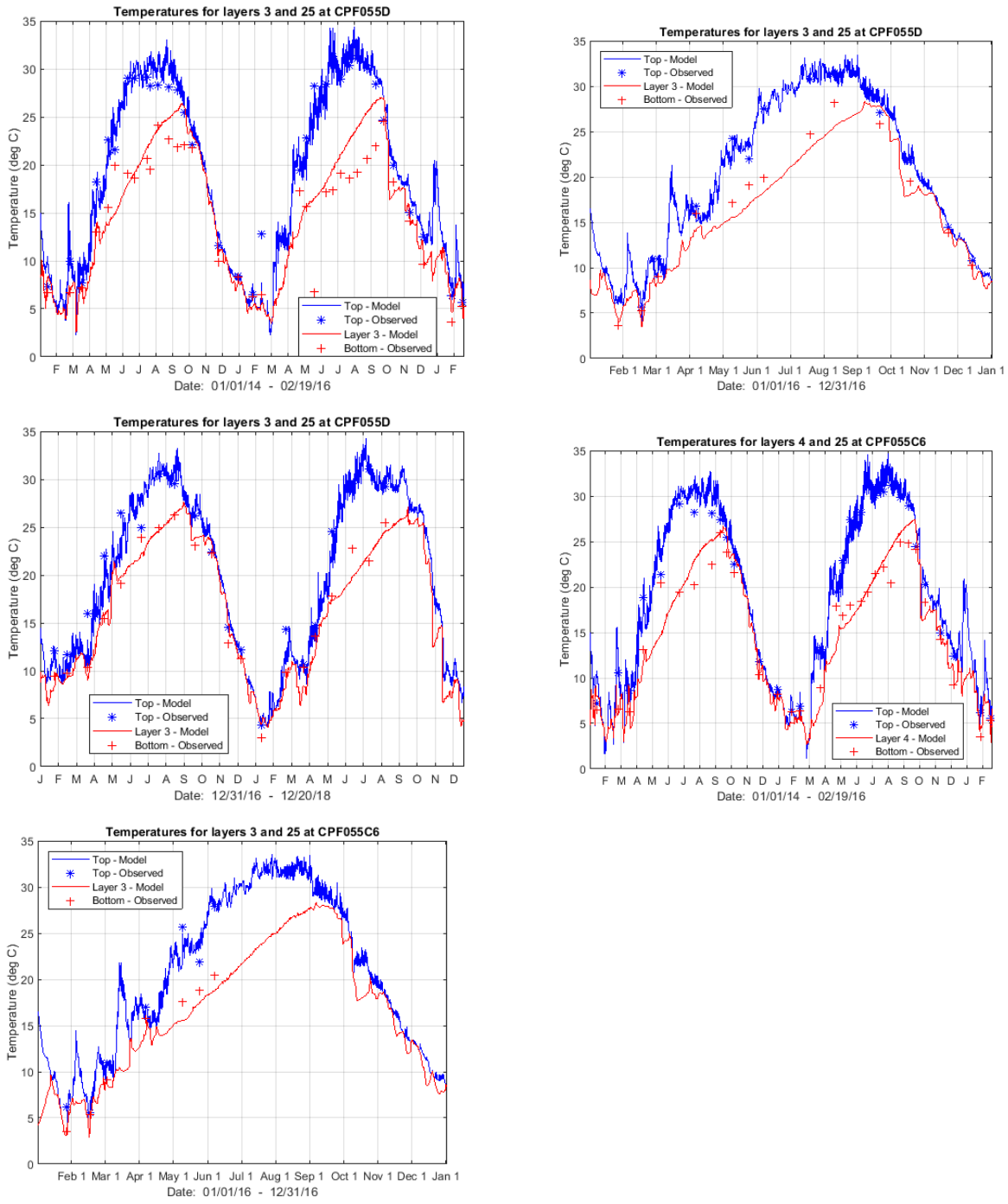

Figure A2.6. Top and bottom (blue and red), observed (symbols) and model predicted (solid lines) temperature time histories for three model time periods (Jan. 2014 - Feb. 2015, Jan. 2016 – Dec. 2016, Jan. 2017 – Dec. 2018) at stations CPF055D and CPF055C6.

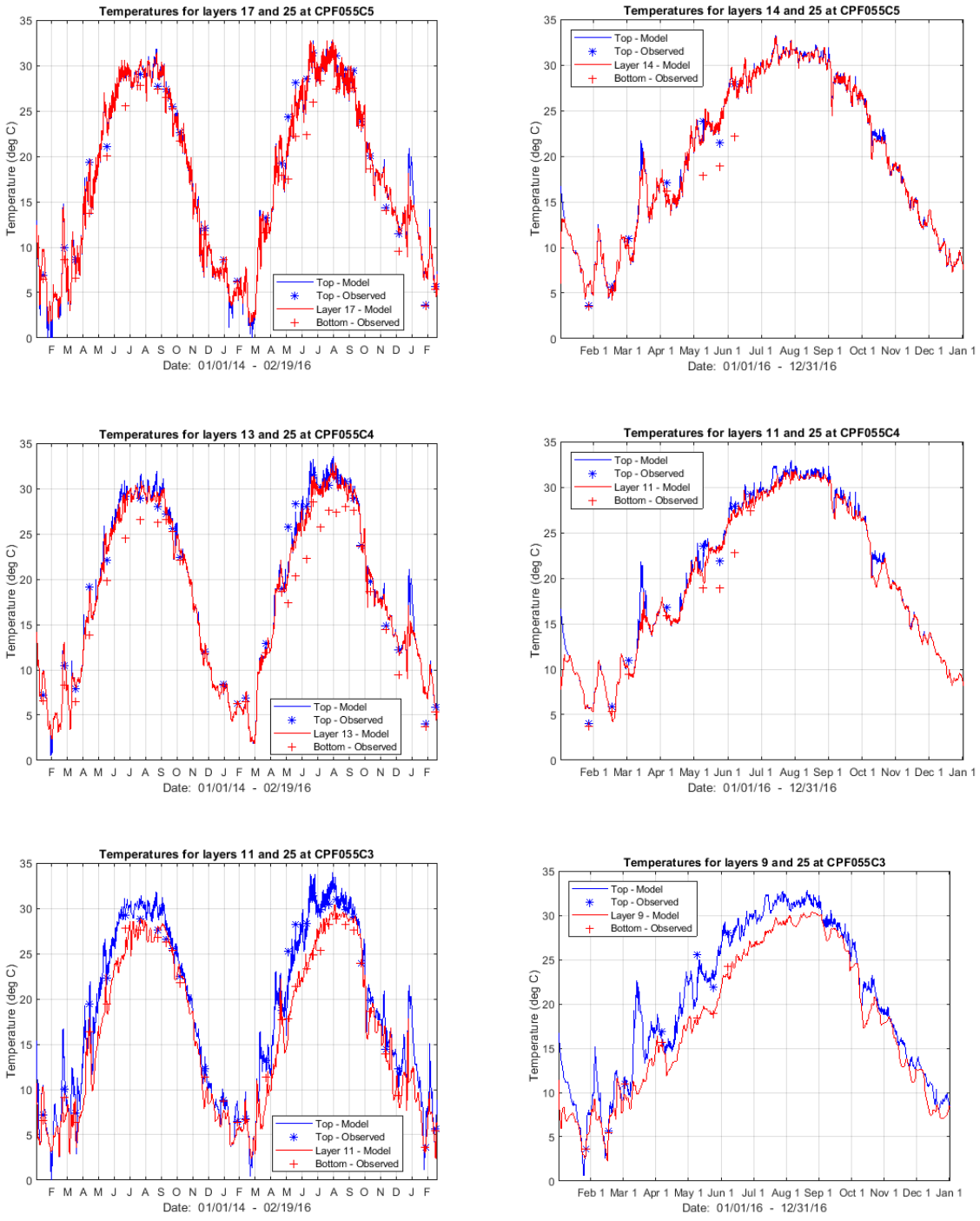

Figure A2.7. Top and bottom (blue and red), observed (symbols) and model predicted (solid lines) temperature time histories for two model time periods (Jan. 2014 - Feb. 2015, Jan. 2016 – Dec. 2016) at stations CPF055C5, CPF055C4 and CPF055C3.

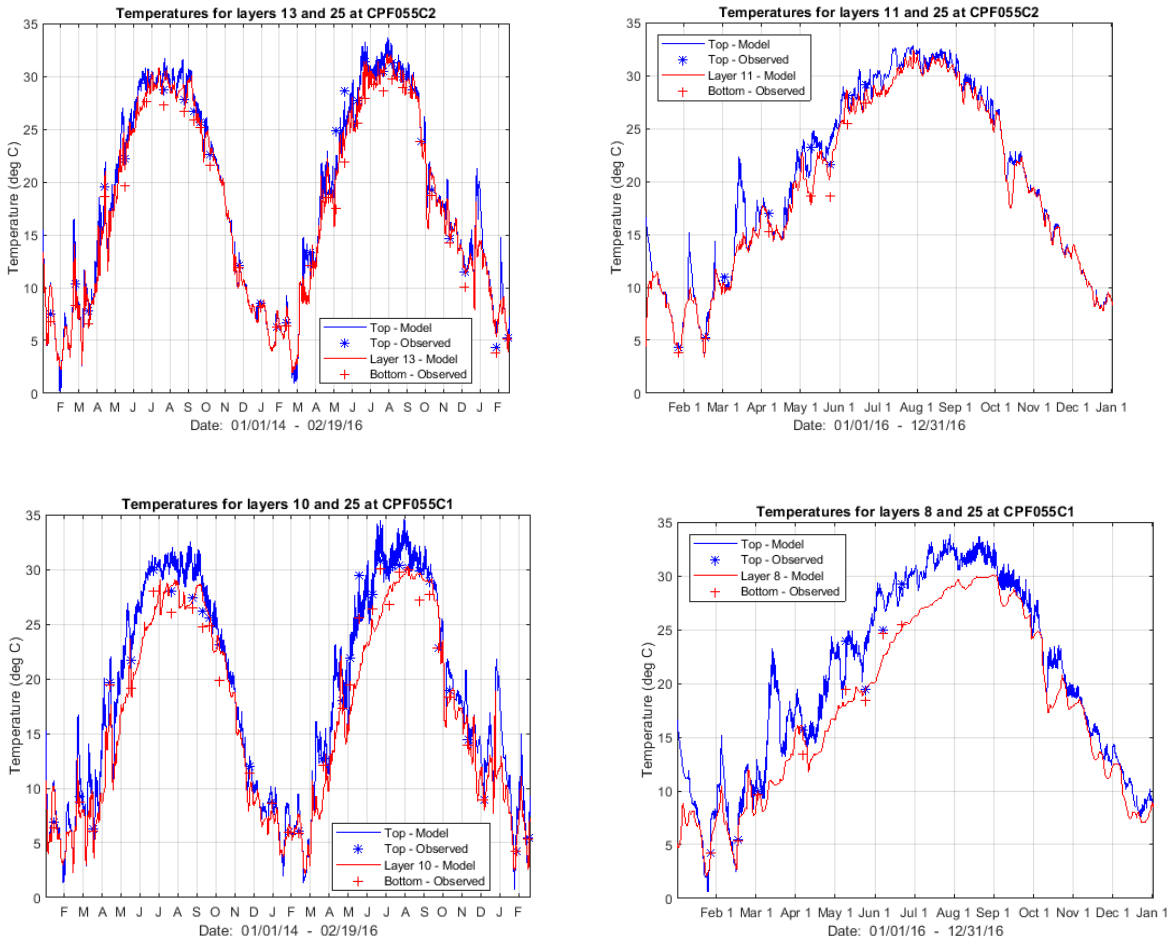

Figure A2.8. Top and bottom (blue and red), observed (symbols) and model predicted (solid lines) temperature time histories for two model time periods (Jan. 2014 - Feb. 2015, Jan. 2016 – Dec. 2016) at stations CPF055C2, and CPF055C1.

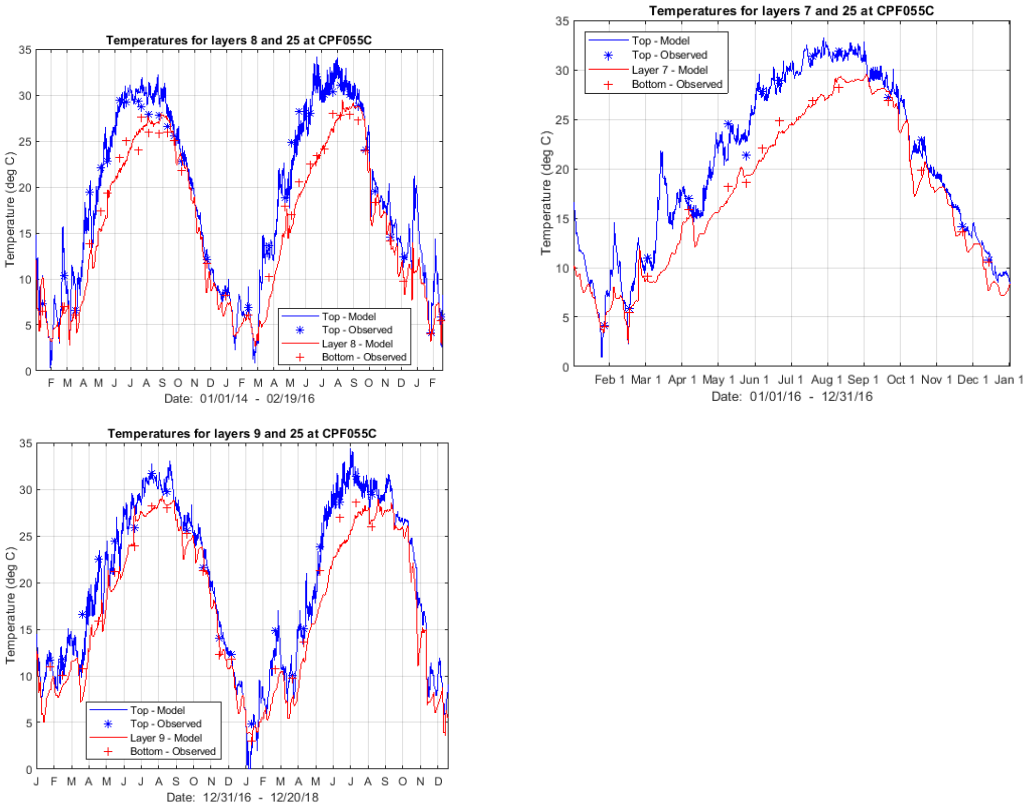

Figure A2.9. Top and bottom (blue and red), observed (symbols) and model predicted (solid lines) temperature time histories for three model time periods (Jan. 2014 - Feb. 2015, Jan. 2016 – Dec. 2016, Jan. 2017 – Dec. 2018) at station CPF055C.